

1 The Mediterranean Sea Heat and Mass Budgets : Estimates, Uncertainties and 2 Perspectives

3
4 G. Jordà (1), K. Von Schuckmann (2), S. A. Josey (3), G. Caniaux (4), J. García-Lafuente (5), S. Sammartino
5 (5), E. Özsoy (6), J. Polcher (7), G. Notarstefano (8), P.-M. Poulain (8), F. Adloff (4), J. Salat (9) , C. Naranjo
6 (5), K. Schroeder (10), J. Chiggiato (10), G. Sannino (11), D. Macías (12)

- 7
8 (1) Institut Mediterrani d'Estudis Avançats (IMEDEA, UIB - CSIC), Esporles, Spain
9 (2) Mediterranean Institut of Oceanography; La Garde, France
10 (3) National Oceanography Center (NOC), Southampton, UK
11 (4) CNRM UMR 3589, Météo-France/CNRS, Toulouse, France
12 (5) University of Malaga (GOFIMA), Málaga, Spain
13 (6) Eurasia Institute of Earth Sciences, İstanbul Technical University, İstanbul, Turkey
14 (7) Laboratoire de Météorologie Dynamique (CNRS/IPSL) , Palaiseau, France
15 (8) National Institute of Oceanography and Experimental Geophysics (OGS), Trieste, Italy
16 (9) Institut de Ciències del Mar (ICM), Barcelona, Spain
17 (10) Istituto di Scienze Marine (ISMAR), Venezia, Italy
18 (11) Italian National Agency for New Technologies, Energy and Sustainable Economic
19 Development (ENEA), Rome, Italy
20 (12) European Commission (Joint Research Center), Ispra, Italy
21
22

23 Abstract

24 This paper presents a review of the state-of-the-art in understanding and quantification of the
25 Mediterranean heat and mass (i.e. salt and water) budgets. The budgets are decomposed into a
26 basin averaged surface component, lateral boundary components (through the Gibraltar and
27 the Dardanelles Straits), a river input component and a content change component. An
28 assessment of the different methods and observational products that have been used to
29 quantify each of these components is presented. The values for the long term average of each
30 component are also updated based on existing literature and a first estimate of heat fluxes
31 associated with the riverine input has been produced. Special emphasis is put on the
32 characterization of associated uncertainties and proposals for advancing current knowledge are
33 presented for each budget component.

34 With the present knowledge of the different components, the Mediterranean budgets can be
35 closed within the range of uncertainty. However, the uncertainty range remains relatively high
36 for several terms, particularly the basin averaged surface heat fluxes. Consequently, the basin
37 averaged heat budget remains more strongly constrained by the Strait of Gibraltar heat
38 transport than by the surface heat flux. It is worth remarking that if a short (~few years)
39 averaging period is used, then the heat content change must also be considered to constrain the
40 heat budget. Concerning the water and salt fluxes, the highest uncertainties are found in the
41 direct estimates of the Strait of Gibraltar water and salt transport. Therefore, the indirect
42 estimate of those transports using the budget closure leads to smaller uncertainties than the
43 estimates based on direct observations. Finally, estimates of Mediterranean heat and salt
44 content trends are also reviewed. However, these cannot be improved through the indirect
45 estimates due to the large temporal uncertainties associated to the surface fluxes and the fluxes

46 through Gibraltar. The consequences of these results for estimates of the Mediterranean
47 temperature and salinity trends obtained from numerical modelling are also considered.

48 **1- Introduction**

49

50 Due to its relatively small size its semi-land locked nature, and its geographical location, the
51 Mediterranean Sea is very sensitive and responds relatively quickly to natural forcing and/or
52 anthropogenic influences. Demographic growth, climate change and overexploitation are
53 exerting exceptional pressure on the Mediterranean environment, its ecosystems, services and
54 resources. Over 150 million people live along its coasts and the basin is of paramount
55 importance for the socio-economics of the surrounding countries. The Mediterranean Sea also
56 hosts a large biodiversity (8% of the known marine species with only 0.8% of the oceanic surface)
57 and is a basin of contrasting ecosystems: from the strongly oligotrophic deep interiors to the
58 fully eutrophic northern Adriatic. Moreover, the Mediterranean region has been identified as
59 one of the hot-spots for climate change in the world (Giorgi, 2006), where expected changes will
60 be largest. Some of the projected changes for the next decades include the warming and
61 salinization of the basin as well as the rise of sea level (e.g Adloff et al., 2015). These changes
62 have been recently detected (e.g., Schroeder et al. 2016, Schroeder et al. 2017) and can
63 potentially have a strong impact on the coastal environment and the marine ecosystems (e.g.
64 Macias et al., 2015). The Mediterranean also plays a role in the evolution of the global ocean,
65 mainly because of its character as a concentration basin. The small catchment area (i.e. relatively
66 low river contribution), the permanent dry conditions in the south and the dry conditions in the
67 north under cold and dry northerlies in winter contribute to evaporation exceeding the
68 contribution of precipitation. Therefore, the basin acts as a source of salty waters for the global
69 ocean. For instance, saline waters outflowing from the Strait of Gibraltar (SoG) are then found
70 in the Atlantic Ocean at a depth of ~1,000 m and might have an impact on the global ocean
71 circulation (Reid 1979; Béthoux 1979; Millot et al. 2006). In this context, the understanding of
72 the functioning of the Mediterranean basin is of paramount importance in order to be able to
73 accurately predict its evolution during the next decades, and its impact on the global ocean.
74 Among all the elements of that functioning, one of the first issues that should be addressed is
75 the monitoring and characterization of the heat and mass content evolution. Although previous
76 attempts have been done (e.g. Lacombe et al., 1981 or Rohling and Bryden, 1992), the significant
77 improvements of the observational systems over the last decades motivate a review of the
78 present knowledge on the Mediterranean heat and mass budgets.

79

80 The variations of heat and mass content of the water in the Mediterranean basin (Figure 1) are
81 directly related to the fluxes of heat and mass across the boundaries of the basin water body.
82 Therefore, the heat budget equation for the Mediterranean can be written as follows:

83

—

(1)

84

85

86
87 where ρ is the density of seawater, θ the potential temperature, C_p the specific heat capacity.
88 V_{Med} and A_{Med} represents the Mediterranean volume and surface area while S_{Gib} and S_{Dard} are the
89 vertical section at the Gibraltar and Dardanelles Straits. u represents the velocity of the flow
90 normal to those sections. QH_{net} refers to the net heat flux through the sea surface (in W/m^2) and
91 Q_{riv} is the river runoff. The last sum is done over all the Mediterranean rivers.

92
93 The left hand side term in (1) represents the changes in the Mediterranean heat content (HC),
94 while in the right hand side we have the heat flux entering into the basin through its boundaries:
95 the air-sea interface (SHF), the Gibraltar Strait (GHF), the Dardanelles Strait (DHF) and the rivers
96 (RHF), respectively (heat exchanges across the seafloor are ignored).

97
98 The mass budget could be expressed in similar terms. In this case it is convenient to split the
99 mass content into two terms: the water and salt contributions. Thus, the equation for water
100 content (WC) can be written like (1):

$$\text{---} \tag{2}$$

101
102 where in this case P and E respectively represent precipitation and evaporation (note again that
103 water exchanges across the seafloor are assumed to be negligible in comparison with the other
104 fluxes at basin scale). It is also worth noting that the heat and water budget equations are closely
105 related as far as water and heat fluxes at surface and lateral boundaries are strongly related
106 since an evaporation driven change in water flux necessarily implies a change in latent heat flux.

107
108 As for the salt content (SC), it can only be modified by the salt fluxes (SF) through the lateral
109 boundaries, in particular through the Gibraltar and Dardanelles straits, since the atmosphere,
110 the rivers or the bottom, do not provide significant salt inputs to the ocean. Therefore
111 considering that S represents the salinity of sea water the salt equation will be reduced to:

$$\text{---} \tag{3}$$

113
114
115 The estimates of the single components of the heat and mass (water and salt) budgets using the
116 above formulae require 'good' information on fluxes at the boundaries that are subject to large
117 uncertainties, as will be shown in the present paper. Therefore, we begin by asking two
118 questions : What is a 'good' flux? And why should we improve the estimates of those fluxes?
119 Ultimately, a good flux is one that provides an accurate representation of the exchanges at the
120 given boundaries on the space and timescales of interest irrespective of whether the underlying
121 approach is observation or model. However, it is instructive to examine how the requirements
122 of the observational and modelling communities can differ for particular applications. For
123 instance, for modellers, air-sea fluxes should be compared with "observations" (*e.g.* from buoys)

124 at fine scales in order to reconstruct the seasonal cycle of some parameters (Sea Surface
125 Temperature (SST), Mixed Layer Depth (MLD)). Good fluxes should permit the correct simulation
126 of the thermohaline circulation, at daily timescales and with spatial resolution of the order of
127 several tens of km, as well as the oceanic deep convection in order to simulate properly dense
128 water mass formation. A correct estimate of net heat or freshwater fluxes, despite
129 compensation errors, should prevent model drifts, even if sometimes it is difficult to know if
130 such drifts exist or not due to the lack of reliable data for model validation (see Section 6). To
131 enable the accurate simulation of some oceanic features, such as the eddies (20-30 km in
132 diameter) observed in the Levantine basin, it is unclear how accurate the fluxes need to be in
133 order to enable accurate simulation. Furthermore, for modellers, the question of timescales is
134 important to solve: fluxes must at least enable reconstruction of the seasonal cycle and not only
135 the annual mean state. Smaller timescales (weekly to daily) can also be required because strong
136 flux events influence directly the formation of new water masses (e.g. deep water formation).
137 In summary, it is very difficult to establish an absolute criterion to determine if a flux is 'good' in
138 all the situations. Therefore, a better approach would be to quantify the uncertainties associated
139 to each flux, so that each user may decide if the quality of the estimate fits the specific needs.

140

141 A joint analysis of the different components merging information from different sources could
142 potentially lead to a significant improvement of the knowledge of the system as a whole. In this
143 context, the project "**Mediterranean Sea mass and heat budget: Understanding its forcing,**
144 **uncertainties and time evolution (MED-MaHb)**" has been initiated under the auspices of
145 ENVIMED/MISTRALS/HYMEX. The principal objective of this initiative is to build up a multi-
146 disciplinary synergic community for Mediterranean Sea climate research aiming to work on a re-
147 evaluation of the mass and heat budgets. This work is based on the assessment of the
148 consistency and uncertainty of the different components in equations (1-3). This assessment is
149 based on different approaches (in situ measurements, remote sensing, ocean synthesis and
150 numerical models) to further understand its forcing and to analyze its time evolution. This
151 initiative follows the objectives of the 6th CLIVAR research focus
152 (www.clivar.org/about/research-foci#six), MedCLIVAR (<http://www.medclivar.eu/>), HyMEX
153 (www.hymex.org) and MedCORDEX (www.medcordex.eu/).

154

155 The goal of the present paper corresponds to the first major step of implementation of the
156 MedMAHB project: to review the state-of-the-art of approaches and estimates of each
157 component of the Mediterranean heat and mass budgets. Particular emphasis will be put on: (i)
158 identifying current advances in research and on the characterization of the associated
159 uncertainties, and (ii) to propose a set of recommendations for future improvements of those
160 estimates. All this will in turn deliver relevant contribution to future advancements of regional
161 climate monitoring and predictions, which have been identified as key challenges for future
162 climate research studies (e.g. IPCC, 2013). In sections 2 to 5 we address the characterization of
163 the fluxes through each one of the boundaries: ocean-atmosphere interface, the Strait of
164 Gibraltar, the Dardanelles Strait and the riverine inputs, respectively. In section 6 the changes
165 in the global heat, water and salt content are characterized, while in section 7 we present a short
166 review of the projected evolution of the different components during the next decades. A
167 general discussion is presented in section 8 prior to concluding with some final remarks.

168

169

170 **2- Mass and heat exchange through ocean-atmosphere interactions**

171

172 **2.1. Overview**

173 Air-sea exchanges of heat and freshwater in the Mediterranean are central to our understanding
174 of its oceanography and role within the wider climate system. The exchanges are difficult to
175 determine as they require knowledge of the latent (equivalently evaporation), sensible,
176 longwave and shortwave heat fluxes, as well as precipitation. This in turn requires estimates of
177 the driving near surface atmospheric meteorological parameters (air temperature, humidity and
178 wind speed), sea surface temperature and cloud amount. Attempts to estimate these fields are
179 severely limited by lack of observations and the subsequent derivation of the flux terms by
180 incomplete knowledge of air-sea exchange physics. Consequently, considerable uncertainty
181 remains in Mediterranean air-sea heat and freshwater exchange fields across a wide range of
182 spatial and temporal scales. These vary from basin mean quantities at decadal timescales to, for
183 example, extreme heat loss associated with winter storms at hourly to daily timescales and
184 spatial scales of tens of kilometres.

185

186 To date, the main obstacle to producing accurate ('good') fluxes from various sources (satellite,
187 numerical weather prediction (NWP) models) is the lack of reference quality flux datasets at key
188 locations (for example, high quality time series from surface flux reference site moorings of the
189 type deployed at several other locations in the global ocean within the Ocean Observatories
190 Initiative). To our knowledge, some observatories do exist in the Mediterranean which collect
191 relevant meteorological variables and radiative fluxes (see for instance the FixO3 network,
192 <http://www.fixo3.eu/observatory/>) although they have not been used yet to evaluate different
193 flux datasets. An alternative approach may be to undertake systematic tests that rely on forcing
194 ocean models with all the available flux fields and compare ocean model results with oceanic
195 data in order to elucidate which forcing dataset is the best. However, this approach is
196 expensive in computational terms and face the problem of errors in the ocean model (i.e. the
197 discrepancies between model and oceanic observations may come from sources other than the
198 forcing fields). One of the main techniques used by modellers is to apply flux correction in the
199 form of restoring or adjustment. That is, to impose a constraint in the fields used to force the
200 ocean models in which the modelled sea surface temperature and/or salinity are relaxed
201 towards a reference dataset. This approach has proven to be useful to avoid model drifts but
202 can only be applied if the required reference datasets are of good quality and available for all
203 the modelled period (i.e. this would not be possible for climate projections). Moreover, an
204 additional question is then to know if at long timescales these corrections affect processes such
205 as convection, the production of dense waters and the global circulation itself and its variability
206 (Simmons and Polyakov, 2004).

207

208

209 **2.2. Methods for Estimating Surface Fluxes**

210

211 Different methods are used to estimate turbulent fluxes (latent and sensible heat, evaporation,
212 wind stress, CO₂ fluxes, etc ...). Local estimates are derived from turbulence measurements of
213 the wind (3 components, with a three-axis sonic anemometer), air temperature and humidity

214 fluctuations at high frequency (20 to 50 Hz sample rate) in the constant flux layer. At sea, typical
215 approaches are the eddy correlation (EC) and the inertial dissipative (ID) methods, that employ
216 measurements from surface moorings (e.g. Weller *et al.*, 2012; Bigorre *et al.*, 2013) or research
217 vessels (e.g. Weill *et al.*, 2003; Bourras *et al.*, 2009).

218

219 The EC method is based on direct calculation of the covariance between vertical wind and
220 temperature or humidity fluctuations, and requires correction of wind, temperature and
221 humidity measurements for ship movements (Edson *et al.*, 1998). This means that the angular
222 and linear accelerations of the ship have also to be measured at high frequency with a six
223 degrees of freedom accelerometer. These additional parameters are not necessary for applying
224 the ID method, which is based on the closure of the turbulent kinetic energy equation in the
225 inertial zone of the wind spectrum. In both cases, however, it is essential to apply corrections to
226 take into account flow distortion and vibrations of the measurement platform (Yelland *et al.*,
227 2002; Dupuis *et al.*, 2003; Bourras *et al.*, 2009). In the best case, measurements have to be
228 performed facing wind (at angles less than 30-40°) and at reduced ship velocity (2-3 kts).

229

230 Other methods for estimating turbulent fluxes at sea can also be used, such as: a) the profile
231 method (derived from high resolution radio-soundings in the constant flux layer) (Dupuis *et al.*,
232 1995) and b) the eddy-accumulation method (Brut *et al.*, 2004), which is well suited for
233 estimating latent heat fluxes, CO₂ fluxes or for scalar fluxes of minor and slowly reacting
234 atmospheric species (DMS, ozone, etc.).

235

236 The method most commonly used by modellers is the bulk method (Fairall *et al.*, 1996, 2003;
237 Weill *et al.*, 2003; Edson *et al.*, 2013; among many others). It is based on the physical properties
238 of the constant flux layer (*cf.* Monin and Obukhov, 1954). The method considers the existence
239 of relationships between turbulent fluxes and “slow” (opposed to turbulent) meteorological and
240 oceanic parameters (*i.e.* wind, temperature, humidity, sea level pressure and SST). The exchange
241 coefficients connecting the fluxes and the slow parameters are determined from local estimates
242 of turbulent fluxes using the ID or EC methods.

243

244 In general, experiments at sea only sample a limited range of conditions (*i.e.* medium wind
245 speeds from 3-5 m/s to 15 m/s; weakly stable stratification to moderate unstable stratification).
246 In these ranges, relatively good agreement exists between various parameterizations found in
247 the literature. However, large disagreements exist at low and high winds and highly unstable
248 stratification, which are largely undersampled (Figure 2). Moreover, the sensible heat flux
249 transfer coefficient is poorly known: these restrictions limit the use of bulk algorithms. In
250 numerical models, bulk formulae are usually extrapolated beyond the conditions under which
251 in-situ estimates are made, and this results in significant spread between flux evaluations (see
252 example given in Figure 3).

253

254 Some physical processes directly affect the estimates of fluxes and several bulk algorithms
255 include sea surface properties such as surface wave characteristics, sea spray, white capping,
256 stability, gustiness factor, the effects of skin temperatures, Webb correction, and cooling due to
257 rain (e.g. Fairall *et al.*, 2003). These effects are generally weak except in some specific cases. Of
258 course, these additional parameterizations (as they depend on an increased number of basic

259 observables) increase the errors in the fluxes themselves. Note that for the Mediterranean Sea,
260 frequent gale force (>20 m/s) winds from September to May, and related young sea state and
261 sea spray (Andreas *et al.*, 2014) need to be taken in account in the estimation of wind stress and
262 latent heat fluxes.

263

264 Besides local flux estimates, fluxes can potentially be retrieved from satellite observations. From
265 brightness temperature measurements in a particular frequency range, it is possible to estimate
266 both the shortwave and longwave radiative fluxes (Brisson *et al.*, 1994; Schluessel *et al.*, 1995).
267 Produced operationally at the Centre de Météorologie Spatial (CMS, Météo-France) and at fine
268 time and space scales (1h and 0.1° longitude and latitude), longwave and shortwave radiations
269 are compared systematically with local measurements (*e.g.* buoys in the Atlantic) (Le Borgne *et*
270 *al.*, 2007). As reported in Table 1 and reference herein, the comparison of daily satellite
271 retrievals compare quite well with ship and mooring data in the Atlantic, with bias less than 2
272 W/m² and RMS ranging from 10 to 20 W/m², except for some specific cases (in presence of
273 smoke aerosols or Saharan dust aerosols) . Unfortunately, a similar comparison in the
274 Mediterranean has not been yet done.

275

276 SSTs are nowadays retrieved as a blend of satellite microwave sensors. They perform quite well
277 even through cloudy conditions and infrared observations provide accurate SST analyzed fields
278 (Donlon *et al.*, 2002, 2007). For instance the accuracy of ENVISAT radiometer is in the range of
279 0.1-0.3°C (Embury *et al.*, 2012) and systematically compared with in-situ measurements, SEVERI
280 has a bias of -0.16°C with a root mean square error of 0.5°C (Marullo *et al.*, 2007). Like for
281 radiative fluxes, limitations also do exist in the presence of aerosols.

282

283 Wind stress is currently estimated from scatterometry which provide the wind relative to surface
284 currents at spatial scales of the order of 10-15 km. Sampling problems exist with these retrievals
285 since the time interval between two passages of the satellite at the same spot is of the order of
286 some days and no data are available less than 30 km from the coast. Other limitations exist at
287 weak wind speeds (less than 3 m/s) and for high winds (*e.g.* in tropical cyclones), as well as in
288 presence of strong surface currents, of rain (Weissman *et al.*, 2012), or due to the influence of
289 waves on the stress. Moreover, the space resolution along oceanic fronts and mesoscale
290 features (eddies, filaments) is generally too coarse.

291

292 For retrieving turbulent fluxes from satellite, one requires near-surface wind, air temperature,
293 humidity, SST and sea level pressure with the best accuracy as well as the use of a state-of-art
294 bulk algorithm (*e.g.* Bourras, 2006). Several attempts have been performed to get turbulent flux
295 fields from satellite (Chou *et al.*, 2003) or a net heat balance. Nevertheless the determination
296 of near surface moisture and air temperature still need to be improved in order to get reliable
297 turbulent fluxes (Bourassa *et al.*, 2010; Kent *et al.*, 2014).

298

299 Estimating rain is clearly important for the Mediterranean Sea. However, precipitation is difficult
300 to measure over oceans and seas, both because of instrumental errors (flow distortion on the
301 sensor, difficulty in differentiating sea spray and precipitation at high wind, etc.), and of
302 sampling errors due to the representativeness of local measurement with the surroundings.
303 This problem is more complicated in the case of convective precipitation, due to the highly

304 patchy and intermittent nature of rain. Moreover, precipitation measurements at sea are very
305 scarce. All these factors contribute to the difficulty in evaluating satellite retrievals of oceanic
306 precipitation or numerical model outputs or reanalyses with in-situ data. Satellite retrievals face
307 the question of the temporal sampling window (e.g. where the scanned area is limited to once
308 or twice a day sampling), a problem exacerbated in the case of convective precipitation. Some
309 products combine satellite datasets with reanalyses (Xie and Arkin, 1996) although important
310 biases remain in reanalyses (e.g. Serreze *et al.*, 2005). Additionally some observational products
311 based on in-situ reports from ships have been produced (e.g. ICOADS, <http://icoads.noaa.gov/>).
312 However, these products suffer from the scarcity in time and space of the observations, so the
313 sampling error can be very large. A complementary source of information can be the
314 precipitation estimates from coastal radar measurements. At present many of the
315 Mediterranean countries have radars that measure precipitation till 50-150 km from the coast
316 (e.g. <http://www.eumetnet.eu/radar-network>). Although the whole basin is not completely
317 covered by the radars they can provide useful information for the calibration/validation of other
318 precipitation datasets. The main difficulty is that the data is managed by many different
319 providers and there is not a centralized database where all the radar data is unified and
320 homogenized. Furthermore, the radar measures reflectivity which has to be converted to
321 precipitation intensity relies on more or less complex relationships that can induce
322 uncertainties.

323

324 Finally, flux fields can be provided from operational NWP model outputs (e.g. ECMWF, NCEP,
325 ARPEGE...). However, models have errors related to parameterizations used in the atmospheric
326 boundary layer (including turbulent flux bulk methods), and to radiative schemes which affect
327 cloud cover and radiative fluxes. Moreover, microphysical schemes and formation of clouds, rain
328 bands etc. affect the estimate of precipitation and thus the fresh-water balance at the sea
329 surface. An example of the uncertainties introduced by all those factors is the large discrepancies
330 in the mean heat and water flux over the Mediterranean shown by different regional climate
331 models (RCMs) even when all are driven by the same global reanalysis. For instance, Sánchez-
332 Gómez *et al.* (2011) analysed an ensemble of atmospheric RCMs driven by the ERA40 reanalysis.
333 While the long term mean of the surface heat flux in ERA40 was -15 W/m^2 , the RCMs driven by
334 ERA40 provided values ranging from -40 to $+12 \text{ W/m}^2$. For the net surface water flux the results
335 were similar: the ERA40 mean was 781 mm/yr and the RCMs results ranged from 602 to 1087
336 mm/yr .

337

338

339 **2.3. Reliability of Surface Flux Estimates**

340

341 Surface fluxes estimated by the ID or EC methods are generally compared to assess which
342 method gives better results. For example, from the AMMA/EGEE campaign, Bourras *et al.* (2009)
343 gets weak biases between the ID and EC wind stress and sensible heat fluxes ($<2 \text{ W.m}^{-2}$) but
344 larger biases affect latent heat fluxes when humidity fluctuations were measured with different
345 instruments (18 Wm^{-2} when evaluated with a LICOR and 33 Wm^{-2} when evaluated with a
346 refractometer). These results show that the evaluation of exchange coefficients is affected by
347 some errors: such errors have thus to be evaluated when using a bulk algorithm.

348

349 Errors in turbulent bulk fluxes result from: 1. the accuracy of the input observables (humidity,
350 wind velocity, temperature, SST, sea level pressure); 2. the bulk algorithm itself, which
351 corresponds to the uncertainty affecting the exchange coefficients; 3. the iterative method used,
352 since most bulk algorithms solve the constant flux layer equations iteratively until convergence.
353 Generally point 2 and point 3 errors are computed as a percentage of the mean flux values.

354

355 Moreover, observable errors increase in cases of undersampling, for instance associated with
356 diurnal cycles, when aggregating fluxes over heterogeneous areas etc. Note that the
357 Mediterranean Sea experiences frequent summer SST oscillations associated with diurnal cycles
358 of the order of 0.5°C (Stuart-Menteth *et al.*, 2003; Marullo *et al.*, 2014), a phenomenon largely
359 increased under weak winds and strong diurnal heating conditions. The difference between bulk
360 and skin SST may induce a difference of 0.2° C at night and several degrees during the day
361 (Gentemann and Minett, 2008). According to Webster and Lukas (1992), a 1°C skin SST variation
362 affects upward longwave radiation, sensible heat and latent heat fluxes by 1.3%, 23.3% and
363 16.2% respectively.

364

365 In Table 2, the expected errors are reported for the fluxes estimated at the LION buoy in the
366 north-western Mediterranean Sea. The figures were obtained by taking the mean values of the
367 observables and fluxes estimated with the COARE3.0 bulk algorithm at the buoy for the period
368 2011-2013. The error on the net heat flux mostly comes from the errors on the latent heat flux
369 (12 W/m²) and the net longwave radiation (7 W/m²). The error on the net heat flux reaches 15
370 W/m², a figure close to those reported by Colbo and Weller (2009) in the sub-tropics and or by
371 Cronin *et al.* (2014) for the tropical Pacific. When the bulk algorithm error is considered, the
372 total error on the net heat flux rises to 20 W/m². It is important to notice that this estimate of
373 the heat flux uncertainties has been obtained at the LION buoy and is not representative of the
374 whole Mediterranean. Unfortunately, up to now it is not possible to directly assess the
375 uncertainties associated with basin averaged fluxes because mooring observations are restricted
376 to a limited number of sites that do not adequately sample the range of conditions across the
377 basin.

378

379

380 Concerning the water fluxes various studies show that the bias between satellite retrievals of
381 precipitation and rain gauge can be significant (up to 25% even for long time series, e.g. Bowman
382 *et al.*, 2009). Also Romanou *et al.* (2010) have estimated the uncertainties in the annual mean
383 evaporation over the Mediterranean provided by HOAPS-3 to be ~20-35 % of annual estimate.
384 There are no studies quantifying the uncertainty of products based on ship observations and
385 only a comparison among products is possible. In particular, the different in-situ observational
386 products analyzed by Mariotti *et al.* (2002) provide a range for the long term mean of
387 precipitation (evaporation) of 310-700 mm/yr (1120-1570 mm/yr). The discrepancies among
388 products can be due to the data included in the product as well as to the interpolation procedure
389 used to generate the basin averages. Regarding the numerical models and reanalyses,
390 precipitation depend largely on the dynamics (humidity transport) and on the parameterizations
391 of warm and/or cold microphysics and radiative transfer, leading to significant biases in
392 precipitation positioning and intensity in comparison with satellite datasets (Xie and Arkin, 1996;
393 Béranger *et al.*, 2006; Pfeifroth *et al.*, 2013). As an example, the Mediterranean average

394 precipitation in the reanalyses analyzed by Mariotti et al. (2002) ranged from 300 to 500 mm/yr
395 while the average evaporation ranged from 920 to 1200 mm/yr.

396

397

398 **2.4. Evaluation of Flux Estimates**

399

400 Evaluations of surface flux datasets rely on both large scale (e.g. budget closure, see Discussion
401 section) and local (i.e. high quality surface flux reference site measurements) constraints (Josey
402 and Smith, 2006). At local scales, some flux datasets exist that have gathered high quality data
403 measured at sea and can potentially be used for model and satellite flux product evaluation (e.g.
404 AUTOFLUX, Larsen *et al.*, 2000; ALBATROS, Weill *et al.*, 2003; SAMOS, Smith 2004). For the
405 Mediterranean, the Fetch experiment specifically documented fluxes under low winds and
406 under gale force winds in the Gulf of Lion, as well as associated sea states (Hauser et al., 2003).
407 Surface flux reference site data from flux moorings at several locations in the Mediterranean
408 Sea would clearly be highly desirable to complement those datasets. To our knowledge, only a
409 very limited amount of data exist for the Mediterranean Sea, at periods of time of the order of
410 one year or longer, which are necessary for evaluation of flux products. One candidate of such
411 dataset is the network of Mediterranean buoys that is currently operated by different
412 institutions. A description of most of the existing sites can be found in the FIX03 project website
413 (<http://www.fix03.eu/observatory/>). Most of the buoys do not measure precipitation, radiative
414 fluxes or the parameters required to derive the turbulent fluxes but there are some exceptions
415 (see Figure 1). The Lion and the Azur buoys operated by Météo-France
416 (<http://mistrals.sedoo.fr/HyMeX/>) provide subdaily observations of those parameters since year
417 2000 (radiative fluxes after 2011). The W1-M3A buoy, located in the Ligurian Sea and operated
418 by CNR (<http://www.odas.ge.issia.cnr.it>), have been measuring air-sea fluxes (turbulent and
419 radiative fluxes and precipitation) at subdaily frequency since 2009 (Canepa et al., 2015). The
420 E2-M3A buoy, located in the South Adriatic and operated by the OGS measure the same
421 parameters except precipitation since 2014. The E1-M3A site, managed by HCMR
422 (<http://www.poseidon.hcmr.gr/>) have also observations of the relevant parameters since 2009,
423 although with large gaps in some of the parameters. Finally, the OOCs observatory operated by
424 the CEAB-CSIC in the Catalan Sea (<http://www2.ceab.csic.es/oceans/>) also provides the same
425 parameters (except precipitation) since 2009. Although most of the data is publicly available,
426 they should be quality-controlled and homogenized before they can be used as a reference
427 dataset. Moreover, it has to be noticed that most of the observations are located in the
428 northwestern Mediterranean, which is a problem in terms of the representativity of the
429 reference dataset. Therefore, having a continuous monitoring of air-sea fluxes in the central and
430 southern parts of the basin would be advisable

431

432 Additionally the measurements of atmospheric data from vessels (see for instance
433 <http://icoads.noaa.gov/>) could be a complementary source of information. As mentioned above,
434 the sparse spatial and temporal coverage of those data pose a serious problem for the estimate
435 of basin average quantities. However, that dataset could be used to assess the quality of the
436 products at the time the observations were taken, and thus identify which product (if any) is
437 more reliable. Finally, radar observations of precipitation could be used to assess the quality of
438 the products. However, as mentioned above, this is not straightforward as the reflectivity data

439 provided by different radars should be first homogenized and transformed into precipitation
440 intensity.

441

442 A complementary approach is to use the budget closure at basin or subbasin scales for closing
443 the observed heat and water budgets (Caniaux *et al.*, 2005a, 2005b). The results obtained from
444 this inverse method over the north-western Mediterranean basin are encouraging and the
445 adjusted flux fields, including adjusted precipitation, could potentially be used as a reference for
446 evaluation, model forcing or process studies (Caniaux *et al.*, 2017).

447

448 The heat transport observations at the Strait of Gibraltar provide useful constraints on the basin
449 mean averaged fluxes that have been the subject of many studies over the years (e.g. Gilman
450 and Garret, 1994; Sanchez-Gomez *et al.*, 2011; Schroeder *et al.*, 2012). A common approach in
451 those studies has been to use the results of Macdonald *et al.* (1994) who determined, from
452 water temperature measurements at a few points of the water column across the Strait, a value
453 for the constraint on the basin mean heat flux of $-5.2 \pm 1.3 \text{ W/m}^2$ (where negative values imply
454 an ocean heat loss). It is important to remark, though, that Macdonald *et al.* (1994) used less
455 than one year of observations and did not use observations in the upper 100 m of the water
456 column. Therefore, as acknowledged by those authors, the uncertainty provided is probably
457 underestimated. Historically, observation based flux datasets have not been able to satisfy this
458 constraint. Instead they have basin mean values typically in the range 20 to 30 W/m^2 (e.g. Gilman
459 and Garrett, 1994). However, this has been recognised as being due in part to the use of radiative
460 flux formulae that have been developed in large scale ocean basins (e.g. North Atlantic) and thus
461 do not reflect conditions typically experienced in the Mediterranean. Consequently, various
462 causes for this imbalance have been proposed including the neglected influence of aerosols on
463 the shortwave radiation and the need for revised longwave parameterisations specific to the
464 Mediterranean (Bignami *et al.*, 1995).

465

466 Even with reasonable adjustments for these processes in place, the basin mean heat flux with
467 the NOC ship based product is about 5 W/m^2 i.e. a positive bias relative to the Gibraltar based
468 constraint of the order of 10 W/m^2 (Sanchez-Gomez *et al.*, 2011). By combining the NOC based
469 radiative fluxes with satellite based (HOAPS) estimates for the turbulent fluxes these authors
470 were able to obtain a more realistic basin mean value of $-3 \pm 8 \text{ W/m}^2$ for which closure with
471 the Macdonald *et al.* (1994) value is obtained within the stated error bounds. Sanchez-Gomez
472 *et al.* (2011) also considered budget closure across a range of regional climate models and find
473 a large range but a mean value that does satisfy the Gibraltar constraint; for the ensemble of
474 models considered the basin mean net heat flux is $-7 \pm 21 \text{ W/m}^2$ datasets. The large spread
475 indicates the need for substantial further effort to reduce model uncertainty but such models
476 may ultimately provide a useful indicator of the processes responsible for the biases in
477 observation based Mediterranean Sea air-sea flux datasets.

478

479 **2.5. Perspectives**

480 Based on the published results cited above, the NOC/HOAPS estimate from Sánchez-Gómez *et al.*
481 *et al.* (2011) of the basin average Mediterranean surface heat flux of $-3 \pm 8 \text{ W/m}^2$ is closest to the
482 Gibraltar based value of $-5.2 \pm 1.3 \text{ W/m}^2$ (Macdonald *et al.*, 1994). In a further study, Pettenuzzo
483 *et al.* (2010) attempt to use various satellite and in situ observational data to construct spatially

484 varying corrections to the ERA-40 reanalysis air-sea fluxes and obtain a climatological mean net
485 surface heat flux of -7 W/m^2 (note they do not provide an uncertainty range) which is also
486 consistent with the Gibraltar based value. We take both the Sánchez-Gómez et al. (2011) and
487 Pettenuzzo et al. (2010) values to be indicative of plausible surface flux based estimates of the
488 basin mean heat budget in the discussion in Section 8. It should be stressed that there is no
489 single 'best estimate' set of fluxes for the Mediterranean, hence our decision to select these two
490 papers as a reflection of recent efforts and ongoing uncertainty in the surface flux fields. As
491 these estimates have been obtained with knowledge of the Strait of Gibraltar constraint, it is
492 not useful to employ the surface flux estimates to indirectly estimate the other heat budget
493 components. Regarding the surface water flux the basin average is estimated to be -750 ± 190
494 mm/yr. The uncertainty here has been estimated as the spread of the different products
495 analyzed in Mariotti et al., (2002) and Sánchez-Gómez et al. (2011).

496

497 At present different products based on observational and modelling approaches are available
498 for the Mediterranean air-sea fluxes. Qualitatively, the strengths and weakness of each one is
499 relatively well known but the bottleneck that prevents the improvement of such products and a
500 more accurate estimate of the associated uncertainties is the lack of reference in-situ datasets.
501 The gathering and homogenization of all the above mentioned datasets could lead to such
502 reference dataset and eventually to an improved estimate of the surface fluxes.

503

504

505

506 **3 - Exchanges through the Strait of Gibraltar**

507

508 **3.1 Overview**

509 The vigorous water exchange through the Strait of Gibraltar (SoG hereinafter) is an issue of
510 compelled analysis in the study of the mass and energy budgets of the Mediterranean Sea, since
511 it is its most important open lateral boundary and the only connection to the global ocean. Not
512 surprisingly, its study has aroused great interest and much effort has been paid to put reliable
513 figures to the size of the exchanged flows.

514

515 The highly irregular topography of the SoG (Figure 4), and the remarkable strength of the tidal
516 currents interacting with this topography pose severe difficulties for estimating the size of the
517 exchanged flows and their variability (Lacombe and Richez, 1982; Armi and Farmer, 1988;
518 Bryden et al., 1994; García Lafuente et al., 2000; Sannino et al., 2004; Sánchez Román et al.,
519 2009; Sannino et al. 2009; Sánchez-Garrido et al., 2011; Sannino et al., 2015). The attempts to
520 provide a reliable estimate are traced back to the beginning of the 20th century (see Table 3) and
521 can be sorted out into three categories. In the first one are the theoretical approaches based on
522 the volume and salt conservation for the Mediterranean, which require the previous knowledge
523 of the net evaporation over the basin (or at least a realistic guess of it) as well as the salinity
524 difference between the connected water bodies. The weakness of this approach is the above-
525 mentioned poorly constrained values of the evaporation. More sophisticated approaches
526 include energy considerations that bring the problem to the field of the hydraulics (Bryden and
527 Stommel, 1984; Armi and Farmer, 1985; 1988; Bryden and Kinder, 1991). The second category
528 gathers the attempts based on observations, whose history is more recent due to the formidable

529 technical challenge of deploying scientific equipment in such a harsh environment. The third one
 530 is the numerical modelling (Sannino et al., 2004; 2007; 2009; 2014a; Sánchez Garrido et al., 2011;
 531 Peliz et al., 2013; Boutov et al., 2014) whose usefulness is arguable as models require feedback
 532 from observations to be calibrated. Table 3 shows the values provided by the first two categories
 533 and illustrates how the theoretically-based estimations are systematically larger than those
 534 based on observations. Estimations from numerical models are not included in Table 3 because
 535 of their reliance on the observations used for calibration. However, numerical models are highly
 536 valuable to address other flow properties and to draw important conclusions, as it will be shown
 537 below. Table 3 also provides an estimation of the net flow through the SoG as the mean of the
 538 values based on observations (no-shaded rows), which is 0.065Sv (1Sv = 10⁶m³/s). Taking the
 539 standard deviation of these values as the accuracy, then the net flow through the SoG from
 540 historical observations would be $Q_{net}=0.065\pm0.033$ Sv, which could be rewritten as
 541 $Q_{net}=0.82\pm0.42$ m/yr in terms of the rate of net water loss (E-P) in the Mediterranean basin (1
 542 Sv across the SoG is equivalent to 1260 mm/yr of evaporation in the basin).

543

544 **3.2 Recent estimations of the exchanged fluxes from observations**

545

546 The volume transport, or flow, through a given section is defined by:

547

$$(4)$$

548

549

550 where subscript i is for Atlantic or Mediterranean flows, u_i is the water velocity (considered
 551 positive to the east, negative to the west), and the integral is extended to the cross area of the
 552 section from the lower (LS) to the upper (US) limit. These limits are the seafloor and the interface
 553 for the Mediterranean water ($i=M$), and the interface and the free surface for the Atlantic water
 554 ($i=A$). The net flow $Q_{net}=Q_A+Q_M$ is a small quantity achieved as the sum (actually the difference,
 555 since Q_M is negative) of two much greater numbers, making it very sensitive to the accuracy of
 556 the summands. This is a relevant issue regarding the computation of net fluxes through the SoG.

557

558 The final figure provided by Sammartino et al. (2015) for the outflow at the westernmost section
 559 of the SoG (Espartel sill section, ES, see Figure 4) using this approach was -0.85 Sv. The outflow
 560 variability has to be considered at different time scales. It is dominated by tidal fluctuations
 561 whose standard deviation at ES is ± 0.39 Sv, quite close to the amplitude of the M2 tidal
 562 constituent over there. For long-term studies, in which tidal variability is filtered out, this interval
 563 is unrealistic. The main remaining source of variability after removing tides stems from the
 564 atmospheric forcing and shows a standard deviation of 0.15 Sv, less than half the previous value
 565 (Figure 5). For annual time scales, the meteorologically-driven fluctuations are averaged out and
 566 the variability is further reduced (± 0.08 Sv), the seasonal cycle prevailing over the rest of
 567 contributions. It shows maximum outflow in late winter-early spring and minimum outflow in
 568 late summer (Figure 6). At even longer time scales, the interannual variability drops to ± 0.03 Sv,
 569 which is the uncertainty assigned by Sammartino et al. (2015) to their long-term estimation of

570 the outflow at ES based on ten years of observations. A very small trend of -4.6×10^{-4} Sv/yr was
571 reported by these authors, although it was not significant at the 95% confidence level.

572

573 The conversion from volume to mass transport is easy since the Mediterranean water density
574 variations around a central (3D spatially-averaged) value of $\rho_0 = 1028.5 \text{ kg m}^{-3}$ in the SoG are
575 smaller than 1 kg m^{-3} . It gives a relative variation ~ 40 times less than the relative uncertainty in
576 the estimated flows and it can be assumed as constant. With that value for ρ_0 , the mass outflow
577 at ES would be $(8.74 \pm 0.31) \times 10^8 \text{ kg s}^{-1}$. Because of this straightforward conversion, we will only
578 speak of volume transport (flows).

579

580 Heat (QH) and salt (QS) transport are computed similarly to the flows in eq. (4):

581

$$\rho \tag{5}$$

$$\tag{6}$$

582

583 where subscript i is again for layers, ρ_i is the density, ϑ_i and S_i are the potential temperature and
584 salinity, respectively, and $c_{p,i}$ the specific heat of seawater at constant pressure, which depends
585 very slightly on ϑ_i and S_i . The units for QH_i and QS_i are W and kg s^{-1} , respectively. The net heat
586 and salt transport is the sum of the inflow and outflow contributions. Notice that the negative
587 sign of u_M implies negative heat and salt Mediterranean transports (QH_M, QS_M).

588

589 The practical problem to compute these flows from observations is the necessity of having a
590 good representation of the spatial distribution of ϑ and S . First, there is the need of sampling
591 the water column to have vertical profiles of ϑ and S , due to their strong dependence with depth
592 in the SoG. The same practical problem exists for the flow computation using eq. (4), but this
593 problem can be sorted out by a bottom-moored uplooking ADCP, as it is the case in the ES
594 monitoring station. The horizontal variability could be addressed in a similar way as in
595 *Sammartino et al. (2015)* for the outflow computation if a time series of a single vertical profile
596 of ϑ and S were available, which is not the case. Presently, such time series do not exist and the
597 only feasible estimations of heat or salt transports based on observations come from
598 simultaneous measurements of the u , ϑ and S fields collected by CTD probes with ADCP installed
599 on it during oceanographic surveys. The resulting estimation has the important drawback of
600 being strongly contaminated by the time variability of the velocity field. Figure 7 is a clear
601 illustration of this situation for the case of heat transport. None of the displayed estimations are
602 even close to the expected mean value. Yet more, the estimations carried out during the same
603 oceanographic cruise at the two sampled sections differ noticeably because the sections were
604 sampled at different moments of the tidal phase. The same is applicable to the salt transport,
605 since the main source of variability in eq. (4) to (6) is u_i , especially at tidal time scales. With this
606 fact in mind, the best way of addressing heat and salt transports nowadays, or at least some
607 aspects of them, is numerical modelling.

608

609

610 **3.3 The exchanged fluxes from numerical models**

611

612 Numerical models offer useful insight on relevant features of the exchange hydrodynamics,
613 although the accuracy of the size of the flows computed from their outputs must be considered
614 cautiously. Different factors affect the reliability of numerical models of the SoG, which have to
615 deal with an unusually high spatial and temporal variability and short-scale pronounced
616 bathymetric features. Tidal forcing must be explicitly included because the highly non-linear
617 dynamics caused by the strong flow-topography interaction produces a tidally-driven increase
618 of the long-term exchange (Bryden et al, 1994; García Lafuente et al., 2000; Sannino et al., 2004).
619 A good assessment of the effect of this topographic control on the water flow requires a precise
620 bathymetry of the model domain associated with a very high spatial resolution in both horizontal
621 and vertical directions. From a intercomparison modeling study, Sannino et al., (2014a) were
622 able to assess the minimum requirements needed by an ocean model to reproduce a reliable
623 hydraulic regime of the exchange through the SoG. The requirements suggested are: a minimum
624 horizontal resolution of 500 m and a minimum vertical resolution of about 10 meters. Moreover,
625 while the non-hydrostatic feature is crucial for the generation and propagation of the well-
626 known internal bore and associated large-amplitude internal waves, it is not strictly necessary
627 for simulating the hydraulic regime. Such a very high resolution demands expensive
628 computational systems, which finally provide global figures and spatial patterns that would be
629 impossible to infer from the limited pool of observations. For instance, they resolve the cross-
630 strait structure of the flow, a fact employed by Sánchez Román et al. (2009) and Sammartino et
631 al, (2015) to refine the outflow estimated from observations at ES using the vertical profiles of
632 velocity collected at a single point of the section.

633

634

635 Two hindcasts produced by the Massachusetts Institute of Technology general circulation model
636 (MITgcm) model adapted to the SoG domain (see inset in Figure 4) are now applied to estimate
637 heat and salt transports. Details about the model initialization and validation can be found in
638 Sanchez-Garrido et al. (2011, 2013) and Sammartino et al. (2014). The first hindcast covers the
639 period from March 12 to June 24, 2011, and the second one from September 1 to November 17,
640 2011.

641

642 Table 4 summarizes results from these hindcasts, which are discussed next. A first topic to deal
643 with is the change of the inflow and outflow from one section of the SoG to the other (columns
644 Q_A and Q_M), rising the question of which value is the best one, if any. The classical salt
645 ($Q_M S_M + Q_A S_A = 0$) and volume ($Q_A + Q_M = E$) conservation relationships, valid for steady state
646 exchange and often used to get estimations of the flows (see caption of Table 3), can be
647 combined to give $(S_M - S_A) \times Q_M = S_A \times E$. Since S_A and E are constants, the product $\Delta S \times Q_M$ ($\Delta S = S_M - S_A$)
648 must be constant too, a result pointed out by Bryden et al. (1994), who termed it Outflow Salinity
649 Transport (*OST*). They remarked the fact that a value of the outflow is not meaningful unless it
650 is accompanied by the salinity difference under which the exchange is computed.

651

652 In the SoG this subtlety minds because the entrainment that the active layer¹ exerts on the
653 passive layer increases the exchanged flows (García Lafuente et al., 2013) and diminishes their
654 averaged salinity difference with regards to what happens in Camarinal Sill (CS hereinafter). Last
655 column of Table 4 confirms that the *OST* is the same in all sections in both runs with an accuracy
656 greater than 2% ($OST = -1.81$ Sv PSU), which is not true for the outflow. The discussion above
657 also suggests that the reference flows should be those measured in CS because it is the section
658 of maximum salinity contrast, which implies that it is the section where the entrainment
659 influence is the least. And, therefore, it shall be the section with the minimum size of the
660 exchanged flows. This result is of practical interest for the numerical models that do not resolve
661 the SoG domain properly. Such models are computing flows that correspond to those at CS in
662 our discussion, as they do not resolve the entrainment. According to the results in Table 4, the
663 outflow at ES should be reduced by 12% to obtain the representative value at CS. This
664 percentage is greater than the 5% put forward by García Lafuente et al. (2011) based on near
665 bottom salinity observations at ES and CS. With a 12% reduction, the outflow at CS during the
666 period analyzed in Sammartino et al. (2015) should be -0.77 ± 0.03 Sv. The same considerations
667 apply to the inflow Q_A in Table 4, but not to the net flow, that must be constant throughout all
668 the sections of the SoG in each hindcast. Column Q_{net} in Table 4 suggests that, in fact, it is.

669
670

671 In the light of this discussion, the question then arises as to why the flows are not observed at
672 CS if it is the most representative location? The answer may be found in Table 5, which shows
673 the eddy-flux contribution to all the transports during hindcast II. Eddy fluxes have their origin
674 in the positive correlation between tidal currents and interface vertical oscillations. They
675 increase the long-term exchange (Bryden et al., 1994; Vargas et al., 2006; Sannino et al., 2004,
676 2007, 2015; Naranjo et al., 2014) and modify the way in which the exchange is achieved. The
677 eddy-fluxes contributions to the long-term volume, heat and salt transports depend on the
678 section, being maxima at CS where it represents between 35% and 40% of the total transport in
679 hindcast II (Table 5; similar outcome is produced in hindcast I -not shown), which agrees well
680 with the findings of Bryden et al., (1994). They are greatly reduced at the ending sections of the
681 SoG. Considering the difficulty to estimate eddy-fluxes from observed ADCP velocity profiles,
682 and that their estimations are affected by noticeable uncertainty, it is concluded that CS is not
683 well-suited to observe the outflow. ES gathers more appropriate conditions to this aim, whereas
684 the inflow is better monitored near the eastern exit of the SoG.

685

686 Figure 8 shows a fragment of the heat and salt transports produced by the numerical model and
687 helps to explain the large spreading of the observation-based transports displayed in Figure 7. It
688 confirms that the transports are fully dominated by the tidal variability, a result even more
689 evident in CS section (not shown), where the transports change sign periodically within each
690 layer due to the flooding of the hydraulic control. At ES, the transport within the Mediterranean
691 layer is always negative except for very short and sporadic moments, while the change of sign is
692 the rule for the Atlantic and, hence, the net transports.

693

¹ We shall refer to as *active* and *passive* the layers that flow faster and slower, respectively. West of Camarinal sill, the *active* and *passive* layers are the Mediterranean and Atlantic layers, respectively. The opposite happens to the east of Camarinal sill where the *active* layer is the Atlantic one.

694 The mean values of heat and salt transports in both hindcasts at the selected sections of the SoG
695 are shown in Table 4. An uncertainty has been ascribed to each mean, which has been estimated
696 as half the standard deviation of the subinertial time series, in agreement with the analysis
697 carried out in Sammartino et al. (2015)².

698

699 Within the uncertainty interval, the net salt transport ($QS_{net} = -1.5 \pm 6.5 \cdot 10^6 \text{ kg s}^{-1}$) is null. Actually,
700 it is slightly negative, suggesting a prevalence of the Mediterranean layer, but the mean of the
701 net transport is less than one order of magnitude the transport within each layer. It could also
702 have been the result of an enhanced negative barotropic fluctuation that affected the hindcast
703 periods. Whatever the cause, the assigned uncertainty, which is 3 to 7 times greater than the
704 mean, suggests that the salt transport is balanced or, if it is not, the numerical simulation cannot
705 give an accurate figure for the imbalance. In other words, the classical salt conservation
706 relationship ($Q_M S_M + Q_A S_A = 0$) would hold.

707

708 The net heat transport is towards the Mediterranean Sea with a mean value greater than the
709 associated uncertainty and almost identical numerical values of $\sim 11.5 \text{ TW}$ in hindcast I and ~ 10.5
710 TW in hindcast II in the three sections (Table 4). Dividing the heat transport by the area of the
711 Mediterranean Sea ($2.5 \cdot 10^{12} \text{ m}^2$), we obtain the equivalent heat flux through the Mediterranean
712 Sea surface required to balance the heat transport across the SoG. The resulting figures are 4.6
713 W m^{-2} and 4.2 W m^{-2} with a similar uncertainty of $\sim 4 \text{ W m}^{-2}$. They are in good agreement with
714 the only estimate carried out from the already mentioned direct temperature observations at
715 the SoG (Macdonald et al., 1994) and with reported values in the literature based on
716 Mediterranean Sea heat budgets (Bunker et al., 1982; Garrett et al., 1993).

717

718

719 **3.4 Perspectives**

720 Estimations of the size of the exchanged flows through the SoG and their uncertainty based on
721 observations require long-term monitoring stations such as the one currently running at the
722 westernmost section of ES. The quality and accuracy of the time series employed to this aim
723 would be improved by deploying, at least, a second twin monitoring station at a different site of
724 the section that allows for addressing explicitly the cross-strait structure of the velocity field and,
725 hence, for performing more robust computations of the flow. On the other hand, the peculiar
726 hydrodynamics of the region strongly suggests the selection of specific locations for deploying
727 the monitoring stations. Considering that eddy-fluxes are hard to estimate from observations,
728 the best places for monitoring the inflow and outflow are the eastern and westernmost
729 boundaries of the Strait, respectively, because the influence of the eddy-fluxes is minimized in
730 these sections. While the outflow is rather satisfactorily monitored by the single station

² The ascribed uncertainty should reflect the medium-to-long term variability of the transports, that is, the variability after removing short-term fluctuations, which are the tidal and meteorologically driven fluctuations. The length of the hindcasts is not enough to assess the uncertainty of the long-term scale, but it does allow for the satisfactory removal of tidal variability. Sammartino et al. (2015) shows that the medium-to-long term variability of the outflow is about half the variability of the subinertial series obtained after filtering out the tidal variability. This has been our criterion to assign the uncertainties to all variables in Table 4. Should we have taken the standard deviation of the original series, the uncertainty in, say, the heat transport through ES during hindcast I would have been 120.7 TW instead of 5.43 TW showed in Table 4. The first number is not a realistic long-term uncertainty at all.

731 currently deployed at ES, the inflow is not. Notice that, nowadays, the inflow estimations are
732 almost uniquely based on an indirect approach using the hydrological budget of the
733 Mediterranean, which is not well constrained, and the direct observations of the outflow (see
734 for instance Soto Navarro et al., 2010). Monitoring the inflow requires a good sampling of the
735 top tens of meters of the water column through which a considerable fraction of the inflow
736 occurs. Monitoring stations based on moored up-looking ADCPs miss most of this layer because
737 of the acoustic reflection at the sea surface. Stations based on down-looking ADCPs located at
738 the surface are unfeasible due to the heavy ship traffic. The development of High Frequency
739 Radar stations (HFR) that measure the surface currents open new possibilities for observing the
740 inflow, although the accuracy of HFR observations need to be further improved. A HFR network
741 installed by Puertos del Estado (Spain) in the eastern part of the SoG
742 (<http://www.puertos.es/en-us/oceanografia/Pages/portus.aspx>) is presently running and
743 providing surface velocity fields that can be suitably used, in combination with moored up-
744 looking ADCPs sampling the interior, to obtain long time series of the inflow. Recently Jordà et
745 al. (2016) have demonstrated that a reduced order optimal interpolation scheme is a feasible
746 approach to combine both sources of information and to get accurate estimates of the inflow.

747

748 While the new monitoring systems have obvious potential to improve the volume transport
749 estimates, the continuous sampling of temperature and salinity necessary to estimate heat and
750 salt transports at the same sections where velocity is observed poses challenges that are not
751 overcome yet. The approximately four-month interval sampling of the ES and easternmost
752 sections using a CTD probe equipped with a Lowered ADCP (LADCP) to measure velocity and the
753 properties of the water column simultaneously, which is accomplished routinely by the Spanish
754 Institute of Oceanography since the beginning of this decade, is a significant step forward, but
755 insufficient due to the strong contamination introduced by tides. Supra-tidal sampling interval
756 is required to filter out this noise. One possibility would be to install ADCP in the commercial
757 vessels that cross the Strait routinely. This would provide a large amount of information about
758 the structure of the velocity field and, after a proper filtering out of the tidal signal, an estimate
759 of the water transports. Concerning the hydrographic properties, the required information could
760 be obtained by deploying gliders programmed to sail across the Strait. Two important problems
761 must be envisaged: the heavy ship traffic and the noticeable currents that will probably drift the
762 glider away from the programmed track. An alternative solution that could partially overcome
763 those problems would be to deploy a moored profiler that could take vertical profiles of
764 temperature and salinity autonomously. This solution, however is not exempt of technical
765 difficulties either.

766

767 **4- Exchanges through the Dardanelles Strait**

768

769 **4.1 Overview**

770 The Turkish Straits System (TSS), located at the junction of the Asian and European continents,
771 provides a restricted connection between the large inland basins of the Mediterranean and
772 Black Seas (Figure 9). The Sea of Marmara (surface area 11,500 km²) connects the Aegean and
773 Black Seas through the Dardanelles (western limit, length 75 km, min. width 1.3 km) and
774 Bosphorus (eastern limit, length 35 km, min. width 0.7 km) Straits. Three elongated depressions

775 (max. depth ~1350 m) interconnected by sills (depth ~600 m) and adjoining continental shelves
776 of 40 and 10 km wide, respectively on the southern and northern sides, are found within the Sea
777 of Marmara. The entire TSS is two-layer stratified (Andersen and Carmack, 1984; Ünlüata et al.,
778 1990), with a sharp pycnocline at 25 m separating water masses of Black Sea and Mediterranean
779 Sea origin. The wind-mixed upper layer transits through the system as it responds to seasonal
780 changes, while the lower layer waters transported from the Aegean Sea (Beşiktepe et al., 1993,
781 1994, 2000), supply limited oxygen to the deep basins (Beşiktepe et al., 1993, 1994).

782 Besides the density (hence baroclinic pressure) differences between the two basins,
783 atmospheric pressure and wind effects in the adjacent basins create additional pressure
784 gradients that maintain the exchange through the Bosphorus (Özsoy et al., 1998). Turbulent
785 entrainment and interfacial mixing modify waters in transit through the two straits (Beşiktepe,
786 et al., 1993, 1994; Gregg and Özsoy, 1999, 2002; Gregg et al., 1999; Özsoy et al., 2001), with the
787 highest rates of change of upper layer salinity occurring in the southern Bosphorus and also in
788 the western part of the Dardanelles.

789 Current-meters and both ship-mounted and bottom mounted ADCP measurements in the
790 Bosphorus (Pektaş, 1953; De Filippi et al., 1986; Gregg and Özsoy, 1999; Çetin, 1999; IMS-METU,
791 1999; Özsoy et al., 1998, 2009; Gregg and Özsoy, 2002; Jarosz et al., 2011a,b, , Özsoy and Altıok,
792 2016; Tutsak, 2013; Tutsak et al., 2016; Özsoy et al., 2016c) and Dardanelles (Jarosz et al., 2012,
793 2013), as well as bottom pressure measurements at their junctions (Book et al., 2014) have
794 revealed many different time-scales of oscillations in the TSS, ranging from inertial, semi-diurnal,
795 diurnal to several days periods influenced by the adjacent basins (Yüce, 1993; IMS-METU, 1999;
796 Tutsak, 2013; Tutsak et al., 2016; Özsoy et al., 2016c). Tidal oscillations are exceptionally small,
797 on the order of ~10 cm in the TSS, especially east of the Nara Pass of Dardanelles. Basin
798 oscillations with periods of 2-5h have been observed in sea level records (Alpar and Yüce, 1998).
799 Coupled Helmholtz mode oscillations of the Black Sea and the TSS (e.g. Ducet et al., 1999) with
800 14.7d and 1.9d periods and a two-layer exchange adjustment time scale of 42d have been
801 estimated (Özsoy et al., 1998). The spectral analyses of current velocity measurements provided
802 by Jarosz et al. (2013) appear to support oscillations at those low frequencies.

803 The narrow geometry and topographical complexity of the straits support fast currents leading
804 to nonlinear processes of hydraulic controls and turbulence. With hydraulic controls operating
805 at a sill outside its Black Sea exit and a contraction and a sill in the southern part, the Bosphorus
806 is a good example of the maximal exchange regime (Farmer and Armi, 1986), operating in the
807 full range of weak to strong transient barotropic component. The Dardanelles Strait flow
808 appears to be in the submaximal regime, subject to a single hydraulic control at the mid-strait
809 contraction (Ünlüata et al., 1990).

810 **4.2. Observations**

811 CTD station data collected by the R/V BILIM of the IMS-METU has the highest rate of sampling
812 during the 1985-2001 when intensive studies were carried out at seasonal to annual repetition
813 periods in the TSS (Ünlüata et al., 1990; Latif et al., 1991; Özsoy et al., 1998) and has been
814 continued sporadically in many other scientific cruises since then. A most detailed joint
815 experiment in the Bosphorus and its Black Sea exit, covering also some turbulence and fine

816 structure measurements was carried out in 1994 (Gregg et al., 1999; Gregg and Özsoy, 1999,
817 2002, Özsoy et al., 2001). Detailed mapping of the Bosphorus currents and hydrography was
818 undertaken in 1998-1999, when ADCP and CTD measurements were extended to cover small
819 bays and bends (IMS-METU, 1999). Recent measurements have been acquired from automated
820 coastal meteorology, sea level and ADCP stations (<http://moma.ims.metu.edu.tr>) operated
821 under a coastal network (Özsoy et al., 2009, Tutsak, 2013, Tutsak et al., 2016). During this
822 experiment, a unique set of continuous current profiles were obtained at 15 min. intervals,
823 continued for several years (2008-2012) from a cabled bottom mounted ADCP system deployed
824 near the narrow southern section of the Bosphorus. The sea-level stations established in the
825 project have been operational since 2008. Unfortunately the ADCP measurements have been
826 concentrated mostly at the Bosphorus area and measurements other than CTD are relatively
827 rare and results based on existing data have not been sufficiently reported in the Dardanelles
828 Strait, except for the analyses reported in IMS-METU (1999). A bottom deployed ADCP was
829 placed in the Dardanelles Strait in 2008, though the measurements were terminated after the
830 cable had been pulled out and damaged by fishermen. Further detailed measurements were
831 obtained during the recent SESAME European project (2007-2008) and the following TÜBİTAK
832 research projects (Özsoy et al., 2015). Additionally, a remarkable experiment surveying the full
833 Turkish Straits System with multiplatform observations has been carried out during 2008-2009,
834 by the CMRE (Centre for Maritime Research and Experimentation, formerly NATO Undersea
835 Research Centre, NURC) in collaboration with the Turkish Office of Navigation, Hydrography and
836 Oceanography (SHOD) and the US Naval Research Laboratory (Jarosz et al, 2011a,b, 2012, 2013;
837 Chiggiato et al., 2012; Book et al., 2014; Gerin et al., 2013). As part of this experiment, a one-
838 year time series of bottom mounted ADCP in the straits allowed the computation of water fluxes.
839 These measurements (Jarosz et al., 2013) confirm the order of magnitude of the earlier
840 measurements and provide detailed characterization of the multiple scales of motion in the TSS.
841 A critical review of the past time-series measurements through the TSS can be found in Özsoy
842 and Altıok (2016a,b).

843 **4.3 Modelling results**

844 Although a summary of the modeling is beyond the present scope, it is worth mentioning the
845 grand challenge of predicting the TSS exchange currents and material fluxes that is being taken
846 in a number of steps, using models of increasing complexity. In terms of the complexity of its
847 dynamics and the observational and modeling challenges posed, the TSS is very similar to the
848 Strait of Gibraltar, and on many accounts even more challenging because of the hydrodynamic
849 coupling between three adjacent sea basins and two narrow straits. Advanced three-
850 dimensional modeling studies of the Bosphorus Strait (Sözer, 2013, Sözer and Özsoy, 2017)
851 based on ROMS, as well as curvilinear grid MITgcm (Sannino et al., 2017) and unstructured grid
852 FEOM (Gürses et al., 2016) models of the entire TSS have recently been used for solving the
853 circulation of the entire TSS through the use of high performance computation, thereby fully
854 resolving the current dynamics of the narrow Bosphorus and Dardanelles Straits. Modelling
855 results obtained so far on the structure of the currents and on the exchanged water fluxes
856 through the TSS confirm the ranges obtained in experimental measurements, and verify the
857 limits when either the upper or the lower layer gets blocked. It is also shown that the Marmara
858 Sea circulation and the exchange with the adjacent basins are sensitively determined by the
859 nonlinear, strongly stratified, turbulent dynamics of the exchange flows at the straits. These

860 results show the sensitivity of the response to the net flow through the TSS, as well as other
861 immediate and remote forcing factors, confirming the need for integrated modelling of the
862 entire TSS, with the Marmara Sea, the Dardanelles and Bosphorus Straits coupled together, in
863 order to account for, and eventually be able to fully understand the dynamical interactions and
864 exchange between the adjacent basins of the Mediterranean and Black Seas.

865

866 **4.4 Water fluxes**

867 In the Black Sea, the total freshwater input ($P=300 \text{ km}^3/\text{yr}$ and $R=350 \text{ km}^3/\text{yr}$) is twice as large as
868 the loss term ($E=350 \text{ km}^3/\text{yr}$) which means that the annual net water budget ($Q=P+R-E$) is
869 positive and results in a net flux towards the Mediterranean. Making use of an assumption of
870 steady state mass balance, and multi-year averages of salinity measurements at the junctions of
871 the straits, Ünlüata et al. (1990) have computed the annual average fluxes through the TSS from
872 a two-layer box model, updated later with a seasonal version provided by Tuğrul et al. (2002)
873 and Beşiktepe (2003). An updated description is provided here based on the review given in
874 Schroeder et al. (2012).

875 The annual two-layer volume fluxes of the TSS are shown in Figure 10a. The exchange through
876 the TSS increases in the spring-early summer, and weakens markedly in autumn (within a margin
877 of about ~40% of the annual mean) in response to the freshwater input to the Black Sea (Tuğrul
878 et al., 2002). The input into the Marmara Sea by the upper layer flow of the Bosphorus is
879 estimated as $657 \text{ km}^3/\text{yr}$ and the outflow into the Black Sea in the lower layer is estimated as
880 $318 \text{ km}^3/\text{yr}$ (Figure 10a) based on the measurements during the years 1985-1995 (Tuğrul et al.
881 2002). The input into the Aegean Sea by the upper layer flow of the Dardanelles was found to
882 be $1331 \text{ km}^3/\text{yr}$ and the outflow into the Marmara Sea in the lower layer was $1010 \text{ km}^3/\text{yr}$ in the
883 same period (Tuğrul et al. 2002). The net flow at both sections is then $321 \text{ km}^3/\text{yr}$ which, if
884 divided by the area of the Mediterranean Sea ($2.5 \times 10^{12} \text{ m}^2$) results in an equivalent contribution
885 to the Mediterranean budget of $128 \text{ mm}/\text{yr}$.

886 Bosphorus fluxes computed from ADCP data (Özsoy et al., 1998) show the same seasonal
887 behaviour as reviewed above, but reveal maxima of about $Q_1 = 1600 \text{ km}^3/\text{yr}$ and $Q_2 = 630 \text{ km}^3/\text{yr}$
888 for the upper and lower layers respectively, including blocked cases, indicating instantaneous
889 fluxes 2-3 times larger than the annual mean. Despite large scatter in data due to sampling,
890 overall average values of $Q_1 = 537 \text{ km}^3/\text{yr}$ and $Q_2 = 112 \text{ km}^3/\text{yr}$ were computed, thus leading to
891 a net average value of $425 \text{ km}^3/\text{yr}$ ($170 \text{ mm}/\text{yr}$ of equivalent sea level change in the
892 Mediterranean Sea). It has to be noted that the lower layer flux Q_2 is possibly underestimated
893 as a result of data loss near the bottom, which implies net transport to be overestimated.

894 Based on two layer (1D) modeling results, Oğuz et al. (1990) concluded that the upper or lower
895 layer flows would be blocked when the net flux exceeds $-580 \text{ km}^3/\text{yr}$ or $800 \text{ km}^3/\text{yr}$, in respective
896 directions. The different sources of data and model results in Figure 11 reveal $-630 \text{ km}^3/\text{yr}$ and
897 $950 \text{ km}^3/\text{yr}$ respectively as the approximated limiting values beyond which either the lower or
898 the upper layer are expected to be blocked. Figure 11 compares various sets of observations
899 (Merz and Möller, 1928; Özsoy et al., 1998) and results from two different models (Sözer, 2013;
900 Sözer and Özsoy, 2017; Sannino et al., 2017), establishing the relative upper and lower layer
901 exchange fluxes as a function of the net flux imposed on the Bosphorus Strait. Although the

902 fluxes reported in Figure 11 are for the Bosphorus Strait rather than the Dardanelles, they
903 indicate the range of fluxes expected and the net flux Q_1-Q_2 is of course the same between the
904 two Straits assuming that volume in the Marmara Sea does not change significantly at long time
905 scales.

906 Indirect estimates of the net transport through the Bosphorus (i.e. equivalently through the
907 Dardanelles) based on long-term water fluxes and sea-level variations in the Black Sea (Stanev
908 and Peneva, 2002) indicate seasonal anomalies (Figure 10b), with variations of the order of ~75%
909 of the mean, that is considerably larger than the ~40 % estimated by Tuğrul et al. (2002) from
910 the seasonal based mass budget. These differences arise from data uncertainties as well as
911 differences in the averaging (monthly versus seasonal) applied to the data. However, both
912 methods yield the same general pattern of seasonal variability.

913 Jarosz et al. (2012, 2013), based on ADCP data gathered during 12 months in 2008-2009 in both
914 ends of the Dardanelles, have found that the input into the Aegean Sea by the upper layer flow
915 of the Dardanelles was 1157 km³/yr and the outflow into the Marmara Sea in the lower layer
916 was 999 km³/yr, the net flux therefore amounting to 158 km³/yr (63 mm/yr of equivalent
917 Mediterranean sea level change). Figure 12 shows the fluxes collected in 2008/2009 at the
918 southern section of the Dardanelles Strait and it is worth remarking the large variability observed
919 in the flows. The volume fluxes exchanged between the Aegean and Marmara Seas via
920 Dardanelles Strait are subject to a wide range of oscillations that are especially amplified in
921 winter months and often two times larger than the mean fluxes (Jarosz et al. 2013). It is also
922 observed that the net barotropic fluxes are even of greater amplitude and oscillate about a
923 much smaller mean value. The minimum and maximum values of the upper layer flux
924 respectively were -2593 and 149 km³/yr during the measurement period. For the lower layer
925 the extremes were -434 and 3375 km³/yr, and for the net fluxes one finds -2368 and 3513 km³/yr
926 for the respective minimum and maximum values.

927 Concerning the uncertainties in the estimates of the net water fluxes (reviewed by Özsoy and
928 Altıok, 2016), up to our knowledge there are no accurate estimates of them yet. The
929 retrospective evaluations of long-term average fluxes should take into account the instrumental
930 accuracy, the uncertainties in the estimates of the fluxes from limited observations and the
931 influence of inter-annual variations. Therefore, up to now only the comparison among different
932 published estimates (see Table 6) can be used as a rough approximation of the uncertainty. By
933 doing this, the net water flux is 275 + 59 km³/yr towards the Mediterranean (or 110 + 24 mm/yr
934 in equivalent sea level change in the Mediterranean Sea).

935 **4.5 Heat and salt fluxes**

936 To our knowledge there are no published estimates of the heat and salt fluxes through the
937 Dardanelles Strait. In order to get a first estimate of those fluxes we do a simple computation
938 using published values for the temperature and salinity of the upper and lower layers. In
939 particular, we estimate the net heat flux as $(Q_1 \cdot T_1 + Q_2 \cdot T_2)$ and analogously the net salt flux as
940 $(Q_1 \cdot S_1 + Q_2 \cdot S_2)$, where subindex 1 and 2 represent the upper and lower layer, respectively. For the
941 temperature and salinity we use $T_1=14^\circ\text{C}$, $T_2=16^\circ\text{C}$, $S_1=35$ psu and $S_2=39$ psu, similar to the values
942 observed in the Dardanelles (e.g. Jarosz et al. 2013). Then, in order to take into account the time
943 variability in the water fluxes and the uncertainty in those estimates we assume a random error

944 of $200 \text{ km}^3/\text{yr}$ for Q_1 and Q_2 , which is based on the std of observed fluxes by Jarosz et al. (2013)
945 and the spread among estimates shown in Table 6. Similarly we consider an uncertainty of 2°C
946 for the temperature and 2 psu for the salinity, although sensitivity tests have shown that
947 uncertainties in the temperature and salinity have a second order importance in front of the
948 uncertainties in the water fluxes. The estimated inflow, outflow and net heat fluxes are $0.90 \pm$
949 0.15 W/m^2 , $-0.80 \pm 0.17 \text{ W/m}^2$ and $0.10 \pm 0.16 \text{ W/m}^2$, respectively (here positive indicates
950 towards the Mediterranean). The estimated inflow, outflow and net salt fluxes are 1.35 ± 0.20
951 10^6 kg/s , $-1.18 \pm 0.22 10^6 \text{ kg/s}$ and $0.20 \pm 0.22 10^6 \text{ kg/s}$, respectively.

952

953 **4.6 Perspectives**

954 At present there are no monitoring systems that can provide continuous estimates of the fluxes
955 through the Dardanelles Strait. However, previous studies have shown that this is technically
956 feasible. A monitoring system similar to the observational system used by Jarosz et al. (2013)
957 could allow an accurate estimate of the water fluxes in the Dardanelles Strait. That system
958 should be complemented with routine measurements of temperature and salinity profiles at
959 least on the limits of the Strait in order to compute heat and salt fluxes. However, up to our
960 knowledge there are no plans to implement and maintain such system. A complement to the
961 observational approach would be the operational implementation of numerical models fully
962 resolving the dynamical and mass balances of the adjacent basins and straits (i.e. similar to those
963 presented above). Those models could be calibrated and/or validated using a more limited set
964 of observations (i.e. from short term monitoring periods) and then provide continuous estimates
965 of the heat and mass fluxes into the Mediterranean.

966

967

968 **5- Riverine input**

969 **5.1 - Overview**

970 The rivers carry to the sea the residual of precipitation and evaporation over the entire
971 continental catchment of the Mediterranean Sea. This area covers about $7.9 10^6 \text{ km}^2$, or three
972 times the area of the sea itself and goes from tropical Africa up to Russia. This area is drained by
973 some of the largest rivers of the world, like the Nile ($2.9 10^6 \text{ km}^2$) or the Danube ($0.8 10^6 \text{ km}^2$).
974 Large parts of this drainage basin are located in arid areas (northern Africa), thus leading to
975 relatively low net rainfall (precipitation minus evaporation) and river discharge. The
976 Mediterranean catchment is also strongly populated and men since millennia have regulated
977 the flow of water in order to make the best usage of it. Today, most of the Mediterranean
978 countries practice an irrigated agriculture which essentially takes water from rivers in order to
979 enhance evaporation and crop productivity. In the countries on the southern shores more than
980 80% of the net rainfall is used for irrigation (Margat 2008). It is thus a process which cannot be
981 ignored when quantifying the riverine input.

982

983 **5.2 - The reliability of observational based estimates**

984 The largest rivers are being gauged by national agencies but such data is not always publicly
985 available or reliable. The societal importance of the water flux available in the rivers also makes
986 this information sensitive from an economical or geopolitical point of view. Therefore the data
987 is not always made available or only after having been treated to remove the impact of some

988 agronomic or industrial activities. Thus many of the data publicly available are either outdated
989 or with incomplete information on possible treatments applied to remove the impact of water
990 usage. Obviously taking into account the contribution of un-gauged rivers is even more difficult.
991 Especially in semi-arid regions where overland flows are the prime source of water for irrigation.
992 Concerning the data reliability, on the one hand a gauging station has to be as close as possible
993 to the mouth of the river in order to be as much representative as possible of the entire
994 catchment, but on the other hand it has to be unaffected by estuarine processes and thus free
995 of saline intrusions or tidal effects. A further complication to the observational based estimates
996 is that many large rivers in the Mediterranean region form a delta. Observing the river discharge
997 upstream the delta neglects the strong evaporation on such fertile grounds, which are often the
998 heartland of agricultural activities and thus of human water usage.

999
1000

1001 The World Meteorological Organization (WMO) sponsored Global Runoff Data Centre (GRDC)
1002 has assembled river discharge data from most basin agencies around the world and thus offers
1003 today the most complete data set. But this data comes without indication on the quality of the
1004 observations. It is unknown to which precision the basin agency has monitored the transect of
1005 the river or which assumptions were used in the velocity measurements. Nevertheless, GRDC
1006 data can be the basis for an observational derived freshwater input into the Mediterranean. This
1007 effort has been undertaken at CEFREM (Centre de Formation et de Recherche sur les
1008 Environnements Méditerranéens) by identifying for each coastal point on a regular latitude
1009 longitude grid the available data and computing an estimate of the annual mean influx (Ludwig
1010 et al. 2009). As the last station on the river before its mouth can be before the confluence of
1011 other tributaries, some corrections are applied to add the flux which has not been observed. In
1012 the CEFREM data set only about 63% of the total flux is based on observations. For coastal points
1013 where un-gauged rivers end, the authors have applied a simple annual water balance model
1014 which assumes that the total annual rainfall over the basin minus an estimate for average
1015 evaporation yields the flux into the ocean. The limitation to annual mean fluxes is justified by
1016 the fact that human regulation of rivers mostly affects the seasonal cycle of discharge. The
1017 CEFREM is available in 2 versions which differ by the resolution at which they have been
1018 established and the period they have covered. In both versions the same methodology is used
1019 but different atmospheric data are considered for the water balance model.

1020

1021 The riverine input estimate by CEFREM is currently the best observational based product
1022 available. It estimates that the total freshwater influx is 780 km³/yr for the Mediterranean and
1023 Black seas over the period 1960-1969 and 710 km³/yr for the period 1991-2000 (Both averages
1024 are computed with version 1 of the data, see Figure 13). A reduction is also found when the total
1025 discharge is separated in different subbasins. For the period 1960-1969 the discharge in the
1026 western Mediterranean, the eastern Mediterranean and the Black Sea are 137, 253 and 390
1027 km³/yr, respectively. For the period 1991-2000 the values are 115, 213 and 382 km³/yr,
1028 respectively. This reduction is attributed by the authors to changes in the climate forcing using
1029 a simple precipitation/runoff model. The CEFREM products inherit the uncertainties inherent to
1030 the observed discharge discussed above and which cannot be quantified because of the lack of
1031 meta-information on observational methods or the post-processing applied to remove the

1032 human influence. It is also limited by the simple runoff model used for un-gauged basins and the
1033 fact that only annual mean values are proposed.

1034

1035 **5.3 - The case of the Nile**

1036 To illustrate the complexity of the human management of the rivers it is interesting to examine
1037 in more detail the case of the Nile. This river has the third largest drainage area in the world but
1038 has probably always contributed less fresh water to the Mediterranean than the Danube. Over
1039 the last centuries a number of dams have been built to regulate its flow, produce hydro-power
1040 and develop irrigation based agriculture. In its lower basin the first major dam to be built was
1041 the lower Aswan dam which was filled in 1902. The Aswan gauging station reports a mean annual
1042 discharge of 112 km³/yr over the 1871-1900 period (Vörösmarty et al. 1998). The same station
1043 reports for the period 1903-1960 an annual mean value of 88km³/yr indicating a reduction of
1044 the water carried by the river. In 1976 the high Aswan dam reached its capacity and the
1045 downstream station reported for the final period over which data is available (1976-1984) an
1046 average discharge of 59km³/yr.

1047

1048 But the abstractions of water are not limited to the dams built upstream of the city of Aswan.
1049 Vörösmarty et al (1998) and GRDC report data for the 1976-1984 period at a station just before
1050 the delta (El Ekhsase) and which displays an average flow of 40km³/yr. Obviously a significant
1051 fraction of the water observed in El Ekhsase will evaporate within the delta or reach the sea via
1052 canals, drains or groundwater. Nixon (2003) estimates that in 1984, 14 km³/yr reached the sea.

1053

1054 Since the high Aswan dam was filled, agriculture and other water usages have increased in Egypt.
1055 Based on the reported discharge at the Aswan station, the infrastructure could have made
1056 available for Egypt's development 29km³/yr (difference between the 1903-1960 and 1976-1984
1057 periods) which are carried north through a network of channels. If this water had been
1058 evaporated over the area of Lake Nasser (5000 km²) and the irrigated surfaces in Egypt (3 10⁴
1059 km² FAO 2005) this would have meant an increase of 2.27 mm/d of the flux to the atmosphere.
1060 Considering that maximal evaporation of crops in similar climates are rarely above 6mm/d
1061 during the growing season (Duchemin et al. 2008, Garatuza-Payan et al. 1998), this seems to be
1062 a unrealistic increase of annual mean evaporation following the construction of the Aswan high
1063 dam and hints to the fact that a large part of the water lost on the way to the sea could have
1064 infiltrated into the soils. This water would then flow to the Mediterranean after passing through
1065 the aquifers.

1066

1067 This discussion of the Nile river suggests that probably a significant fraction of the water entering
1068 Egypt still reaches the sea but it is not accounted for by the gauging station as it flow to the
1069 ocean through canals, drains and aquifers. Smaller arid basins of the Mediterranean will
1070 probably pose similar observational problems but at smaller scale.

1071

1072 We propose here to quantify the annual mean riverine input into the Mediterranean basin based
1073 on the CEFREM data as it is based, for a large part, on observed discharges. In particular we use
1074 the average of the V1 and V2 products which differs in the period spanned, the spatial resolution
1075 and the atmospheric forcing used to infer the discharge of un-gauged rivers. The observed
1076 discharge in monitored basins is the same in both version of the product. The average discharge

1077 for the period 1960-2010 we obtain is 767 km³/yr, which can be split in 125, 250 and 392 km³/yr
1078 for the western Mediterranean, eastern Mediterranean and Black Sea. As the direct uncertainty
1079 cannot be estimated it is suggested to use the uncertainty from the ORCHIDEE model as a
1080 surrogate (see next section). It has to be reminded that a significant fraction of the freshwater
1081 inflow in the CEFREM data is based on a simple water balance model because of a lack of
1082 hydrological data. Based on this hypothesis we obtain an uncertainty of 107km³/yr for the entire
1083 basin. It is important to note that this assumed error of 14% hides a very contrasted picture. In
1084 the basins where the hydro-meteorological data are reliable, ORCHIDEE simulates correctly the
1085 major rivers and the error can be as small as 10%. In contrast for Mediterranean sub-basins
1086 affected by irrigation and poor observational networks, the errors can be in excess of 100%.

1087

1088 **5.4 - Modelling riverine inputs**

1089 Riverine input can also be obtained through global hydrological models. Their objective is to
1090 simulate the continental water cycle under given atmospheric conditions by representing in as
1091 much detail as possible the transfer of water and its usage. These models are often validated
1092 and calibrated on observed discharge and thus can be considered as the most reliable
1093 predictions of river flows. One such model is WaterGAP3 (Döll et al. 2003) which has been used
1094 to study in detail the water cycle of the Mediterranean basin (aus der Beek et al. 2012). It is able
1095 to predict, at a daily time step, realistic discharge values for most rivers and provide an estimate
1096 of the water withdrawals for irrigation. WaterGAP3 predicts a riverine input into the
1097 Mediterranean (including the Black sea) of 924 km³/yr for the period 2002-2009.

1098

1099 Alternatively, forcing a state of the art land surface model (LSM) with bias corrected atmospheric
1100 conditions allows also to produce estimates of the freshwater inflow into the Mediterranean.
1101 The LSMs have been developed to represent continental processes in climate models and
1102 include complex parameterizations for plant and bare soil evaporation as well as for hydrological
1103 processes and simulate the water and energy exchange at a sub-diurnal time step. In some cases
1104 they have even introduced representations for irrigation and floodplains in order to estimate
1105 water taken from the streams to sustain or augment the evaporation of crops and wetlands.
1106 One such model is ORCHIDEE developed at the Institut Pierre Simon Laplace (IPSL). It has been
1107 validated over a number of catchments of the world, and most recently over the Amazon basin
1108 (Guimberteau et al. 2012). Using the WATCH atmospheric forcing data bases (WFD and WFDEI)
1109 (Weedon et al. 2011, Weedon et al. 2014), the total fresh water flowing into the Mediterranean
1110 can be estimated with ORCHIDEE. Such an exercise is presented in Figure 13 where the
1111 simulations with different atmospheric forcings are compared to the estimates of CEFREM. It
1112 has to be noted that the model reproduces well the observed inter-annual variability of the
1113 riverine input and the uncertainty in the forcing introduces errors which are similar to the
1114 difference between the two versions of the CEFREM product.

1115

1116 These integrated numbers over the entire basin hide a number of large discrepancies. This can
1117 be well illustrated again with the case of the Nile. WaterGAP3 and ORCHIDEE produce discharges
1118 of over 300 km³/yr which is well above the values observed at Aswan before the dams or the
1119 modern irrigation infrastructure of Egypt were installed. This can be explained by the limited
1120 capacity of the models to represent the floodplains of the upper Nile, the lack of regulation by
1121 the Nalubaale Dam at the outflow of Lac Victoria and not the least the poor atmospheric forcing

1122 over the tropical part of the basin. More generally, ORCHIDEE overestimates the inflow into the
1123 ocean of arid basins and thus underestimates the continental evaporation there. Certainly the
1124 irrigation parameterization of ORCHIDEE is too simple (de Rosnay et al. 2003) but one may also
1125 wonder if the observations represent correctly the water cycle in these basins which are not
1126 often not well monitored.

1127

1128 **5.5 - Heat flux contribution of rivers**

1129 To our knowledge there is no database of temperatures for streams flowing into the
1130 Mediterranean. This is generally a topic which is lacking attention for the research community,
1131 probably because of the complexity of the processes involved. We are not aware either of efforts
1132 under way to include this parameter in land surface models or global hydrological models. Some
1133 isolated effort have been undertaken, as for instance by Beaufort et al. (2015) for the Loire, but
1134 a generalization to all water flows on continents is desperately lacking.

1135

1136 A first approximation for the total contribution of rivers to the heat budget can be derived
1137 assuming that the temperature of the river waters is similar to the temperature in the sea. For
1138 each river considered by ORCHIDEE we obtain the closest sea surface temperature from the SST
1139 product of Marullo et al. (2007). Then, we estimate the heat flux for each river and do the
1140 integration for the whole basin. In order to take into account the different sources of uncertainty
1141 in this estimate we first consider that the temperature in the river can be $\pm 5^{\circ}\text{C}$ the sea
1142 temperature. Then, we also assume that the uncertainty in the river flow is a 15% of the total
1143 value (section 5.3). The result of this estimate show a marked seasonal cycle (see Figure 14) with
1144 a maximum in November ($1.1 \pm 0.2 \text{ W/m}^2$) and a broad minimum from May to July ($\sim 0.3 \pm 0.1$
1145 W/m^2). This annual minimum is relatively constant along time, while the annual maximum shows
1146 significant variability ranging from 1 to 2 W/m^2 . The long term annual average of the heat
1147 contribution from the rivers is $0.6 \pm 0.4 \text{ W/m}^2$.

1148

1149 **5.6 - Perspectives**

1150 In view of the difficulty of accessing discharge data close to mouth of the rivers flowing into the
1151 Mediterranean and knowing how much of the total flux they actually capture, the
1152 observationally based approach will always be affected by large uncertainties. Models are
1153 plagued by large errors today, but they offer a good potential for improvements. The quality of
1154 their atmospheric forcing will certainly improve. Developments will enhance their ability to
1155 represent irrigated areas and floodplains as well as groundwater processes. With irrigation
1156 playing such an important role in arid basins, reducing the uncertainty in the manmade
1157 enhancement of evaporation will be key in refining our estimate of the riverine inputs.
1158 Furthermore satellite information can be used to validate lake levels, irrigated areas or the total
1159 continental water storage. Also, observed discharges throughout the basin can be used to verify
1160 the models or correct the predictions with assimilation methods. Finally, the temperature of the
1161 river waters should be measured, at least in the largest rivers, in order to estimate the heat flux
1162 associated to the river runoff. Once that data will be available it could be compared to sea
1163 surface data from satellite observations to identify up to which extent the sea temperature can
1164 be used as a proxy for the river temperature.

1165

1166

1167 **6 - The Mediterranean Sea heat and mass content**

1168

1169 **6.1 - Overview**

1170 Direct estimates of the Mediterranean heat and salt contents can only be obtained from in-situ
1171 measurements of temperature and salinity, respectively. Those measurements represent a
1172 discrete set of observations with typically large gaps in the spatial and/or the temporal coverage.
1173 Thus, the in-situ observations have to be averaged using more or less sophisticated approaches
1174 in order to produce basin or sub-basin integrated quantities. Therefore, the accuracy of the heat
1175 and salt content estimates will depend not only on the accuracy of the measurements but
1176 especially on their spatial and temporal distribution as well as on the properties and the tuning
1177 of the algorithm used to integrate those measurements. For instance, Vargas-Yáñez et al, (2009)
1178 have shown that the method used to define anomalies (e.g. removing a monthly or a yearly
1179 climatology) can lead to large differences in the estimates of the western Mediterranean
1180 temperature and salinity trends (i.e. more than 50% depending on the method used). Also,
1181 Vargas-Yáñez et al. (2012) have shown that computing trends from an interpolated product
1182 instead of using the raw profiles can also lead to large discrepancies (e.g. from non significant
1183 trends for the upper layer temperature in the western Mediterranean to a significant trend of
1184 0.02°C/yr, respectively).

1185

1186 The water mass content has to be estimated indirectly since it cannot be directly measured. In
1187 order to better understand the links between the changes in the volume and mass of the basin
1188 we present first some basic concepts. For a water column of area A , a change in the sea surface
1189 elevation (η) can be due to changes in the density of the water column (ρ ; steric component)
1190 and/or to changes in the mass of the water column (m):

$$\Delta \eta = \frac{1}{\rho_0} \Delta \rho + \frac{1}{\rho_0} \Delta m \tag{7}$$

1191 Assuming a simple linear approach for the (temporal and spatial) changes of density with
1192 temperature and salinity — we get:

$$\Delta \rho = \alpha \Delta T + \beta \Delta S \tag{8}$$

1193 where α and β are the thermal expansion and haline contraction coefficients, respectively.
1194 Equation (8) expresses that changes in the volume of the water column can be associated to
1195 changes in the thermal content (thermosteric), the salt content (halosteric), the mass content
1196 of salt and the mass content of water. It is important to highlight that any change in the salinity
1197 of the water column implies a change in the salt content. For more details on these concepts
1198 and the implications for the Mediterranean basin the reader is referred to Jordà and Gomis
1199 (2013).
1200

1201 Concerning the quantification of the changes in the water mass content, on one hand
1202 gravimetric observations (as those provided by the Gravity Recovery and Climate Experiment or
1203 GRACE mission) provide a measure of the changes in the total mass. However, it has to be noted
1204 that this includes both changes in the water content and in the salt content (last two terms in
1205 (8)). I.e.: GRACE cannot distinguish if the mass change is due to a salinification of the basin or to
1206 an increase in the amount of water. Therefore, a complementary estimate of the changes in the
1207 salt content (e.g. from the in-situ observations mentioned above) has to be provided in order to
1208 deduce the changes in the water mass content. On the other hand, observations of sea level (i.e.
1209 from altimetry or tide gauges), can be used to measure changes in the total volume of water in
1210 the basin (the left hand side term in (8)). In this case, though, it has to be noted that changes in
1211 the volume may be due to an expansion/contraction of the water column without necessarily
1212 implying a change in the water mass content. Therefore, the thermosteric component, the
1213 halosteric component and the changes in the salt content of the basin have to be estimated with
1214 complementary datasets.

1215

1216 In the following we summarize the different types of temperature and salinity observations that
1217 are currently available for the Mediterranean, the choices that are typically used to integrate
1218 those observations to compute the heat and salt content, the different methods to estimate the
1219 water content changes and, finally, we discuss the contribution of numerical modelling.

1220

1221 ***6.2 – In situ observations of temperature and salinity in the water column***

1222

1223 Since the first decades of the XXth century different kinds of instruments were available to
1224 measure temperature and salinity of the water column. The first measurements were obtained
1225 with Nansen bottles which were equipped with reversing thermometers. This system provided
1226 observations of temperature and salinity at a limited number of vertical levels and a non-
1227 negligible uncertainty existed in the estimate of the depth at which the measurements were
1228 obtained. Also, the Mechanical BathyThermograph (MBT) was widely used until the end of the
1229 70's. The MBT provided profiles of temperature vs depth for the upper part of the water column.
1230 Its accuracy was low ($\sim 0.05^{\circ}\text{C}$) and recently a bias in the MBT data has been identified which can
1231 induce an error of up to $0.2\text{-}0.4^{\circ}\text{C}$ (Gouretski and Koltermann, 2007). MBT was substituted by
1232 the expandable BathyTermograph (XBT) which is still used in different applications. The XBT
1233 provides profiles of temperature vs. depth down to large depths but its accuracy is low ($\sim 0.05\text{-}$
1234 0.1°C) and also suffer from biases in the determination of the depth, which translate into errors
1235 of up to $0.2\text{-}0.4^{\circ}\text{C}$. In this case, however, there is less consensus about how to correct those
1236 biases on the historical data (Cowley et al., 2013). Most MBT/XBT data can be found in the
1237 databases although usually uncorrected. However, it is worth noting that Vargas-Yáñez et al.
1238 (2010) have shown that including or not MBT/XBT data in heat content estimates of the western
1239 Mediterranean does not significantly change the results.

1240

1241 Also since the early '70s, oceanographic vessels used to collect temperature and salinity data
1242 from surface waters underway (thermosalinometers). This procedure has been extended to
1243 "ships of opportunity" (SOOP) such as ferries or liners that cover a repeated route across the
1244 Mediterranean (e.g. MedGOOS).

1245

1246 At the end of the 70s, when CTD (Conductivity, Temperature and Depth) instruments reached a
1247 reasonable accuracy, they started to be widely used everywhere, including the Mediterranean.
1248 CTDs provide a continuous vertical profile of temperature and conductivity (which is converted
1249 into salinity) at a given station, from the surface to the bottom. Up to now, it is agreed that CTDs
1250 provide the most accurate measurements of temperature and salinity (accuracy of 0.001°C and
1251 0.001 psu, respectively). Generally both salinity and conductivity sensors are calibrated on a
1252 regular basis and the measurements are checked on board with reversing thermometers and
1253 with water samples that are analyzed directly with a salinometer. Ship-based hydrography
1254 represents the only method for obtaining high vertical resolution measurements over the whole
1255 water column. Presently the Mediterranean Argo network (described below) samples only the
1256 upper 2000 m of the sea. If one considers that 20% of the Mediterranean volume lies below
1257 2000 m, where significant changes have been recently observed, it appears clear that ship-based
1258 full-depth CTD data become essential to reduce uncertainties in freshwater, heat and sea level
1259 budgets and to assess the long-term steric contribution to Mediterranean sea level (Schroeder
1260 et al., 2015). In addition, ship-based hydrographic measurements provide a standard for
1261 validating new autonomous sensors and a reference data set for other observing systems such
1262 as Argo profiling floats, expendable bathythermographs, and gliders. However, even if there is
1263 a large amount of CTD data available in the international databases, there is still a non-negligible
1264 fraction of the total dataset acquired that is only available upon request submitted to the
1265 responsible institutions.

1266

1267 Since the turn of the century, profiling floats have been deployed in the Mediterranean as part
1268 of the international Argo program (Poulain et al., 2007) to measure profiles of temperature and
1269 salinity at intervals of 5 or 10 days, between the surface and maximal depths of 2000 dbar.
1270 Nearly 30,000 profiles have been collected throughout the Mediterranean basin between 2001
1271 and 2015. The number of floats operating simultaneously has reached a maximum of about 80
1272 in mid-2015 and future deployments aim at maintaining an active Argo fleet of 60-70 floats in
1273 the Mediterranean Sea. The Argo data are accurate ($\pm 0.002^\circ\text{C}$, ± 0.002 psu, ± 2 dbar for
1274 temperature, salinity and pressure respectively, for SBE 41 CP model) and although the pumped
1275 measurements are not as reliable in the upper 5 m it provides a reasonably well distributed
1276 coverage reaching regions which are traditionally not surveyed by oceanographic campaigns.
1277 Also, the Argo data are centralized and subject to homogeneous quality checks. However, it is
1278 worth noting that the calibration of the instrument remains a very sensitive issue. More
1279 information on the Mediterranean Argo float data can be obtained at the Coriolis data center
1280 and the Mediterranean Regional Argo Center (<http://nettuno.ogs.trieste.it/sire/medargo/>).

1281

1282

1283 During the first decade of the XXI century several autonomous underwater vehicles (gliders)
1284 have started to be operated in the Mediterranean. These vehicles allow to obtain a very spatially
1285 dense set of quasi-vertical profiles with reasonably good accuracy (0.004°C and 0.01 psu for
1286 temperature and conductivity respectively, for the GPCTD model). Also for these platforms,
1287 calibration is an important issue, along with problems related to the fact that not all CTDs
1288 mounted on gliders are pumped (which leads to a systematic salinity offset between descending
1289 and ascending profiles). The glider data are quite unified in the databases and efforts are being
1290 devoted to homogenize the quality control applied to the data. Additionally it has to be

1291 mentioned that the very large contribution of the gliders during the last years can be misleading
1292 (see Figure 15): glider data can be redundant because profiles can be very close to each other,
1293 hundreds of meters apart. Concerning the salinity measured by the gliders it has to be
1294 mentioned that both are affected by the thermal lag problem (Garau et al., 2011), which causes
1295 that the conductivity observations can be inaccurate when the instrument crosses a strong
1296 vertical temperature gradient. This kind of problem has been extensively studied and corrected
1297 for the standard ship-based CTDs in the past. Lueck and Picklo (1990) have proposed a numerical
1298 model of the thermal inertia of the Sea-Bird conductivity cells. Analyzing temperature-salinity
1299 diagrams, Morison et al. (1994) have estimated the correction to be applied to the thermal lag
1300 error. However the Sea-Bird CTD probes installed on gliders do have additional problems that
1301 make it difficult to apply the traditional corrections. In particular, (i) they are not always pumped,
1302 so the water flux velocity within the sensors depends on the glider velocity, and (ii) the sampling
1303 frequency on gliders is reduced compared to ship-based CTD casts (0.5 Hz vs 24 Hz). Garau et al.
1304 (2011) have therefore proposed a new method for the thermal lag correction for unpumped
1305 CTDs on gliders, which takes into account the variable velocity of the instrument itself.

1306

1307

1308 Finally, it is worth mentioning that continuous time series of temperature and salinity at given
1309 depths have been obtained using moored instruments (see for instance the CIESM
1310 HydroChanges Programme, Schroeder et al., 2013). The accuracy of the temperature
1311 measurements can be as good as those of the CTD (at least the more recent ones), while the
1312 accuracy of the salinity measurements is lower (~ 0.01 psu). Also, in certain areas and depths,
1313 biofouling may be a critical issue in the stability of the sensor response with time. The temporal
1314 resolution of these data is generally very high, but the drawback of the mooring data is the
1315 discrete coverage in depth and that often present temporal discontinuities, either due to
1316 malfunctioning of the instruments or to discontinuities in the monitoring program. Also, it is
1317 possible to have drifts in the salinity measurements that should be corrected. Conversely, its
1318 very good temporal coverage (typical temporal resolution is 1 hour at least) allows to filter out
1319 the high frequency signals that can contaminate the climate signals. An additional problem of
1320 the mooring data is that they are not unified in the databases and most of the data have not
1321 been delivered to them.

1322

1323 The relative importance of all the above mentioned types of measurements has evolved with
1324 time (see Figure 15), from the beginning, when only bottles and MBT were used till the present
1325 when the Argo and glider data have become the largest contributors to the databases. This
1326 evolution also implies that the typical accuracy of the temperature and salinity measurements
1327 have evolved with time. This is especially important prior to the mid 60s when only bottle and
1328 MBT observations were available. Also, it is important to underline the fact that until the late
1329 70s the only information for salinity was provided by bottles. This heterogeneity in the type of
1330 observations requires a multiplatform cross-calibration in order to homogenize the information
1331 but this is often not available.

1332

1333 Besides the instrumental error we have to consider the representativity errors, which are usually
1334 much larger than the instrumental ones. Typically, we are interested in monthly or yearly
1335 estimates of the temperature/salinity 3D field in order to infer the basin heat/salt content.

1336 However, the measurements obtained at a given time may not be representative of the
1337 monthly/yrly average due to the influence of higher frequency processes (i.e. typically
1338 mesoscale features). As an example, the rms difference between hourly temperature
1339 observations at 100 m depth with respect to the monthly mean in a point located in the NW
1340 Mediterranean is 0.1 °C, much larger than the nominal accuracy of the instrument. Also, the
1341 number of observations during summer is much higher than during winter for the ship-based
1342 observations, so a careful treatment of the seasonal heterogeneities should be applied in order
1343 to avoid a bias towards the summer values when year-averaged estimates are computed.

1344

1345 The spatial coverage is also inhomogeneous across the basin and in depth (Figure 16), mainly
1346 because the hydrographic data, except the Argo and some mooring data, were obtained in the
1347 framework of targeted studies and not with the aim of monitoring long term signals. Some
1348 regions, especially the southern part of the basin, are rarely sampled (or if sampled the data are
1349 not in public databases). Also, the upper layers are better sampled than the intermediate or
1350 deeper layers, because of technical limitations or specific goals of the surveys (e.g. lowering a
1351 CTD until the bottom floor requires significantly more operation time and for most biological
1352 applications it is not needed). Although the spatial and temporal variability of the temperature
1353 and salinity fields at those depths is much lower than in the upper layers, this lack of information
1354 can hamper the ability to identify long term trends in the deeper layers (Llasses et al., 2015).

1355

1356 Long-term ship-based repeated full-depth CTD stations are a useful tool to assess the relative
1357 importance of different layers in the water column in determining the variability of the integrate
1358 heat and salt contents. In the Mediterranean such a station is for instance the DYFAMED station
1359 (bottom depth 2000 m), located in the north-western Mediterranean, east of the Gulf of Lion.
1360 Schroeder et al. (2010) used these CTD data, collected almost every month by the Observatoire
1361 Océanologique de Villefranche sur Mer Service d’Observation (<http://www.obs-vlfr.fr/sodyf/>) to
1362 observe the temporal evolution of heat and salt contents in the Ligurian Sea, for the period
1363 1995–2008 (see Figure 7 in Schroeder et al., 2010). Further analyses of the time series
1364 concerning the integral heat and salt contents and the contribution of the different layers to the
1365 total variance of heat and salt contents, reveal that the heat content changes of the whole water
1366 column are mostly explained (> 93% of explained variance) by the heat content changes of the
1367 first 1000 m, so that glider and Argo datasets could be sufficient to guarantee to capture this
1368 signal (obviously if a spatially dense enough network was established). However, concerning the
1369 salt content changes of the whole water column, the variance explained by the first 1000 m is
1370 only about 70%, so there is at least a 30% of the variance which is missed when not using full
1371 depth profiles. This is important to be taken into account when choosing the depth range for
1372 the assessment of the heat and salt content changes in the Mediterranean Sea.

1373

1374 Concerning the public databases where the hydrographic observations can be retrieved, the
1375 data obtained until the 90’s were gathered and quality controlled in the frame of the
1376 MEDAR/MEDATLAS project (<http://www.ifremer.fr/medar/>). The SeaDataNet project
1377 (www.seadatanet.org/) also gathers the metadata of most of the available observations and
1378 provides a portal for contacting the data providers. Also, a large part of the data are available in
1379 the World Ocean Database (https://www.nodc.noaa.gov/OC5/WOD/pr_wod.html) and in the
1380 Hadley Center repository (<http://hadobs.metoffice.com/en4/>). The homogenized and quality

1381 controlled Argo dataset can be retrieved from the Coriolis data center (www.coriolis.eu.org/),
1382 while the glider data are stored and disseminated through the EGO-network ([http://www.ego-](http://www.ego-network.org/)
1383 [network.org/](http://www.ego-network.org/)) and the Coriolis data center. Moreover, there are other data portals that include,
1384 at least partially, those datasets (e.g. EMODNET, <http://www.emodnet-physics.eu/>; MonGOOS
1385 <http://oceanobs.mongoos.eu/>); MyOcean-Copernicus, <http://marine.copernicus.eu/>). It has to
1386 be reminded, though, that not all the existing data are included in those databases and that the
1387 consistency among databases is not always guaranteed. The data distributed to the data centers
1388 have not always passed a quality control prior to their submission (raw data are often
1389 submitted). Moreover, the quality control applied in the different center may significantly differ.
1390 Finally, the calibration of the instruments is a very important element to ensure consistency
1391 among different observations, but unfortunately it is not always correctly tracked.

1392

1393 **6.3 – Computing heat and salt content**

1394 The available discrete temperature and salinity data have to be integrated in order to produce
1395 estimates of heat and salt content. Often, before computing basin averages the discrete data is
1396 interpolated on a regular grid to reduce the impact of the heterogeneous spatial distribution.
1397 The interpolated field is typically obtained through a weighted average whose general
1398 expression is:

(9)

1399 That is, the interpolated value at point j is a combination of a first guess (or background field) at
1400 that location plus a weighted sum of the observed anomalies
1401). There are different ways to define the weights w_i . They can be constant, a function of distance
1402 or obtained as the result of a statistical optimization (e.g. optimal interpolation, Bretherton et
1403 al., 1976). The way the background field is defined is also an open issue. Sometimes it is simply
1404 zero or a low order polynomial although often the background is defined as a long term average
1405 and depends on the month of the year and the spatial location.

1406

1407 A note of caution is required concerning the interpolation of the discrete data. The averaging
1408 often can mask problems with the observations, so it is very important that the observations
1409 considered have been quality controlled before the interpolation. Also, the analysis of the
1410 uncertainty linked to the interpolated product is not straightforward. There are different sources
1411 of uncertainty: observational and representatively errors, inhomogeneous data sampling and
1412 the limitations of the interpolation/averaging method. Considering all of them is a difficult task
1413 and often the uncertainties are underestimated. Also, some interpolation methods produce a
1414 formal error map that depends on the analysis choices and the selected parameters, so they are
1415 up to certain level arbitrary. Furthermore, once the 3D field is integrated to produce the heat or
1416 salt content value, that uncertainty should be propagated, but there is not a simple way of doing
1417 so (i.e. the spatial covariances between the errors at different grid points should be
1418 characterized somehow).

1419

1420 Some representative examples of different approaches followed to integrate the heat and salt
1421 content are the following. D’Ortenzio et al, (2005) and Houpert et al., (2014), in the study of the

1422 seasonal mixed layer depth and the heat storage rate have followed a similar approach. Data
1423 from all available platforms has been used. In a first step the data was binned in 1° boxes, then
1424 the median was obtained for each box and month and a spatial filter was applied to remove
1425 small scales. The uncertainty is estimated from the standard deviation (std) of temperature at
1426 each box and then propagated into the heat storage rate estimate using a MonteCarlo approach.

1427

1428 Other authors have generated monthly 3D maps of temperature and salinity using algorithms
1429 based on optimal interpolation (e.g. Rixen et al., 2005; Llasses et al. 2015; and
1430 Jordà et al., 2016). In those cases the data from all the available platforms were used and
1431 interpolated in a ~0.2° grid. The background was generated from the same dataset and kept
1432 either constant or evolving on time. The uncertainty analysis is generated as the formal OI error
1433 (Rixen et al., 2005) or more accurately using surrogate data from a numerical model (Jordà et
1434 al., 2016). It must be mentioned that there are also global products that cover the
1435 Mediterranean area and which provide gridded 3D maps at a spatial resolution of 1° like the
1436 one from the JMST Center (rda.ucar.edu/datasets/ds285.3/), Ishii and Kimoto, 2009) or the
1437 Hadley Center EN4 (hadobs.metoffice.com/en4, Good et al., 2013).

1438

1439 In order to illustrate the type of results that are provided by the above mentioned products the
1440 Mediterranean 3D basin averaged temperature and salinity time series obtained from Jordà et
1441 al. (2016) are shown in Figure 17 along with the uncertainty estimates. It can be seen that the
1442 uncertainties before the '80s are larger than the interannual variability, thus suggesting that
1443 probably there are not enough observations to characterize that variability. After the '80s the
1444 temperature variability can be better tracked and a warming trend seems clearly captured. The
1445 salinity changes are typically more difficult to capture and only after year 2000, with the
1446 contribution of Argo data the uncertainty range could be narrowed. The relatively high
1447 uncertainties in the salinity are due to two factors: first, there are less salinity observations (i.e.
1448 until the 80s salinity was measured using bottles); second, the salinity field is dominated by short
1449 scale features (i.e. the variations at short spatial scales <~50-100 km are more important than
1450 those at longer spatial scales), so it is more difficult to identify the large scale features with
1451 discrete measurements (Llasses et al., 2015).

1452

1453 ***6.4 Observational estimates of the water content.***

1454

1455 Changes in the volume of the basin can be obtained from two main sources of information. On
1456 one side there are the coastal tide gauges, which measure sea level relative to the coast. Some
1457 of the records span more than 100 years (e.g. the Marseille tide gauge, Wöppelmann et al.,
1458 2014) and for the last decades there is a good spatial coverage along the northern side of the
1459 basin. Conversely, very few data along the southern coast is included in the databases. The
1460 accuracy of hourly measurements is ~1 mm and for the monthly averages the accuracy is higher
1461 than 0.01 mm. Most of the tide gauge data are available through the Permanent Service for
1462 Mean Sea Level (www.psmsl.org, Holgate et al., 2013). The tide gauge data has to be quality
1463 controlled to avoid spurious peaks and changes in the reference level as well as to remove the
1464 effects of land movements. The drawbacks of this type of data is that they provide observations
1465 at discrete locations which are not necessarily representative of the basin average.

1466

1467 The other main source of information concerning the volume of the basin is satellite altimetry,
1468 which is operational since 1993, and measures sea level relative to the geoid along given tracks.
1469 Then the data from different satellites can be merged and interpolated on regular grids to
1470 produce weekly maps of sea level anomalies. Along-track and gridded products are distributed
1471 by several data centers (e.g. AVISO, www.aviso.altimetry.fr ; CSIRO,
1472 http://www.cmar.csiro.au/sealevel/sl_data_cmar.html; University of Colorado,
1473 <http://sealevel.colorado.edu/>). The accuracy of along-track is estimated to be ~2 cm while the
1474 gridded maps accuracy is estimated to be ~2- 4 cm for the weekly maps. It has to be noted,
1475 though, that the number of available satellites has not been constant in time, so the accuracy of
1476 the maps was not constant either. Also, for long-term trend estimates there can be an error due
1477 to instrumental and processing errors of ~1 mm/yr at regional scales (Henry et al., 2014).

1478
1479 The long time coverage of the tide gauge data can be combined with the good spatial coverage
1480 of altimetry in order to produce long time series of basin averaged sea level. This has been done
1481 using reduced order optimal interpolation techniques (e.g. Calafat and Gomis, 2009, Meyssignac
1482 et al., 2011, Calafat and Jordà, 2011). These techniques combine the spatial covariance patterns
1483 of sea level variability characterized from satellite altimetry or models with the time variability
1484 provided by tide gauges. Using this approach the basin averaged sea level for the last six decades
1485 has been reconstructed and the associated uncertainty has been estimated in less than 1 cm for
1486 the monthly values (Calafat and Jordà , 2011). Then, using hydrographic data to quantify the
1487 three first terms in the RHS of equation (8) the time series of water content can be derived
1488 (Figure 18, adapted from Jordà and Gomis, 2013).

1489
1490
1491 The changes in water mass content can be also derived using gravimetric observations. The
1492 GRACE mission measures changes in the gravity field which in turn can be converted, after
1493 several corrections, into mass variations. In order to reduce the noise in the mass estimates a
1494 smoothing filter with a characteristic length scale of ~300-500 km is typically applied, so the
1495 spatial resolution of the GRACE data products is relatively coarse. Also, the Mediterranean
1496 region suffers from the handicap of being surrounded by a complex coastline which can
1497 contaminate the solution (e.g. Calafat et al., 2010; Fenoglio-Marc et al., 2012). Different
1498 products derived from GRACE can be obtained from GRACE-Tellus data center
1499 (<http://grace.jpl.nasa.gov/>). The accuracy of the monthly maps is estimated to be ~1 cm of
1500 equivalent water thickness (Johnson and Chambers, 2013), although a detailed estimated of the
1501 products accuracy for the Mediterranean has not been yet conducted. Once the mass estimates
1502 are available, they have to be corrected for the changes in the salt mass content in order to infer
1503 the changes in the water content (Eq. 8). Unfortunately, the uncertainties in the salt content
1504 change are large: the uncertainty for the salt content change during the period 2004-2010 is
1505 $\pm 0.32 \cdot 10^6$ kg/s (Figure 17), which translated to equivalent water thickness would be ± 3.9 mm/yr
1506 much larger than the estimated mass change ~ 1 mm/yr (Calafat et al., 2010).

1507
1508 **6.5 Contribution of numerical modelling**

1509 The numerical models are tools that can also give a different insight in the evolution of the heat
1510 and mass content of the Mediterranean. Numerical simulations covering the whole
1511 Mediterranean run with different numerical codes, with several spatial resolutions (from 1/6°

1512 to 1/36^o) and temporal coverage (from 20 to 60 years) are presently available in different
1513 repositories (e.g. www.medcordex.eu; Ruti et al., 2015; <http://marine.copernicus.eu/>). Here we
1514 specifically consider free-surface 3D primitive equation models which provide temperature,
1515 salinity and sea level fields as outputs. As a note of caution it has to be mentioned that the state-
1516 of-the-art models for the Mediterranean use the Boussinesq approximation. This implies that
1517 models cannot reproduce the effects of a net thermal expansion, so such effect has to be added
1518 a posteriori as a spatially constant but time varying factor (Greatbach 1994). Besides this, the
1519 main limitations for the realism of modelled sea level is that most models usually does not
1520 account for the atmospheric pressure effects and that the contribution of the global ocean must
1521 be accurately prescribed through the lateral boundary conditions.

1522

1523 The models distribute inside the basin the heat and mass that is introduced through the surface
1524 and the lateral boundary conditions. The internal dynamics generated by the model can partially
1525 modify the air-sea fluxes through changes in the sea surface temperature and/or salinity, the
1526 characteristics of the lateral outflow through the Strait of Gibraltar and/or the Dardanelles Strait
1527 and up to certain extent the inflow in those straits. However, in general, it is found that the
1528 evolution of the model simulations is strongly constrained by the forcings imposed at the
1529 boundary conditions (e.g. Harzallah et al., 2015). Also, imbalances between the initial conditions,
1530 the forcing through the sea surface and/or the lateral boundaries can lead to spurious long term
1531 drifts that may be misinterpreted as climate change signals. In summary, if the numerical models
1532 were correctly configured and the forcing fields were accurate enough, they could provide an
1533 accurate representation of the evolution of heat and mass content and the mechanisms behind
1534 it. Unfortunately those two assumptions are difficult to fulfill and at present the numerical
1535 estimates of the Mediterranean heat and mass content are not considered more reliable than
1536 observational based estimates. However, it is worth mentioning that several international
1537 initiatives (e.g MedCORDEX, ENVIMED/TANGRAM) are devoting lots of efforts to advance in this
1538 field in order to produce more accurate and reliable numerical simulations.

1539

1540 A complementary tool that merges the benefits of numerical model with observational-based
1541 estimates are the ocean reanalyses. By reanalysis we refer to numerical simulation in which a
1542 data assimilation procedure has been implemented to incorporate the information from
1543 observations into the model trajectory. The reanalyses can be viewed as a sophisticated way of
1544 interpolating data providing, in statistical sense, the best estimate of the true state of the ocean.
1545 Therefore, in theory, they should provide a more realistic picture of the ocean state than
1546 statistically based interpolations as those discussed in section 6.3. However, they also suffer
1547 from some of the above mentioned problems that models have concerning long term drifts and
1548 the impact of errors in the forcing fields as well as the lack of data to constrain the model in
1549 certain regions and/or periods. For the Mediterranean, there exists only a limited number of
1550 reanalyses (Adani et al., 2011; Hamon et al., 2015) and up to our knowledge no multi-product
1551 assessment has been performed yet. In any case, they are a promising alternative for a better
1552 estimate of the Mediterranean heat and mass budgets.

1553

1554 **6.6 Perspectives**

1555 The recent improvements in the observational networks, especially since the development of
1556 the Argo program in the Mediterranean starting in the early 2000s, has allowed a significant

1557 reduction of the uncertainties associated to heat and mass content estimates in the
1558 Mediterranean. However, some improvements could be still brought through a coordinated
1559 effort for the collection and homogenization of hydrographic data that are not yet in the public
1560 databases. In that sense it is important to highlight the existing discrepancies in the historical
1561 data collected in different databases. A careful review and homogenization of the past
1562 observations including a tracking of the calibration procedures would also be very beneficial,
1563 especially for those observations obtained in low-sampled areas or periods.

1564

1565 Concerning ship-based hydrography, until now the Mediterranean has been sampled at irregular
1566 intervals during national expeditions, while it has been neglected by the global sampling
1567 programs such as WOCE and GO-SHIP (www.go-ship.org). Med-SHIP is a new program that aims
1568 at filling this gap, by regularly sampling the Mediterranean along two meridional transects in
1569 each basin (western and eastern, to be repeated every 3 years) and one zonal transect from the
1570 Strait of Gibraltar to the easternmost Mediterranean (to be repeated every 6 years (last
1571 repetition in 2011; see Tanhua et al., 2013) and next one planned for 2017-2018). In particular
1572 the zonal transect, repeated on a low-frequency basis is thought to allow the assessment of
1573 long-term variations in the heat and salt budgets, with a focus on the deeper layers that are less
1574 influenced by small-scale features (Schroeder et al., 2015). It is important to mention that Med-
1575 SHIP aims at following GO-SHIP standards, which include a fully open-access data policy.

1576

1577 Regarding the distribute network of open ocean moorings there are different initiatives that
1578 gather some of the existing data (a large fraction of the mooring data is kept by the institutions
1579 and not held in the databases). For instance, the FIX03 program
1580 (<http://www.fix03.eu/observatory/>) includes 10 sites in the Mediterranean that obtain
1581 hydrographic observations. The data is available in the data center of each observatory. Also, a
1582 complementary network is the CIESM HydroChanges Programme, which its ultimate goal is to
1583 detect long-term variations, abrupt changes and events, especially of the deep waters. An
1584 special concern in HydroChanges is to ensure a careful calibration of the existing sensors on
1585 long-term observatories especially for those measuring at large depths where the variations are
1586 much smaller than in the upper layers. Very importantly, future commitments of the
1587 HydroChanges community includes the set-up of a common database and metadatabase, or
1588 alternatively, to promote the submission of the collected data to existing databases (e.g., the
1589 Mediterranean in-situ TAC, MonGOOS). However, as happens with the ship based data, most
1590 of the existing data are not in the databases yet.

1591

1592 A more important issue that has to be mentioned is that, with the exception of Argo, there are
1593 few long-term monitoring programs that can allow a correct observation of climate signals.
1594 Therefore, a first concern is that the Mediterranean Argo network should be maintained and
1595 sustained. Several Mediterranean countries and the Euro-Argo ERIC (www.euro-argo.eu) are
1596 already committed to guarantee this sustainability. Besides this, an internationally coordinated
1597 effort that ensure a regular monitoring of key regions of the Mediterranean could allow a much
1598 better estimate of the Mediterranean mass and heat content evolution. This also includes the
1599 deployment of floats capable of collecting data as deep as 4000 dbar in selected areas of the
1600 Mediterranean to measure the variability of the heat and salt content below 2000 dbar. The

1601 determination of those key regions would require a devoted study that exceeds the goals of this
1602 paper.

1603

1604

1605 **7- 21st Century scenarios for the budget components**

1606 ***7.1-Overview***

1607 An important concern about the Mediterranean heat and mass budget is the future evolution
1608 of their different components in a context of global warming. The Mediterranean is located at
1609 the frontier between the arid climate of North Africa and the continental European climate. So,
1610 small perturbations of the conditions either in Europe or in Africa may induce significant changes
1611 in the Mediterranean. This section aims at giving a short overview of the projected changes in
1612 the different components of the Mediterranean heat and mass budgets. These projections are
1613 based on numerical simulations that aim to reproduce the evolution of the climate under certain
1614 scenarios of the future greenhouse gases (GHG) concentrations. On one hand, the
1615 Mediterranean is not isolated from the global climate system, so in order to properly simulate
1616 the evolution of this region it is important to simulate the evolution of the whole globe. In this
1617 sense, the global climate models (GCMs) are the first required step. However, on the other hand
1618 the Mediterranean has several characteristics (i.e. large spectrum of mesoscale processes, water
1619 mass formation, strait dynamics,...) that require a relatively high spatial resolution in the models
1620 in order to produce a realistic behaviour. Therefore, regional climate models (RCMs) nested into
1621 GCMs are necessary to properly model the Mediterranean and to produce regional projections.

1622 It is also important to highlight that the projections are inherently affected by a significant degree
1623 of uncertainty. First, they are based on assumptions on the unknown future GHG concentrations.
1624 Second, being the result of numerical simulations, the projections are affected by uncertainties
1625 linked to the accuracy of the modelling system. In particular to uncertainties in the GCMs and
1626 also in the RCMs. And finally, the climate system has a natural multidecadal variability which is
1627 not linked to the GHGs concentrations and that is reproduced by the models. In other words,
1628 some changes simulated by the models may be due to natural variations and not to changes in
1629 the GHGs concentrations. This has to be taken into account when the projection only span few
1630 decades, as the changes due to GHGs and those due to natural variations are more difficult to
1631 distinguish. A common technique to characterize the uncertainties in the modelling system and
1632 to filter out the natural variations is to produce a large number of simulations forced by the same
1633 GHG concentrations. Then, the ensemble average is considered to be the best approximation to
1634 the real evolution while the ensemble spread is a measure of the uncertainties linked to the
1635 models and the natural variability. Unfortunately, the computational cost of the regional
1636 simulations is high, so at present the number of Mediterranean regional projections is reduced
1637 and the results must be interpreted with care.

1638

1639

1640 ***7.2- Water fluxes through the surface and the lateral boundaries***

1641 Table 7 summarizes projected changes of the different component of the freshwater budget
1642 obtained by different authors. Most of the compiled studies predict a decrease in precipitation
1643 over the basin with a reduction between -5 and -15% although some projections reach up to a -
1644 28 % reduction. Also, the evaporation tends to increase a similar amount with some models

1645 projecting up to 18 % more evaporation. River runoff and Black Sea water net inflow both
1646 decrease respectively up to -87 % and -102 %. It is interesting to notice that the latter means
1647 that some studies even predict that the Black Sea would become an evaporative basin and thus
1648 the net water flow through the Dardanelles Strait would change its direction (from the
1649 Mediterranean to the Black Sea). Finally, the net water inflow through Gibraltar could increase
1650 up to 60 %, as the result of the increase in the freshwater deficit. Adloff et al. (2015) have also
1651 shown that the changes in the components of the water budget are strongly linked to the chosen
1652 socio-economic scenario: for higher GHG emissions, the water flux response is larger. [Note that
1653 the other studies referenced in Table 7 are based on a single scenario].

1654

1655 ***7.3- Heat fluxes through the surface and the lateral boundaries***

1656 Table 8 compiles the projected changes in the heat fluxes through the surface and the Strait of
1657 Gibraltar. The surface heat loss of the Mediterranean is decreasing in all available climate
1658 projections. This positive surface heat change ranges from +25 % to +118 %, which means that
1659 some model predict that the Mediterranean could even gain heat through the surface in the
1660 future. As for the water fluxes component, the changes in surface heat fluxes are tightly related
1661 with the GHG concentrations in the scenarios. It is worth noting that results from the CIRCE
1662 project compiled in both Dubois et al (2012) and Gualdi et al. (2013) refer to changes over the
1663 2021-2050 period. Much larger changes are expected for the period 2061-2099 if the CIRCE
1664 simulations would have been performed up to 2099. Concerning the net heat exchange through
1665 Gibraltar, the ensemble of the CIRCE simulations displays a range between -11 % and +3 % (2021-
1666 2050 vs. 1961-1990), while the simulations carried up to the end of the 21st century predict an
1667 increase from 0 % to +40 % (2070-2099 vs. 1961-1990). The increase in the heat flux is linked to
1668 a combination of (i) an enhanced water flux required to compensate the increase in the water
1669 losses through the surface inside the Mediterranean and (ii) the increase in the temperature of
1670 the Atlantic waters flowing into the Mediterranean.

1671

1672 ***7.4- Heat and mass content changes***

1673 Most of the studies on the future climate of the Mediterranean Sea have projected a significant
1674 warming and salinization at the end of the 21st century (Table 9). This is consistent with the
1675 above mentioned results on the surface fluxes. An increase of the global temperature would also
1676 lead to a reduction of the heat loss through the sea surface and to an increase of the
1677 temperatures of the incoming Atlantic waters through the Strait of Gibraltar. This altogether
1678 would lead to an increase of the Mediterranean heat content. Also, an increase of the water loss
1679 through the sea surface would lead to a salinization of the basin, since more salty water will enter
1680 the basin to compensate the fresh water deficit. However, the expected salinity of the Atlantic
1681 waters is not a straightforward issue. On one hand, some global models project an increase in
1682 the northeast Atlantic salinity due to increase evaporation in that region. On the other hand
1683 other models suggest that the ice melting in the Arctic would imply a water freshening that can
1684 be advected towards the northeast Atlantic. In the latter case the waters entering the
1685 Mediterranean through the Strait of Gibraltar may be fresher and could compensate, at least
1686 partially, the effects of enhanced evaporation.

1687 Although most models agree on the general picture, the projected amount of change is quite
1688 diverse among the different studies. Somot et al. (2006), using a single simulation forced under

1689 the SRES-A2 scenario, have projected an increase in the basin averaged temperature (T3D) of
1690 1.5°C and of 0.23 psu in the salinity (S3D) in 2099 with respect to the values in year 2000. Carillo
1691 et al. (2012), performed two simulations for the period 1950-2050 under the scenario SRES-A1b.
1692 The difference between the two simulations was on the Atlantic boundary conditions, specially
1693 on the salinity. The simulated changes for the period 2001-2050 with respect to the period 1950-
1694 2000 was +0.38°C and +0.42°C for T3D and +0.03 and -0.08 psu for S3D, for the two simulations
1695 respectively. Adloff et al. (2015) performed an ensemble of six projections under three different
1696 GHG scenarios (B1/A1b/A2) and with varying Atlantic, riverine and atmospheric conditions.
1697 Their results projected an averaged change for the period 2070-2099 with respect to 1961-1990
1698 of +0.93°C to +1.35°C for the temperature and +0.28 and +0.52 psu for salinity (Table 9). Finally,
1699 Macías et al. (2015) have projected an increase for the period 2096-2099 with respect to 2014-
1700 2017 of +1.30 and +2.50 °C (+0.6 and 0.9 psu) for the temperature (salinity) using respectively
1701 the scenario RCP4.5 and RCP8.5. Part of the discrepancies among these studies are linked to the
1702 model characteristics and the way they simulate basic features of the basin. Another part should
1703 be attributed to the different configuration of the experiment (model chosen to provide
1704 boundary conditions and/or GHG scenario) and the diagnostics performed (analysed period).

1705 The sea level in the Mediterranean will be affected by changes in the thermal content of the
1706 basin through the thermal expansion. The changes in the salt content are expected to have a
1707 minor effect (Jordà and Gomis, 2013). Concerning the thermal expansion, Carillo et al. (2012)
1708 computed that thermosteric sea level would reach 5cm and 7cm by 2050, although one should
1709 keep in mind that the largest part of the oceanic response to climate change appears in the
1710 second half of the 21st century. The simulations of Adloff et al. (2015) projected a thermal
1711 expansion from 45 cm to 61 cm by the end of the 21st century. However, it has to be kept in
1712 mind that the Mediterranean sea level is strongly affected by the changes in the nearby Atlantic
1713 (see for instance Tsimplis et al., 2013). This link with the Atlantic has clear consequences for the
1714 future evolution of the Mediterranean. First, the changes in the Mediterranean sea level will be
1715 modulated by the Atlantic: if the Mediterranean sea level rose much more than the nearby
1716 Atlantic the increase in the along-strait pressure in Gibraltar will translate into a reduction of the
1717 net flow in the basin and thus a reduction of sea level. Second, in a similar way sea level changes
1718 in the Atlantic will be transferred to the Mediterranean. In that sense, recent projections for the
1719 nearby Atlantic (Bouttes et al., 2013) show that sea level in that region will be ~10 cm higher
1720 than the global sea level rise. This, in turn, it is projected to be between 50 and 150 cm by 2100
1721 due to the combination of thermal expansion and water addition from land based ice melting.
1722 Therefore, it should be expected that the Mediterranean sea level will rise much more than what
1723 is projected considering only the basin thermal expansion (e.g. Jordà et al., 2012).

1724

1725 **7.5- Perspectives**

1726 As important as the projected changes is the uncertainty associated to those projections. In
1727 consequence it is of substantial importance to get accurate estimates of them. As mentioned
1728 above, one source of uncertainty is related to the modelling system itself. Mediterranean models
1729 do still have room for improvement and several efforts are being carried out in that line (e.g.
1730 MedCORDEX initiative , Ruti et al., 2015 ; the ENVIMED-TANGRAM project). A better
1731 representation of the present climate would increase the robustness of the future projections.
1732 Another source of uncertainty is related to the information introduced through the boundary

1733 conditions, mainly the projected changes in the nearby Atlantic and in the atmospheric forcing.
1734 In order to tackle this it is necessary to have an ensemble of simulations forced by a range of
1735 feasible conditions at the boundaries. Also, such ensemble could be used to filter out the
1736 influence of the natural variability on the projected changes. And last but not least, it has to be
1737 kept in mind that the future GHG concentrations are unknown, so different scenarios should be
1738 taken into account. All this requirements demand a huge amount of human and computational
1739 resources and can only be achieved through sustained and coordinated efforts at the
1740 international level. In this sense, to maintain programs like MedCORDEX is essential to ensure
1741 the improvement of Mediterranean future projections.

1742

1743 **8- Discussion**

1744 A key question that can be addressed is whether the attained accuracy of the different
1745 components of the Mediterranean Sea heat and mass budgets is sufficient. As mentioned in the
1746 introduction, the answer obviously depends on the application where those estimates have to
1747 be used. In our case, we are primarily interested in determining if we can close the heat and
1748 mass budgets with the state-of-the-art estimates and to assess in which components there are
1749 more room for improvements.

1750 A first consideration is that the budgets described in equations (1-3) are independent of the
1751 timescale considered and the relations must hold for any averaging period of time. In practice,
1752 though, the chosen period may affect the reliability of the different components. For instance,
1753 when a long period is considered, the heat and mass content change in equations (1-3) is closer
1754 to zero (i.e. the basin is close to the equilibrium), which would simplify the closure of the budget.
1755 However, the estimates of the different components can be unreliable for past periods when
1756 the observational systems were scarce. Conversely, it is possible to find a short period where
1757 the quality of the different components is better estimated (i.e. because of having a better
1758 observational system). However in that case the content change cannot usually be neglected
1759 and has to be estimated somehow. Moreover, the accuracy of the trends (i.e. the rate of content
1760 change) is directly linked to the record length, so shorter periods are prone to show higher
1761 uncertainties.

1762 A second issue closely linked to the closure of the budget is the quantification of the uncertainty
1763 associated to each component. This will determine the accuracy of the closure and the capability
1764 to indirectly estimate the different components. Ideally, the characterization of the uncertainty
1765 should involve the comparison with independent observations. Unfortunately this is almost
1766 never possible due to the lack of such observations, so other alternatives are envisaged.
1767 Sometimes the temporal standard deviation is used as a measure of the error in the mean.
1768 Strictly speaking, the statistical uncertainty of the average of a collection of N samples $\{X_i\}$ is
1769 defined as $\text{std}(\{X_i\})/N^{0.5}$ when the samples are assumed to be uncorrelated. Therefore, this
1770 quantity would measure the inaccuracies in the estimate of the mean provided we have a short
1771 record (i.e. that is what we should use if we wanted to estimate the long term average of a
1772 quantity when only few years of data are available). However two important remarks are
1773 needed. The first one is that this would be correct only if the samples are uncorrelated. In
1774 practice this requirement is almost never satisfied as the geophysical variables have a long term
1775 memory. For autocorrelated time series (i.e. those with low frequency signals on it), N should

1776 be replaced by N^* , the effective degrees of freedom. To determine N^* is not straightforward
1777 and depends on the relation between the length of the record with respect to the characteristic
1778 time scales on it. Therefore, in those cases where the records are short the uncertainties
1779 obtained from the std are probably underestimated. The second remark is that the std is only a
1780 measure of the statistical uncertainty associated to the averaging, but by no means can be
1781 viewed as a measure of the total uncertainty. The latter should include also the uncertainties
1782 linked to the accuracy of the data and/or the methodological approach used to estimate the
1783 derived quantities (i.e. the fluxes). This part of the uncertainty is not easy to quantify but it is
1784 very important as it is usually the dominant contributor. A common approach has been to use
1785 an ensemble of products (e.g. surface heat fluxes from different models) and consider that the
1786 ensemble spread encompasses the observational and methodological errors. However, this
1787 approach can highly underestimate the uncertainty: most models/reanalyses are not
1788 independent as they are based on similar codes and the observations used to constrain and/or
1789 to calibrate them are often the same. Moreover, the number of available products is typically
1790 small so the inter-product spread is probably underestimating the actual spread. Alternatively
1791 other approaches base on sensitivity experiments using synthetic data from numerical models
1792 to test the accuracy of the methodology and the propagation of the observational and
1793 representativity errors to the derived quantities. This approach can lead to more realistic
1794 estimates of the uncertainties. Some examples can be found in Sánchez-Román et al. (2009) for
1795 the estimates of the Gibraltar outflow or Llasses et al. (2015) for the Mediterranean heat and
1796 salt content. Unfortunately this strategy is not always easy to implement and at present is not
1797 available for most of the components of the budgets.

1798 The next step is to summarize the different estimates of the components in (1-3) along with
1799 their associated uncertainties in order to evaluate in which cases the budgets can be closed. For
1800 illustrative purposes we consider a long term average for the period 1980-2010 as well as the
1801 short period 2005-2010. The summary of the results for the heat budget (eq. 1) is presented in
1802 Table 10. The long-term mean surface heat flux is estimated to be $-3 \pm 8 \text{ W/m}^2$ from ship/satellite
1803 observation based (Sánchez-Gómez et al., 2011) and where the uncertainty is computed as the
1804 temporal std. This value also encompasses the -7 W/m^2 value obtained by Pettenuzzo et al.
1805 (2010) from atmospheric reanalyses..It has to be noted that the selection of these two estimates
1806 has been done implicitly considering the Gibraltar constraint. Without that knowledge, the
1807 actual uncertainty in the mean surface heat flux would be much larger. For the period 2005-
1808 2010 we have analysed the results from the MedCORDEX ensemble of regional ocean models.
1809 The results indicate that during that period there was no significant difference with the long
1810 term mean or the intermodel spread. For the net heat flux through the Strait of Gibraltar, the
1811 estimated value is $4.5 \pm 4.1 \text{ W/m}^2$. This value arises from a numerical simulation, as far as no
1812 direct observations are available, and the uncertainty has been estimated as half the std of the
1813 subinertial time series. Alternatively, assuming an uncertainty of 15 % in the inflow, outflow or
1814 the temperatures would lead to a similar degree of uncertainty. For the period 2005-2010 there
1815 is no information that can be used to assess significant changes in the heat flux through
1816 Gibraltar. For the Dardanelles Strait we use the estimate presented in Section 4.5 of 0.1 ± 0.2
1817 W/m^2 , which is based on published values for the temperature and transport of the two-layer
1818 system. The uncertainties have been derived assuming an uncertainty of 2°C in the
1819 temperatures and $200 \text{ km}^3/\text{yr}$ in the transport. The latter is based on the observed std of the

1820 low frequency time series. Again, there is no data that allow to assess a significant change during
1821 the 2005-2010 period. For the rivers, the estimate performed in section 5.5 was $0.6 \pm 0.4 \text{ W/m}^2$
1822 where the uncertainty has been obtained assuming an uncertainty in the river runoff of 15% and
1823 $5 \text{ }^\circ\text{C}$ in the river temperature. No significant difference is observed for the period 2005-2010.
1824 For the heat content change the value estimated for the period 1980-2010 is $0.3 \pm 0.3 \text{ W/m}^2$
1825 while for 2005-2010 is one order of magnitude larger $3.5 \pm 3.0 \text{ W/m}^2$.

1826 The summary of the water mass budget components is presented in Table 11. The averaged
1827 water flux through the surface is estimated to be $-0.8 \pm 0.2 \text{ m/yr}$ based on published results (see
1828 section 2.5) where the uncertainty comes from the interproduct spread. For the period 2005-
1829 2010, the reanalyses and RCM models show a slight increase in the water loss, being -0.9 ± 0.2
1830 m/yr . The Gibraltar net water flux is estimated to be $0.8 \pm 0.2 \text{ m/yr}$ based on historical estimates
1831 and with the uncertainty computed as the spread of those estimates. For the shorter period
1832 2005-2010, there is no direct estimates of the flux but based on the indirect computation of
1833 Soto-Navarro et al. (2010), the net water flux should have increased to $0.85 \pm 0.2 \text{ m/yr}$ during
1834 that period. The net water flux through the Dardanelles is estimated to be $0.1 \pm 0.02 \text{ m/yr}$, with
1835 the uncertainty computed also as the spread of historical estimates. For the period 2005-2010
1836 there is no information to assess eventual changes in that component. The river contribution is
1837 considered to be $0.2 \pm 0.01 \text{ m/yr}$ and none of the independent estimates show significant
1838 changes on the mean during the period 2005-2010. The change in the freshwater content for
1839 both periods is not significantly different from 0: $0.5 \pm 1.0 \text{ mm/yr}$ and $1 \pm 3 \text{ mm/yr}$, respectively
1840 (note that these values refer to the change in the freshwater content and not the total sea level;
1841 i.e. the thermal expansion effects are not considered).

1842 Finally, the different components of the salt mass budget are presented in Table 12. The mean
1843 net salt flux through Gibraltar is estimated to be $-1.5 \pm 6.5 \cdot 10^6 \text{ kg/s}$ and no information is available
1844 to assess if any change existed during 2005-2010. The salt flux through the Dardanelles Strait is
1845 estimated to be $0.2 \pm 0.2 \cdot 10^6 \text{ kg/s}$ with the uncertainty computed assuming an error of 2 psu in
1846 the salinity of the exchanged waters (see section 4.5). Again, no information is available to assess
1847 eventual changes during the period 2005-2010. The salt content change is estimated to be $0.1 \pm$
1848 $0.1 \cdot 10^6 \text{ kg/s}$ for the period 1980-2010 and to increase up to $0.3 \pm 0.2 \cdot 10^6 \text{ kg/s}$ during 2005-2010.

1849

1850 Comparing the direct estimates of the different components (Tables 10-12) it can be seen that
1851 the heat, water mass and salt mass budgets are closed within the uncertainty limits. This means
1852 that the each component could be indirectly estimated from the other components using the
1853 equations (1)-(3). However, this would only make sense for the component showing the largest
1854 uncertainty. In particular, for the period 1980-2010, the surface heat fluxes can be better
1855 constrained using this approach (uncertainty reduced from $\pm 8.0 \text{ W/m}^2$ to $\pm 4.3 \text{ W/m}^2$), as well
1856 as the net water flux through the Strait of Gibraltar (uncertainty reduced from $\pm 0.4 \text{ m/yr}$ to \pm
1857 0.2 m/yr ; that is from $\pm 0.03 \text{ Sv}$ to $\pm 0.02 \text{ Sv}$), and the net salt flux through the Strait of Gibraltar
1858 (uncertainty reduced from $\pm 6.5 \cdot 10^6 \text{ kg/s}$ to $0.2 \cdot 10^6 \text{ kg/s}$). For the shorter period 2005-2010 the
1859 same components are better estimated indirectly than from direct computation. It is worth
1860 noting that for that shorter period, the common assumption that the Gibraltar heat transport is
1861 mostly compensated by the heat trough the sea surface is not accurate. The changes in the basin

1862 heat content have to be taken into account as far as they are comparable to the Gibraltar
1863 contribution.

1864

1865 The picture obtained for the heat budget shows that the dominant terms are the fluxes through
1866 the sea surface ($-4.9 \pm 4.3 \text{ W/m}^2$) and the fluxes through the Strait of Gibraltar ($4.5 \pm 4.1 \text{ W/m}^2$).
1867 The contribution of the heat content change (i.e. the temperature trend) is smaller but not
1868 negligible ($0.3 \pm 0.3 \text{ W/m}^2$) and should be taken into account when short periods (\sim few years)
1869 are considered. A new result is that the contribution from the rivers, albeit small is non-negligible
1870 ($0.6 \pm 0.4 \text{ W/m}^2$) and during some periods can be comparable to the heat fluxes through the
1871 Strait of Gibraltar (see section 5.5). The largest uncertainties in the heat budget are associated
1872 to the surface fluxes and the Gibraltar fluxes ($\sim 4 \text{ W/m}^2$). In relative terms, the uncertainties
1873 associated to the Dardanelles are also very high (i.e. roughly twice the estimated value).
1874 However, as that component represents a small contribution to the total budget those
1875 uncertainties are small in absolute terms. Concerning the water mass budget, the flux through
1876 the sea surface is the largest contributor ($-0.8 \pm 0.2 \text{ m/yr}$) and is compensated by a combination
1877 of the flux through Gibraltar ($0.4 \pm 0.2 \text{ m/yr}$), the river runoff ($0.2 \pm 0.01 \text{ m/yr}$) and the flux
1878 through the Dardanelles ($0.1 \pm 0.02 \text{ m/yr}$). It is worth noting that in this case all those
1879 components are of similar magnitude while the change in the water content (i.e. linked to the
1880 non-thermohaline sea level change) is much smaller. Concerning the uncertainties, those
1881 associated with the surface fluxes and the fluxes through Gibraltar are one order of magnitude
1882 larger than the others. Finally, for the salt mass budget, our estimates suggest that the
1883 contribution of the fluxes through the Dardanelles strait would be larger than the estimated salt
1884 content change, so the Gibraltar contribution would be negative (salt export to the Atlantic).
1885 Nevertheless it has to be noted that the uncertainties in the fluxes through the straits are large,
1886 so these results have to be taken with caution.

1887

1888

1889 These results also indicate to which components more efforts should be devoted in the future.
1890 Although the budgets can be closed with the existing estimates, the associated uncertainties are
1891 still very large. It seems clear that the largest improvements in the characterization of the
1892 Mediterranean budgets would be brought by the reduction of the uncertainties in the surface
1893 heat fluxes and in the fluxes through the Strait of Gibraltar. For the surface fluxes more studies
1894 devoted to exploit the available in-situ data and to provide a reference dataset to evaluate the
1895 air-sea fluxes from different products are required. Complementary, a better monitoring of the
1896 Gibraltar Strait, even if it would require a large coordinated effort, would allow to better
1897 constrain the air-sea fluxes estimates and to better explain the changes in the salt content of
1898 the basin. However, some notes of caution are required. The net volume and salt transports are
1899 the difference of two very similar quantities and, therefore, their size is close to zero. Actually,
1900 if the uncertainty is identified with the error of the measurement, neither of them would be
1901 statistically different from zero (Table 4). The fact that these two net transports are more than
1902 one order magnitude less than the intervening terms in the summation makes them be very
1903 sensitive to small errors in the estimate of each term. Even when the net heat transport is
1904 obtained with the same procedure, it exhibits a clear difference with the net flow and salt
1905 transport: it is only a little smaller than the terms in the summation and its time-averaged value
1906 is slightly greater than the associated uncertainty. The reason for this difference stems from the

1907 marked temperature difference between the Atlantic and the Mediterranean waters, which is
1908 greater than the salinity difference in relative terms. Thus, while the net salt transport is virtually
1909 zero, the heat transport is positive.

1910

1911 Another important consequence of the budget analysis performed before is that the
1912 Mediterranean can be used as a test case for the evaluation of air-sea heat flux products. The
1913 indirect estimate of the mean surface heat flux provides a strong constraint that can allow to
1914 elucidate which products are significantly biased. That constraint could even be refined with
1915 complementary monitoring of Gibraltar heat fluxes and, to a less extent, of the rivers and
1916 Dardanelles heat fluxes. Moreover, during the last years air-sea fluxes have been measured in
1917 several open sea locations (see section 2.5), which would provide additional constraints for the
1918 surface heat flux products once the available data is homogenized and quality controlled.
1919 Conversely, for the net surface water flux the indirect estimate cannot be considered an
1920 effective constraint as far as the associated uncertainties are too large. An accuracy of ~ 0.015
1921 Sv in the estimates of net flow through the Strait of Gibraltar would be needed to improve the
1922 direct estimate of the surface water flux. In order to reach such value, an accuracy of ~ 0.01 Sv
1923 would be required for the inflow and outflow (i.e. $\sim 1\%$ of the absolute value). Until that level
1924 of accuracy is attained in the estimates of the Gibraltar water fluxes, the only way to constrain
1925 the surface water flux products is through the development and exploitation of the open-sea
1926 observational network.

1927 An open question that is usually discussed is if there should be a preferred period for the budgets
1928 closure. The results presented in this paper suggest that since 2004 the uncertainties in the heat,
1929 salt and water content change are reduced thanks to the new observing systems. However, no
1930 clear improvement has been brought to the other components of the budgets which in fact
1931 dominate the uncertainty. The estimates of the surface fluxes and the net fluxes through the
1932 Strait of Gibraltar have not been significantly improved during that period, so the accuracy of
1933 the budget closure is basically the same. It has to be noted that some observational systems that
1934 could bring new improvements to those fluxes have been deployed recently (e.g. surface current
1935 radar observations in Gibraltar (see 3.4) or air-sea flux measurements at open sea buoys (see
1936 2.4)). Therefore, the period from 2014 onward could be potentially preferred but only once the
1937 new datasets have been used to improve the air-sea fluxes and the fluxes through the Strait of
1938 Gibraltar.

1939 Finally, it is also worth noting that the indirect estimate of the heat and salt content is less
1940 accurate than what is obtained from in situ observations. The main reason is the large
1941 uncertainties associated to the surface heat flux and the heat and salt fluxes through the Strait
1942 of Gibraltar. An important consequence of this is that the heat and salt content changes
1943 obtained from numerical models would be less reliable than the observational estimates.
1944 Although the models can reproduce the heat and salt redistribution inside the Mediterranean,
1945 the changes in the total heat and salt content are strongly determined by the surface and lateral
1946 boundary conditions, which are highly uncertain. As an example, Vargas-Yáñez et al (2010) have
1947 estimated from in-situ observations a change in the western Mediterranean heat content of 0.3
1948 W/m^2 for the period 1940-2000. This is an order of magnitude lower than the uncertainty
1949 associated to the mean surface heat flux used to force the ocean models. In consequence, the

1950 characterization of temperature and salinity trends in the Mediterranean from models should
1951 be avoided unless until the uncertainties in the forcings are significantly reduced.

1952

1953

1954

1955 **9- Conclusions**

1956 In this paper we have presented a review of the state-of-the-art of the understanding and
1957 quantification of the Mediterranean heat and mass (i.e. salt and water) budgets. The different
1958 components of the budgets have been described in detail and a critical review of the different
1959 methods and observational products that allow their quantification has been presented. Special
1960 emphasis has been put on the characterization of the associated uncertainties, and several
1961 proposals for the advance in the current knowledge are presented for each component of the
1962 budgets.

1963

1964 The *surface fluxes* are mainly characterized using atmospheric reanalyses or regional climate
1965 models as far as little observational data are available over the sea. The uncertainty associated
1966 to those fluxes is the most sensitive part of the heat and water mass budget as they are one of
1967 the dominant components of the budgets. In that sense, an increase of the observations of air-
1968 sea fluxes on the sea (i.e. with moored open sea buoys), as well as a coordinated effort to
1969 combine observational discrete data with numerical model outputs is thus recommended. The
1970 *fluxes across the Strait of Gibraltar* are also an important component of the budgets even if there
1971 are some important lacks. In particular, there are very few direct measurements of the inflow
1972 (and thus of the net water transport) and the heat and salt transports are not routinely
1973 monitored. However, and even with the technical challenges associated with the monitoring of
1974 such complex region, a sustained monitoring of the Gibraltar fluxes would be very beneficial as
1975 it would allow to better constrain the surface heat and water fluxes and to indirectly determine
1976 the changes in the Mediterranean salt content. The uncertainties associated to the *fluxes across*
1977 *the Dardanelles Strait* are even relative larger than for the Strait of Gibraltar. However, due to
1978 its small contribution to the total budget this is not a major shortcoming for the closure of the
1979 Mediterranean budgets. Nevertheless, it is obvious that they have a large impact at regional
1980 scale, so any improvement in the monitoring of those fluxes would lead to a better knowledge
1981 of the dynamics in the Eastern basin. The observations of the *riverine input* are often either
1982 outdated or with incomplete information on possible treatments applied to remove the impact
1983 of water usage. Also, about a 40% of the total flux cannot be estimated from observations.
1984 Different types of numerical models can complement the observational estimates producing
1985 high frequency time series as well as estimates in places where observations are not available.
1986 However they are strongly affected by uncertainties in the water fluxes over land. A first
1987 estimate of the heat flux associated to the river runoff has also been produced showing that
1988 rivers can significantly contribute to the heat budget. Concerning the *heat and salt content*
1989 *change*, the present day observational system has allowed a significant reduction of the
1990 uncertainties, mainly since the introduction of the Argo floats. However, it has been also
1991 identified that more efforts should be devoted to better integrate the existing information,
1992 especially that collected and stored at national level, which is not always available in the public
1993 databases. The changes in the water content are derived from estimates of total sea level

1994 changes that have been corrected for the expansion of the water column (i.e. using hydrographic
1995 data). Alternatively, satellite observations of mass changes can be converted into water content
1996 changes using information on the salt content change. However, the large uncertainties
1997 associated to salt content estimates make this approach still useless in practice.

1998

1999 The state-of-the-art of the different components allow the budget closure in the range of the
2000 uncertainty. This allows to indirectly estimate some of the components of the budget with better
2001 accuracy than the direct estimate. In particular the Mediterranean has proven to be a suitable
2002 test case for the evaluation of air-sea heat flux products (but not for the water flux products).
2003 The accuracy of the indirect estimate of the long term mean is higher than the interproduct
2004 spread and could even be reduced if a monitoring of the Gibraltar heat flux was set up.
2005 Conversely, the indirect estimates of the heat and mass contents are more uncertain than the
2006 direct estimates. The consequence of this is that long term temperature and salinity trends
2007 obtained from numerical modelling must be call into question. The heat and salt content
2008 evolution in numerical models are strongly constrained by the surface and lateral forcings, which
2009 are not accurate enough to lead to accurate modelling of the temperature and salinity trends.

2010

2011 Finally, this review has revealed that the quantification of the uncertainty associated to each
2012 component should also be improved. In most cases it has only been assessed using the temporal
2013 std as a proxy of the error in the mean or using the spread of different products to account for
2014 methodological and observational errors. However, in most cases these approaches lead to an
2015 underestimation of the uncertainties.

2016

2017 **Acknowledgements**

2018 The authors want to acknowledge all the teams that maintain the different long term monitoring
2019 programs and databases in the Mediterranean for their extremely valuable contribution to the
2020 understanding of the Mediterranean functioning. We also want to acknowledge T. Rigo and D.
2021 Gomis for useful discussions on parts of the paper. This work has been partially funded by the
2022 ENVIMED/MISTRALS program through the MedMAHB and TANGRAM projects. G. Jordà
2023 acknowledges a Ramón y Cajal contract (RYC-2013-14714) funded by the Spanish Ministry of
2024 Economy and the Regional Government of the Balearic Islands and the Spanish-funded CLIFISH
2025 project (CTM2015-66400-C3-2-R). Data from the monitoring station at Gibraltar have been
2026 collected within the frame of Spanish-funded INGRES projects (REN03-01608, CTM06-02326 and
2027 CTM2010-21229). J. Chiggiato and K. Schroeder acknowledge the Italian National Project
2028 RITMARE, funded by the Italian Ministry of Education, University and Research and the FP7 EU
2029 Ocean-Certain (GA #603773).

2030

2031

2032

2033 **REFERENCES**

- 2034 Adani M, S. Dobricic and N. Pinardi, 2011: Quality Assessment of a 1985–2007 Mediterranean
2035 Sea Reanalysis. *J. Atmos. Oceanic Technol.*, 28, 569–589. doi:
2036 <http://dx.doi.org/10.1175/2010JTECHO798.1>
- 2037 Adloff F., S. Somot, F. Sevault, G. Jorda, R. Aznar, M. Déqué, M. Herrmann, M. Marcos, C. Dubois,
2038 E. Padorno, E. Alvarez-Fanjul, D. Gomis (2015) Mediterranean Sea response to climate
2039 change in an ensemble of twenty first century scenarios, *Climate Dynamics* Volume
2040 45, Issue 9, pp 2775-2802 doi:10.1007/s00382-015-2507-3
- 2041 Alpar, B. and H. Yüce (1998). Sea-Level Variations and their Interactions between the Black Sea
2042 and the Aegean Sea. *Estuarine, Coastal and Shelf Science*, 46, 609-619.
- 2043 Andersen, J. J. and E. C. Carmack (1984). Observations of Chemical and Physical Fine-structure
2044 in a Strong Pycnocline, Sea of Marmara. *Deep-Sea Res.*, 21, 877-886.
- 2045 Anderson, R.J., 1993: A study of wind stress and heat flux over the open ocean by the inertial-
2046 dissipation method. *J. Phys. Oceanogr.*, 23, 2153-2161
- 2047 Andreas, E.L., L. Mahrt, D. Vickers, 2014: An improved bulk air-sea surface flux algorithm,
2048 including spray-mediated transfer. *Q. J. R. Meteorol. Soc.*, Online publication, 1-Sep-2014.
- 2049 Armi, L., and D. Farmer (1985), The Internal Hydraulics of the Strait of Gibraltar and Associated
2050 Sills and Narrows, *Oceanologica Acta*, 8, 37-46.
- 2051 Armi, L., and D. M. Farmer (1988), The flow of Mediterranean water through the Strait of
2052 Gibraltar, *Progress in Oceanography*, 21(1), 1-103, doi:[http://dx.doi.org/10.1016/0079-
2053 6611\(88\)90055-9](http://dx.doi.org/10.1016/0079-6611(88)90055-9).
- 2054 aus der Beek, T., L. Menzel, R. Rietbroek, L. Fenoglio-Marc, S. Grayek, M. Becker, J. Kusche, and
2055 E. V. Stanev. 2012. Modeling the water resources of the Black and Mediterranean Sea river
2056 basins and their impact on regional mass changes. *J. Geodyn.*, 59-60, 157–167,
2057 doi:10.1016/j.jog.2011.11.011.
- 2058 Baschek, B., U. Send, J. García Lafuente, and J. Candela (2001), Transport estimates in the Strait
2059 of Gibraltar with a tidal inverse model, *Journal of Geophysical Research: Oceans*, 106(C12),
2060 31033-31044, doi:<http://dx.doi.org/10.1029/2000JC000458>.
- 2061 Beaufort, A., Moatar, F., Curie, F., Ducharne, A., Bustillo, V. and Thiéry, D. (2015), River
2062 Temperature Modelling by Strahler Order at the Regional Scale in the Loire River Basin,
2063 France. *River Res. Applic.*, doi: 10.1002/rra.2888
- 2064 Béranger, K., B. Barnier, S. Gulev, and M. Crépon, 2006: Comparing 20 years of precipitation
2065 estimates from different sources over the World Ocean. *Ocean Dyn.*, 56, 104-138.
- 2066 Beşiktepe, Ş. T. (2003). Density Currents in the Two-Layer Flow: An example of Dardanelles
2067 Outflow, *Oceanologica Acta*, 26, p.243-253.
- 2068 Beşiktepe, Ş., E. Özsoy, M. A. Latif ve T. Oğuz (2000). Marmara Denizi'nin hidrografisi ve Dolaşımı,
2069 (Hydrography and circulation of the Marmara Sea), Marmara Sea 2000 Symposium,
2070 İstanbul, Nov. 11-12, 2000, 14 pp. (in Turkish).

- 2071 Beşiktepe, Ş., Özsoy, E. and Ü. Ünlüata (1993). Filling of the Marmara Sea by the Dardanelles
2072 Lower Layer Inflow, *Deep-Sea Res.*, 40, 1815-1838,
- 2073 Beşiktepe, Ş., Sur, H. İ., Özsoy, E., Latif, M. A., Oğuz, T. and Ü. Ünlüata (1994), The Circulation
2074 and Hydrography of the Marmara Sea, *Prog. Oceanogr.*, 34, 285-334.
- 2075 Bethoux, J. P. (1979), Budgets of the Mediterranean Sea. Their dependence on the local climate
2076 and on the characteristics of the Atlantic waters, *Oceanologica Acta*, 2, 157-163.
- 2077 Bignami, F., S. Marullo, R. Santoleri and M. E. Schiano, 1995: Longwave radiation budget in the
2078 Mediterranean Sea. *J. Geophys. Res.*, 100(C2), 2501 - 2514.
- 2079 Bigorre, S.P., R.A. Weller, J. Lord, J.B. Edson, and J.D. Ware, 2013: A surface mooring for air-sea
2080 interaction research in the Gulf Stream. Part II: Analysis of the observations and their
2081 accuracies. *J. Atmos. Ocean. Tech.*, 30, 450-469.
- 2082 Book, J. W., E. Jarosz, J. Chiggiato, and Ş. Beşiktepe (2014), The oceanic response of the Turkish
2083 Straits System to an extreme drop in atmospheric pressure, *J. Geophys. Res. Oceans*, 119,
2084 3629–3644, doi:10.1002/ 2013JC009480.
- 2085 Borghini, M., H.L. Bryden, K. Schroeder, S. Sparnocchia, and A. Vetrano (2014) The
2086 Mediterranean is becoming saltier, *Ocean Sciences*, 10, 693–700, doi:10.5194/os-10-693-
2087 2014
- 2088 Bourassa, M. A., S. T. Gille, D. L. Jackson, J. B. Roberts, and G. A. Wick, 2010: Ocean winds and
2089 turbulent air - sea fluxes inferred from remote sensing. *Oceanography*, 23(4), 36-51.
- 2090 Bourras, D., 2006: Comparison of five derived latent heat flux products to moored buoy data. *J.*
2091 *Clim.*, 19, 6291-6313, doi:10.1175/JCL13977.1
- 2092 Bourras, D., A. Weill, G. Caniaux, L. Eymard, B. Bourlès, S. Letourneur, D. Legain, E. Key, F. Baudin,
2093 B. Piguet, O. Traullé, G. Bouhours, B. Sinardet, J. Barrié, J.P. Vinson, F. Boutet, C. Berthod,
2094 and A. Cléménçon, 2009: Turbulent air-sea fluxes in the Gulf of Guinea during the AMMA
2095 experiment. *J. Geophys. Res.*, 114, C04014, doi:10.1029/2008JC004951.
- 2096 Bouttes N, Gregory JM, Kuhlbrodt T, Smith RS (2013) The drivers of projected North Atlantic sea
2097 level change. *Clim Dyn.* doi:10.1007/s00382-013-1973-8
- 2098 Boutov, D., Á. Peliz, P. M. A. Miranda, P. M. M. Soares, R. M. Cardoso, L. Prieto, J. Ruiz, and J.
2099 García Lafuente (2014), Inter-annual variability and long term predictability of exchanges
2100 through the Strait of Gibraltar, *Global and Planetary Change*, 114(0), 23-37,
2101 doi:<http://dx.doi.org/10.1016/j.gloplacha.2013.12.009>.
- 2102 Bowman, K.P., C.R. Homeyer, and D.G. Stone, 2009: A comparison of oceanic precipitation
2103 estimates in the tropics and subtropics. *J. Appli. Meteor. Climatol.*, 48, 1335-1344.
- 2104 Bretherton, F.P., R.E. Davis, and C.B. Fandry, 1976: A technique for objective analysis and design
2105 of oceanographic experiments applied to MODE-73. *Deep-Sea Research*, 23, 559-582, DOI:
2106 10.1016/0011-7471(76)90001-2.
- 2107 Brisson, A., P. LeBorgne, A. Marsouin, and T. Moreeau, 1994 : Surface irradiances calculated
2108 from METEOSAT sensor data during SOFIA-ASTEX. *Int. J. Remote Sens.*, 15, 197-203.

- 2109 Brut A., D. Legain, P. Durand, and P. Laville, 2004 : A relaxed eddy accumulator for surface flux
2110 measurements on ground-based platforms and aboard research vessels. *J. Atmos. Ocean.*
2111 *Tech.* 21, 3, 411-427.
- 2112 Brut, A., A. Butet, P. Durand, G. Caniaux, and S. Planton, 2005: Air-sea exchanges in the
2113 equatorial area from the EQUALANT99 dataset: Bulk parameterizations of turbulent fluxes
2114 corrected for airflow distortion. *Q. J. R. Meteor. Soc.*, 131, 2497-2538,
2115 doi:10.125/qj.03.185.
- 2116 Bryden, H. L., and H. M. Stommel (1984), Limiting processes that determine basic features of the
2117 circulation in the Mediterranean Sea, *Oceanologica Acta*, 7(3), 289-296.
- 2118 Bryden, H. L., and T. H. Kinder (1991), Steady two-layer exchange through the Strait of Gibraltar,
2119 *Deep Sea Research Part A. Oceanographic Research Papers*, 38, Supplement 1(0), S445-
2120 S463, doi:[http://dx.doi.org/10.1016/S0198-0149\(12\)80020-3](http://dx.doi.org/10.1016/S0198-0149(12)80020-3).
- 2121 Bryden, H. L., J. Candela, and T. H. Kinder (1994), Exchange through the Strait of Gibraltar,
2122 *Progress in Oceanography*, 33(3), 201-248, doi:[http://dx.doi.org/10.1016/0079-
2123 6611\(94\)90028-0](http://dx.doi.org/10.1016/0079-6611(94)90028-0).
- 2124 Bunker A.F., H. Charnock, and R.A. Goldsmith (1982): A note of the heat balance of the
2125 Mediterranean and Red Seas. *Journal of Marine Research*, 40, 73–84.
- 2126 Calafat, F. M., and G. Jordà (2011), A Mediterranean sea level reconstruction (1950–2008) with
2127 error budget estimates, *Global Planet. Change*, 79, 118–133,
2128 doi:10.1016/j.gloplacha.2011.09.003.Calafat et al., 2010;
- 2129 Calafat, F.M., Gomis, D. (2009). Reconstruction of Mediterranean Sea level fields for the period
2130 1945-2000. *Global Planet. Change*, 66(3-4), 225-234.
- 2131 Calafat, F.M., Marcos, M., Gomis, D. (2010). Mass contribution to Mediterranean Sea level
2132 variability for the period 1948–2000. *Global Planet. Change*, 73, 193-201.
- 2133 Candela, J. (2001), Mediterranean water and global circulation, in *Ocean Circulation and Climate*
2134 *Observing and Modelling the Global Ocean*, edited by G. Siedler, J. Gould and J. Church, p.
2135 715, Academic Press
- 2136 Canepa E., Pensieri S., Bozzano R., Faimali M., Traverso P., Cavaleri L. (2015) The ODAS Italia 1
2137 buoy: More than forty years of activity in the Ligurian Sea. *Progress in Oceanography*.
2138 doi:10.1016/j.pocean.2015.04.005
- 2139 Caniaux, G., A. Brut, D. Bourras, H. Giordani, A. Paci, L. Prieur, and G. Reverdin, 2005a: A one
2140 year sea surface heat budget in the northeastern Atlantic basin during the POMME
2141 experiment: 1. Flux estimates. *J. Geophys. Res.*, 110, C07S02, doi:10.1029/2004JC002596.
- 2142 Caniaux, G., S. Belamari, H. Giordani, A. Paci, L. Prieur, and G. Reverdin, 2005b: A one year
2143 sea surface heat budget in the northeastern Atlantic basin during the POMME experiment:
2144 2. Flux correction. *J. Geophys. Res.*, 110, C07S03, doi:10.1029/2004JC002695.
- 2145 Caniaux, G., L. Prieur, H. Giordani, and J.-L. Redelsperger (2017), An inverse method to derive
2146 surface fluxes from the closure of oceanic heat and water budgets: Application to the north-
2147 western Mediterranean Sea, *J. Geophys. Res. Oceans*, 122, doi:10.1002/2016JC012167.

- 2148 Carillo A, Sannino G, Artale V, Ruti PM, Calmanti S, Dell'Aquila A (2012) Steric sea level rise over
 2149 the Mediterranean Sea: present climate and scenario simulations. *Clim Dyn* 39(9–10):2167–
 2150 2184. doi:10.1007/s00382-012-1369-1
- 2151 Carter, D. B. (1956), The water balance of the Mediterranean and Black Seas, *Climatology Drexel*
 2152 *Institute of Technology, Laboratory of Climatology, 9*, 123-175.
- 2153 Çetin, N. (1999). Analysis of the exchange flow through the Bosphorus Strait. M.Sc. Thesis,
 2154 Institute of Marine Sciences, METU, Erdemli, Mersin, 109 pp.
- 2155 Chiggiato, J., E. Jarosz, J. W. Book, J. Dykes, L. Torrisi, P.-M. Poulain, R. Gerin, J. Horstmann, and
 2156 S. Besiktepe (2012), Dynamics of the circulation in the Sea of Marmara: Numerical
 2157 modeling experiments and observations from the Turkish straits system experiment, *Ocean*
 2158 *Dyn.*, 62, 139–159, doi:10.1007/s10236-011-0485-5.
- 2159 Chou, S.H., E. Nelkin, J. Ardizzone, R. M. Atlas, and C. L. Shie, 2003: Surface turbulent heat and
 2160 momentum fluxes over global oceans based on the goddard satellite retrievals, version 2
 2161 (GSSTF2). *J. Clim.*, 16, 3256–3273.
- 2162 Colbo K., and R.A. Weller, 2009: Accuracy of the IMET sensor package in the subtropics. *J. Atmos.*
 2163 *Oceanic Techn.*, 26, 1867-1890, doi:10.1175/2009JTECHO667.1
- 2164 Cowley, R., S. Wijffels, L. Cheng, T. Boyer, and S. Kizu. 2013. Biases in Expendable
 2165 Bathythermograph Data: A New View Based on Historical Side-by-Side Comparisons. *J.*
 2166 *Atmos. Ocean. Technol.* 30: 1195–1225., doi:10.1175/JTECH-D-12-00127.1
- 2167 Cronin, M.F., M. Bourassa, C.A. Clayson, J. Edson, C. Fairall, R.A. Feely, E. Harisson, S. Josey, M.
 2168 Kubota, B.P. Kumar, K. Kutsuwada, B. Large, J. Mathis, M. McPhaden, L. O'Neill, R. Pinker,
 2169 K. Takahashi, H. Tomita, R.A. Weller, L. Yu, and C. Zhang, 2014 : Wind stress and air-sea
 2170 fluxes observations : status, implementation and gaps. *A white paper for the Tropical Pacific*
 2171 *Observing System of 2020 Workshop (TPOS-2020)*.
- 2172 D'Ortenzio, F., D. Iudicone, C. De Boyer Montegut, P. Testor, D. Antoine, S. Marullo, R. Santoleri,
 2173 and G. Madec. 2005. Seasonal variability of the mixed layer depth in the Mediterranean Sea
 2174 as derived from in situ profiles. *Geophys. Res. Lett.* 32: 2–5., doi:10.1029/2005GL022463
- 2175 De Filippi, G. L., Iovenitti, L. and A. Akyarlı (1986). Current analysis in the Marmara-Bosphorus
 2176 Junction. 1st AIOM (Associazione di Ingegneria Offshore e Marina) Congress, Venice, June
 2177 1986, 5-25.
- 2178 DeCosmo, J., K.B. Katsaros, S.D. Smith, R.J. Anderson, W.A. Oost, K. Bumke, and H. Chadwick,
 2179 1996: Air-sea exchange of water vapor and sensible heat: the Humidity Exchange over Sea
 2180 (HEXOS) results. *J. Geophys. Res.*, 101, 12,001-12,016, doi:10.1029/95JC03796.
- 2181 de Rosnay P., J. Polcher, K. Laval, M. Sabre. 2003. Integrated parameterization of irrigation in
 2182 the land surface model ORCHIDEE. Validation over the Indian Peninsula. *Geophysical*
 2183 *Research Letters*, 30(19):1986
- 2184 Döll, P., F. Kaspar, and B. Lehner. 2003. A global hydrological model for deriving water availability
 2185 indicators: model tuning and validation. *J. Hydrol.*, 270, 105–134, doi:10.1016/S0022-
 2186 1694(02)00283-4.

- 2187 Donlon, C.J., I. Robinson, K.S. Casey, J. Vazquez-Cuervo, E. Armstrong, O. Arino, et al. 2007: The
2188 Global Ocean Data Assimilation Experiment High-resolution Sea Surface Temperature Pilot
2189 Project. *Bull. American Meteorol. Soc.*, 88, 1197–1213, doi :10.1175/BAMS-88-8-1197.
- 2190 Donlon, C.J., P.J. Minnett, C. Gentemann, T.J. Nightingale, I.J. Barton, B. Ward, 2002 : Toward
2191 improved validation of satellite sea surface skin temperature measurements for climate
2192 research. *J. Clim.*, 15 (4), 353–369.
- 2193 Dubois C., S. Somot, S. Calmanti, A. Carillo, M. Déqué, A. Dell’Aquila, A. Elizalde-Arellano, S.
2194 Gualdi, D. Jacob, B. Lheveder, L.Li, P. Oddo, G. Sannino, E. Scoccimarro, F. Sevault (2012)
2195 Future projections of the surface heat and water budgets of the Mediterranean sea in an
2196 ensemble of coupled atmosphere-ocean regional climate models, *Clim. Dyn.* 39 (7-8):1859-
2197 1884. DOI 10.1007/s00382-011-1261-4.
- 2198 Ducet, N., Le Traon, P. Y. and P. Gauzelin (1999). Response of the Black Sea mean level to
2199 atmospheric pressure and wind forcing, *J. Mar. Sys.*, 22, 311 – 327.
- 2200 Duchemin B., Maisongrande P., Boulet G., Benhadj I. (2008) , A simple algorithm for yield
2201 estimates: Evaluation for semi-arid irrigated winter wheat monitored with green leaf area
2202 index, *Environmental Modelling & Software*, Volume 23, Issue 7, , Pages 876-892, ISSN
2203 1364-8152, <http://dx.doi.org/10.1016/j.envsoft.2007.10.003>.
- 2204 Dupuis, H., A. Weill, K.B. Katsaros, and P.K. Taylor, 1995: Turbulent heat fluxes by profile and
2205 inertial dissipation methods: analysis of the atmospheric surface layer from shipboard
2206 measurements during the SOFIA/ASTEX and SEMAPHORE experiments. *Ann. Geophys.*, 13,
2207 1065-1074, doi:10.1007/s00585-995-1065-0.
- 2208 Dupuis, H., C. Guérin, D. Hauser, A. Weill, P. Nacass, W. Drennan, S. Cloché, and H. Graber, 2003:
2209 Impact of flow distortion corrections on turbulent fluxes estimated by the inertial
2210 dissipation method during the FETCH experiment on R/V L’Atalante. *J. Geophys. Res.*,
2211 108(C3), 8064, doi:10.1029/2001JC001075.
- 2212 Edson et al., 2013 : On the exchange of momentum over the open ocean. *J. Phys. Oceanogr.*, 43,
2213 1589-1610.
- 2214 Edson, J.B., J.E. Hare, and C.W. Fairall, 1998: Direct covariance flux estimates from moving
2215 platforms at sea. *J. Atmos. Ocean. Tech.*, 15, 547-562, doi:10.1175/1520-0426.
- 2216 Embury, O., C.J. Merchant, and G.K. Corlett, 2012: A reprocessing for climate of sea surface
2217 temperature from the along-track scanning radiometers: initial validation, accounting for
2218 skin and diurnal variability. *Remote Sensing of Environment*, 116, 62-78, doi:
2219 10.1016/j.rse.2011.02.028.
- 2220 Eymard L., S. Planton, P. Durand, C. Le Visage, P.Y. LeTraon, L. Prieur, A. Weill, D. Hauser, J.
2221 Rolland, J. Pelon, F. Baudin, B. Bénech, J.L. Brenguier, G. Caniaux, P. De Mey, E.
2222 Dombrowski, A. Druilhet, H. Dupuis, B. Ferret, C. Flamant, P. Flamant, F. Hernandez, D.
2223 Jourdan, K. Katsaros, D. Lambert, J.M. Lefèvre, P. Le Borgne, B. Le Squere, A. Marsouin,
2224 H. Roquet, J. Tournadre, V. Trouillet, A. Tychensky, B. Zakardjian, 1996: Study of the air-
2225 sea interactions at the mesoscale: the SEMAPHORE experiment. *Ann. Geophysicae.* 14,
2226 986--1015.
- 2227 Eymard, L., G. Caniaux, H. Dupuis, L. Prieur, H. Giordani, R. Troadec, P. Bessemoulin, G.
2228 Lachaud, G. Bouhours, D. Bourras, C. Guérin, P. Le Borgne, A. Brisson, and A. Marsouin,

- 2229 1999: Surface fluxes in the North Atlantic Current during the CATCH/FASTEX experiment.
2230 *Quart. J. Roy. Meteor. Soc.*, 125, 561, 3563-3599.
- 2231 Fairall, C.W., E.F. Bradley, D.P. Rogers, J.B. Edson, and G.S. Young, 1996: Bulk parameterization
2232 of air-sea fluxes in TOGA COARE. *J. Geophys. Res.*, 101, 3747-3767, doi:10.1029/95JC03205.
- 2233 Fairall, C.W., E.F. Bradley, J.E. Hare, A. Grachev, and J.B. Edson, 2003: Bulk parameterization of
2234 air-sea fluxes of TOGA COARE: updates and verification for the COARE algorithm. *J. Clim.*,
2235 16, 571-591.
- 2236 FAO. 2005. AQUASTAT country profile Egypt, FAO, Rome,
2237 <http://www.fao.org/nr/water/aquastat/countries/index.stm>, 06/10/2010
- 2238 Farmer, D. M. and L. Armi (1986). Maximal two-layer exchange over a sill and through the
2239 combination of a sill and contraction with barotropic flow, *J. Fluid Mech.*, 164, 53-76.
- 2240 Fenoglio-Marc L., R. Rietbroek, S. Grayek, M. Becker, J. Kusche, E. Stanev (2012) Water mass
2241 variation in the Mediterranean and Black Sea *Journal of Geodynamics* 59– 60 (2012) 168–
2242 182. doi: 10.1016/j.jog.2012.04.001
- 2243 Garatuza-Payan, J., Shuttleworth, W. J., Encinas, D., McNeil, D. D., Stewart, J. B., deBruin, H. and
2244 Watts, C. (1998), Measurement and modelling evaporation for irrigated crops in north-west
2245 Mexico. *Hydrol. Process.*, 12: 1397–1418. doi: 10.1002/(SICI)1099-
2246 1085(199807)12:9<1397::AID-HYP644>3.0.CO;2-E
- 2247 Garau B., Ruiz S., Zang G.W., Heslop E., Kerfoot J., Pascual A., Tintoré J. 2011. Thermal lag
2248 correction on Slocum CTD glider data, *J. Atmos. Ocean. Tech.* 28: 1065-1074.
- 2249 García Lafuente, J., A. Sánchez Román, C. Naranjo, and J. C. Sánchez Garrido (2011), The very
2250 first transformation of the Mediterranean outflow in the Strait of Gibraltar, *Journal of*
2251 *Geophysical Research: Oceans*, 116(C7), C07010,
2252 doi:<http://dx.doi.org/10.1029/2011JC006967>.
- 2253 García Lafuente, J., E. Álvarez Fanjul, J. M. Vargas, and A. W. Ratsimandresy (2002), Subinertial
2254 variability in the flow through the Strait of Gibraltar, *Journal of Geophysical Research:*
2255 *Oceans*, 107(C10), 3168, doi:<http://dx.doi.org/10.1029/2001JC001104>.
- 2256 García Lafuente, J., E. Bruque Pozas, J. C. Sánchez Garrido, G. Sannino, and S. Sammartino (2013),
2257 The interface mixing layer and the tidal dynamics at the eastern part of the Strait of
2258 Gibraltar, *Journal of Marine Systems*, 117–118(0), 31-42,
2259 doi:<http://dx.doi.org/10.1016/j.jmarsys.2013.02.014>.
- 2260 García Lafuente, J., J. Delgado, A. Sánchez Román, J. Soto, L. Carracedo, and G. Díaz del Río
2261 (2009), Interannual variability of the Mediterranean outflow observed in Espartel sill,
2262 western Strait of Gibraltar, *Journal of Geophysical Research: Oceans*, 114(C10), C10018,
2263 doi:<http://dx.doi.org/10.1029/2009JC005496>.
- 2264 García Lafuente, J., J. M. Vargas, F. Plaza, T. Sarhan, J. Candela, and B. Bascheck (2000), Tide at
2265 the eastern section of the Strait of Gibraltar, *Journal of Geophysical Research: Oceans*,
2266 105(C6), 14197-14213, doi:<http://dx.doi.org/10.1029/2000JC900007>.
- 2267 Garrett C., R. Outerbridge, and K. Thompson (1993): Interannual variability in Mediterranean
2268 heat and buoyancy fluxes. *Journal of Climate*, 6, 900–910.

- 2269 Gentemann, C.L., and P.J. Minnett, 2008: Radiometric measurements of ocean surface thermal
2270 variability. *J. Geophys. Res.*, 113, C08017, doi :10.1029/2007JC004540.
- 2271 Gerin R., Poulain P.-M., Besiktepe S. and Zanasca P. (2013) Surface circulation of the Marmara
2272 Sea as deduced from drifters. *Turkish Journal of Earth Sciences*, 22(6), 919-930.
- 2273 Gilman C. and Garrett C., 1994: Heat flux parameterizations for the Mediterranean Sea: The role
2274 of atmospheric aerosols and constraints from the water budget, *J. Geophys. Res.*, 99(C3),
2275 5119\20135134.
- 2276 Giorgi, F. (2006), Climate change hot-spots, *Geophys. Res. Lett.* 33,
2277 L08707,doi:10.1029/2006GL025734
- 2278 Good, S. A., M. J. Martin and N. A. Rayner, 2013. EN4: quality controlled ocean temperature and
2279 salinity profiles and monthly objective analyses with uncertainty estimates, *Journal of*
2280 *Geophysical Research: Oceans*, 118, 6704-6716, doi:10.1002/2013JC009067
- 2281 Gouretski, V., and K. P. Koltermann (2007), How much is the ocean really warming?, *Geophys.*
2282 *Res. Lett.*, 34, L01610, doi:10.1029/2006GL027834.
- 2283 GRDC : http://www.bafg.de/GRDC/EN/Home/homepage_node.html
- 2284 Greatbatch, R. J., 1994: A note on the representation of steric sea level in models that conserve
2285 volume rather than mass. *J. Geo- phys. Res.*,99, 12 767–12 771
- 2286 Gregg, M. C. and E. Özsoy (1999). Mixing on the Black Sea Shelf North of the Bosphorus, *Geophys.*
2287 *Res. Lett.*, 26, 1869-1872.
- 2288 Gregg, M. C. and E. Özsoy (2002). Flow, Water Mass Changes and Hydraulics in the Bosphorus,
2289 *J. Geophys. Res.*, 107 (C3), 10.1029/2000JC000485.
- 2290 Gregg, M. C., Özsoy E. and M. A. Latif (1999). Quasi-Steady Exchange Flow in the Bosphorus,
2291 *Geophys. Res. Lett.*, 26, 83-86.
- 2292 Gualdi S., S. Somot, W. May, S. Castellari, M. Déqué, M. Adani, V. Artale, A. Bellucci, J. S.
2293 Breitgand, A. Carillo, R. Cornes, A. Dell’Aquila, C. Dubois, D. Efthymiadis, A. Elizalde, L.
2294 Gimeno, C. M. Goodess, A. Harzallah, S. O. Krichak, F. G. Kuglitsch, G. C. Leckebusch, B.
2295 L’Heveder, L. Li, P. Lionello, J. Luterbacher, A. Mariotti, A. Navarra, R. Nieto, K. M. Nissen,
2296 P. Oddo, P. Ruti, A. Sanna, G. Sannino, E. Scoccimarro, F. Sevault, M. V. Struglia, A. Toretì,
2297 U. Ulbrich and E. Xoplaki (2013) Future Climate Projections, In: *Regional Assessment of*
2298 *Climate Change in the Mediterranean*, Volume 1. Eds. Navarra, A., and L. Tubiana, Springer,
2299 Dordrecht, The Netherlands, 53-118.
- 2300 Guimberteau, M., Drapeau, G., Ronchail, J., Sultan, B., Polcher, J., Martinez, J.-M., Prigent, C.,
2301 Guyot, J.-L., Cochonneau, G., Espinoza, J. C., Filizola, N., Fraizy, P., Lavado, W., De Oliveira,
2302 E., Pombosa, R., Noriega, L., and Vauchel, P. 2012. Discharge simulation in the sub-basins
2303 of the Amazon using ORCHIDEE forced by new datasets, *Hydrol. Earth Syst. Sci.*, 16, 911-
2304 935, doi:10.5194/hess-16-911-2012, 2012.
- 2305 Gürses, Ö., Aydoğdu, A., Pinardi, N. and E. Özsoy, 2016. A Finite Element Modeling Study of the
2306 Turkish Straits System, in Özsoy, E. et al. (editors), *The Sea of Marmara - Marine*

- 2307 *Biodiversity, Fisheries, Conservation and Governance*, Turkish Marine Research Foundation
2308 (TÜDAV) Publication #42, 169-184
- 2309 Hamon, M., Beuvier, J., Somot, S., Lellouche, J. M., Greiner, E., Jordà, G., Bouin, M. N., Arsouze,
2310 T., Béranger, K., Sevault, F., Dubois, C., Drevillon, M., and Drillet, Y.: Design and validation
2311 of MEDRYS, a Mediterranean Sea reanalysis over 1992–2013, *Ocean Sci. Discuss.*, 12, 1815-
2312 1867, doi:10.5194/osd-12-1815-2015, 2015.
- 2313 Harzallah A., G. Jordà, C. Dubois, G. Sannino, A. Carillo, L.Li, T. Arsouze, L. Cavichia, J. Beuvier, N.
2314 Akhtar (2015) Long term evolution of heat budget in the Mediterranean Sea from
2315 MedCORDEX forced and coupled simulations. Submitted to *Climate Dynamics*.
- 2316 Hauser D., H. Branger, S. Souffies-Cloch , S. Despiau, W.M. Drennan, H. Dupuis, P. Durand, X.
2317 Durrieu de Madron, C. Estournel, L. Eymard, C. Flamant, H.C. Graber, C. Gu rin, K. Kahma,
2318 G. Lachaud, J.M. Lef vre, J. Pelon, H. Pettersson, B. Pigu t, P. Queff ulou, D. Taillez, J.
2319 Tournadre, and A. Weill, 2003: The FETCH experiment: an overview. *J. Geophys. Res.*,
2320 108(3), doi:10.1029/2001JC001202.
- 2321 Henry, O., M. Ablain, B. Meyssignac, A. Cazenave, D. Masters, R. S. Nerem, and G. Garric (2014)
2322 Effect of the processing methodology on satellite altimetry-based global mean sea level rise
2323 over the Jason-1 operating period. *Journal of Geodesy* Volume 88, Issue 4 , pp 351-361 doi:
2324 10.1007/s00190-013-0687-3
- 2325 Holgate, S. J.; Matthews, A.; Woodworth, P. L.; Rickards, L. J.; Tamisiea, M. E.; Bradshaw, E.;
2326 Foden, P. R.; Gordon, K. M.; Jevrejeva, S.; Pugh, J. 2013 New Data Systems and Products at
2327 the Permanent Service for Mean Sea Level. *Journal of Coastal Research*, 29 (3). 493-504.
2328 10.2112/JCOASTRES-D-12-00175.1
- 2329 Houpert L., P. Testor, X. Durrieu de Madron, S. Somot, F. D'Ortenzio, C. Estournel, H. Lavigne
2330 (2014): Seasonal cycle of the upper-ocean heat rate in the Mediterranean Sea: an
2331 observational approach, *Progress in Oceanography*, accepted, doi:
2332 10.1016/j.pocean.2014.11.004
- 2333 IMS-METU (1999). T rk Boğazlar Sistemi Akıntılarının Değişik Zaman ve Mekan  l eklerinde
2334 İncelenmesi, (A Study of the Turkish Straits System Currents at Various Space – Time Scales),
2335 unpublished report, Institute of Marine Sciences, METU, Erdemli, Mersin, December 1999.
- 2336 IPCC, 2013: *Climate Change 2013: The Physical Science Basis*. Contribution of Working Group I
2337 to the Fifth Assessment Report of the Intergovernmental Panel on Climate Change [Stocker,
2338 T.F., D. Qin, G.-K. Plattner, M. Tignor, S.K. Allen, J. Boschung, A. Nauels, Y. Xia, V. Bex and
2339 P.M. Midgley (eds.)]. Cambridge University Press, Cambridge, United Kingdom and New
2340 York, NY, USA, 1535 pp, doi:10.1017/CBO9781107415324.
- 2341 Ishii, M., and M. Kimoto (2009), Reevaluation of historical ocean heat content variations with
2342 time-varying XBT and MBT depth bias corrections, *J. Oceanogr.*, 65, 287–299
- 2343 Jarosz, E., W. J. Teague, J. W. Book, and Ş. Beşiktepe (2011a). On flow variability in the Bosphorus
2344 Strait, *J. Geophys. Res.*, 116, C08038, doi:10.1029/2010JC006861.

- 2345 Jarosz, E., W. J. Teague, J. W. Book, and Ş. Beşiktepe (2011b). Observed volume fluxes in the
2346 Bosphorus Strait, *Geophys. Res. Lett.*, 38, L21608, doi:10.1029/ 2011GL049557.
- 2347 Jarosz, E., W. J. Teague, J. W. Book, and Ş. T. Beşiktepe (2012), Observations on the
2348 characteristics of the exchange flow in the Dardanelles Strait, *J. Geophys. Res.*, 117, C11012,
2349 doi:10.1029/2012JC008348.
- 2350 Jarosz, E., W. J. Teague, J. W. Book, and S. T. Besiktepe (2013), Observed volume fluxes and
2351 mixing in the Dardanelles Strait, *J. Geophys. Res. Oceans*, 118, 5007–5021,
2352 doi:10.1002/jgrc.20396.
- 2353 Johnson, G. C., and D. P. Chambers (2013), Ocean bottom pressure seasonal cycles and decadal
2354 trends from GRACE Release-05: Ocean circulation implications, *J. Geophys. Res. Oceans* 118
2355 , 4228–4240, doi:10.1002/jgrc.20307.
- 2356 Jordà G., Gomis D., Marcos M. (2012). Comment on “Storm surge frequency reduction in Venice
2357 under climate change” by Troccoli et al. *Climatic Change* 113, Issue 3, pp 1081-1087. doi:
2358 10.1007/s10584-011-0349-5
- 2359 Jordà , G., and D. Gomis (2013), On the interpretation of the steric and mass components of sea
2360 level variability: The case of the Mediterranean basin, *J. Geophys. Res.: Oceans*, 118,
2361 doi:10.1002/jgrc.20060.
- 2362 Jordà, G., Sánchez-Román, A., & Gomis, D. (2017). Reconstruction of transports through the
2363 Strait of Gibraltar from limited observations. *Climate Dynamics*, 48:851.doi:
2364 10.1007/s00382-016-3113-8
- 2365 Jordà G., Houpert L., Gomis D., Bosse A., Testor P., Llasses J., Troupin C. (2016). Mapping the
2366 temperature and salinity of the Mediterranean Sea from 1950 to present. Product
2367 description and sources of uncertainty. Submitted to *Ocean Science*
- 2368 Josey, S. A. and S. R. Smith, 2006: Guidelines for Evaluation of Air-Sea Heat, Freshwater and
2369 Momentum Flux Datasets, CLIVAR Global Synthesis and Observations Panel (GSOP) White
2370 Paper, pp.14. t: <http://www.clivar.org/sites/default/files/documents/gsofpg.pdf>
- 2371 Kanarska, Y., and V. Maderich (2008), Modelling of seasonal exchange flows through the
2372 Dardanelles Strait, *Estuarine Coastal Shelf Sci.*, 79,449–458, doi:10.1016/j.ecss.2008.04.019
- 2373 Kent, E.C., D.I. Berry, J. Prytherch, and J.B. Roberts, 2014: A comparison of global marine surface
2374 humidity datasets from in situ observations and atmospheric reanalysis. *Int. J. Climatol.*, 34,
2375 355-376., doi :10.1002/joc.3691.
- 2376 Lacombe, H., Gascard, J.-C., Gonella, J., and Béthoux, J.-P. (1981). Response of the
2377 Mediterranean to the water and energy fluxes across its surface, on seasonal and
2378 interannual scales. *Oceanol. Acta*, 4:247-255.
- 2379 Lacombe, H., and C. Richez (1982), The Regime of the Strait of Gibraltar, in *Elsevier*
2380 *Oceanography Series*, edited by C. J. N. Jacques, pp. 13-73, Elsevier,
2381 doi:[http://dx.doi.org/10.1016/S0422-9894\(08\)71237-6](http://dx.doi.org/10.1016/S0422-9894(08)71237-6).

- 2382 Larsen, S. E., and Coauthors, 2000: AUTOFLUX: An autonomous flux package for measuring the
2383 air–sea flux momentum, heavy, water vapour and carbon dioxide. Proc. EUROCEAN 2000
2384 Conf., Hamburg, Germany.
- 2385 Latif, M. A., Özsoy, E., Oğuz, T. and Ünlüata, Ü. (1991). Observations of the Mediterranean inflow
2386 into the Black Sea, *Deep-Sea Res.*, 38 (Suppl. 2), 711–723.
- 2387 LeBorgne, P., G. Legendre, and A. Marsouin, 2007: Validation of the OSI SAF radiative fluxes over
2388 the equatorial Atlantic during AMMA experiment. Proceedings of the 2003 EUMETSAT
2389 Meteorological Satellite Conference, Weimar, Germany, 512-519.
- 2390 Llasses J., G. Jordà, D. Gomis (2015) Skills of different hydrographic networks in capturing
2391 changes in the Mediterranean Sea at climate scales. *Clim. Res.* Vol. 63: 1–18, 2015
2392 doi:10.3354/cr01270
- 2393 Ludwig, W., E. Dumont, M. Meybeck, and . Heussner. (2009) ‘River Discharges of Water and
2394 Nutrients to the Mediterranean and Black Sea: Major Drivers for Ecosystem Changes during
2395 Past and Future Decades?’. *Progress in Oceanography* 80, no. 3–4: 199–217.
2396 doi:10.1016/j.pocean.2009.02.001.
- 2397 Lueck, R. G., and J. J. Picklo, 1990: Thermal inertia of conductivity cells: Observations with a Sea-
2398 Bird cell. *J. Atmos. Oceanic Technol.*, 7, 756–768.
- 2399 Macdonald A.M., Candela J. and Bryden H.L. (1994): In La Violette (Ed.), An estimate of the net
2400 heat transport flux through the Strait of Gibraltar, Seasonal and Interannual variability of the
2401 Western Mediterranean Sea, *Coastal Estuarine Stud.*, Vol. 46, AGU, Washington, D.C., pp. 12-
2402 32.
- 2403 Macias DM, Garcia-Gorriz E and Stips A (2015) Productivity changes in the Mediterranean Sea
2404 for the twenty-first century in response to changes in the regional atmospheric forcing.
2405 *Front. Mar. Sci.* 2:79. doi: 10.3389/fmars.2015.00079
- 2406 Margat J. (2008).“L'eau des Méditerranéens”, L'Harmattan, 288 pages, 2008, ISBN : 978-2-296-
2407 06293
- 2408 Mariotti A, Struglia MV, Zeng N, Lau KM (2002) The hydrological cycle in the Mediterranean
2409 Region and implications for the water budget of the Mediterranean Sea. *J Climate* 15:1674–
2410 1690
- 2411 Mariotti A, Zeng N, Yoon J, Artale V, Navarra A, Alpert P, Li L (2008) Mediterranean water cycle
2412 changes: transition to drier 21st century conditions in observations and CMIP3 simulations.
2413 *Env Res Lett.* Doi:10.1088/1748-9326/3/044001
- 2414 Mariotti A, Pan Y., Zeng N, Alessandri A. (2015) Long-term climate change in the Mediterranean
2415 region in the midst of decadal variability, *Climate Dynamics*.
- 2416 Marullo S. , B. Buongiorno Nardelli, M. Guarracino, and R. Santoleri, 2007: Observing the
2417 Mediterranean Sea from space: 21 years of Pathfinder-AVHRR sea surface temperatures
2418 (1985 to 2005): re-analysis and validation. *Ocean Sci.*, 3, 299–310
- 2419 Marullo, S., R. Santoleri, D. Ciani, P. Le Borgne, S. Péré, N. Pinardi, M. Tonani, and G. Nardone,
2420 2014 : Combining model and geostationary satellite data to reconstruct hourly SST filed

- 2421 over the Mediterranean Sea. *Remote Sensing of Environment*, 146, 11-23, doi:
2422 10.1016/j.rse.2013.11.001.
- 2423 Mémery, L., G. Reverdin, J. Paillet, and A. Oschlies, 2005: Intyroduction to the POMME special
2424 section: Therocline ventilation and biogeochemical tracer distribution in the northeast
2425 Atlantic Ocean and impact of mesoscale dynamics. *J. Geophys Res.*,
2426 doi:10.1029/2005JC002976.
- 2427 Merz, A. and L. Möller (1928). *Hydrographische Untersuchungen in Bosporus und Dardanellen*,
2428 Alfred Merz. Bearb. von Lotte Möller, Berlin : E. S. Mittler & Sohn, 1 Atlas of 16 charts, 3
2429 figures, 8 tables of sizes 47 x 39 cm and text 133p.
- 2430 Meyssignac B., F. M. Calafat, S. Somot, V. Rupolo, P. Stocchi, W. Llovel, A. Cazenave (2011) Two-
2431 dimensional reconstruction of the Mediterranean sea level over 1970–2006 from tide gage
2432 data and regional ocean circulation model outputs. *Global and Planetary Change* 77 (1), 49-
2433 61
- 2434 Millot C., Candela J., Fuda J-L, Tber Y. (2006) Large warming and salinification of the
2435 Mediterranean outflow due to changes in its composition. *Deep-Sea Research I* 53 , 656–
2436 666
- 2437 Monin, A.S., and A.M. Obukhov, 1954: Basic laws of turbulent mixing in the surface layer of the
2438 atmosphere. *Trudy Geofiz. Inst. Akad. Nauk SSR*, 24, 1-24.
- 2439 Morison, J., R. Andersen, N. Larson, E. D'Asaro, and T. Boyd, 1994: The correction for thermal-
2440 lag effects in Sea-Bird CTD data. *J. Atmos. Oceanic Technol.*,11, 1151–1164
- 2441 Naranjo, C., J. Garcia Lafuente, G. Sannino, and J. C. Sanchez Garrido (2014), How much do tides
2442 affect the circulation of the Mediterranean Sea? From local processes in the Strait of
2443 Gibraltar to basin-scale effects, *Progress in Oceanography*(0),
2444 doi:<http://dx.doi.org/10.1016/j.pocean.2014.06.005>.
- 2445 Nielsen, J. N. (1912), *Hydrography of the Mediterranean and Adjacent Waters*.
- 2446 Nixon, S. W. 2003. Replacing the Nile: Are Anthropogenic Nutrients Providing the Fertility Once
2447 Brought to the Mediterranean by a Great River? *AMBIO J. Hum. Environ.*, 32, 30–39,
2448 doi:10.1579/0044-7447-32.1.30.
- 2449 Oğuz, T., Özsoy, E., Latif, M. A., Sur, H. İ. and Ünlüata Ü. (1990). Modelling of Hydraulically
2450 Controlled Exchange Flow in the Bosphorus Strait, *Journal of Physical Oceanography*, 20,
2451 945-965.
- 2452 Özsoy, E., Latif, M. A., Beşiktepe, S., Çetin, N., Gregg, N. Belokopytov, V., Goryachkin, Y. and V.
2453 Diaconu (1998). The Bosphorus Strait: Exchange Fluxes, Currents and Sea-Level Changes,
2454 in: L. Ivanov and T. Oğuz (editors), *Ecosystem Modeling as a Management Tool for the Black
2455 Sea*, NATO Science Series 2: Environmental Security 47, Kluwer Academic Publishers,
2456 Dordrecht, vol. 1, 367 pp + vol. 2, 385 pp.
- 2457 Özsoy, E., Beşiktepe, Ş., Gündüz, M. and S. Sancak (1999). Türk Boğazlar Sistemi Akıntılarının
2458 Değişik Zaman ve Mekan Ölçeklerinde İncelenmesi, ODTÜ Deniz Bilimleri Enstitüsü, TURBO

- 2459 Projesi, İkinci Ara Rapor (A Study of the Currents in the Turkish Straits System at Different
2460 Time and Space Scales), 11p + 144 figs. [in Turkish].
- 2461 Özsoy E., Di Iorio D., Gregg M. and Backhaus J. (2001). Mixing in the Bosphorus Strait and the
2462 Black Sea Continental Shelf: Observations and a Model of the Dense Water Outflow, *J. Mar.*
2463 *Sys.*, 31, 99-135.
- 2464 Özsoy, E., Sözer, A., Gündüz, M., Yücel, İ., Yağcı, B., Mert, İ., Yıldız, H., Simav, M. and M. Elge
2465 (2009). Meteorology and Oceanography Network of Excellence (MOMA) – Observation and
2466 Model Forecast Systems, 3rd National Defense Applications Modelling and Simulation
2467 Conference, Ankara, 17-18 June 2009, 27 pp.
- 2468 Özsoy, E., Gürses, Ö. and E. Tutsak (2015). Turkish Straits System and Southern Black Sea:
2469 Exchange. Mixing and Shelf / Canyon Interactions, EGU General Assembly 2015, Vienna,
2470 Geophysical Research Abstracts Vol. 17.
- 2471 Özsoy, E. and H. Altiok (2016a). A Review of Hydrography of the Turkish Straits System, in Özsoy,
2472 E. et al. (editors), *The Sea of Marmara - Marine Biodiversity, Fisheries, Conservation and*
2473 *Governance*, Turkish Marine Research Foundation (TÜDAV) Publication #42, 13-41.
- 2474 Özsoy, E. and H. Altiok (2016b). A Review of Water Fluxes across the Turkish Straits System, in
2475 Özsoy E. et al. (editors), *The Sea of Marmara - Marine Biodiversity, Fisheries, Conservation*
2476 *and Governance*, Turkish Marine Research Foundation (TÜDAV) Publication #42, 42-61.
- 2477 Özsoy, E., Latif, M. A., and Ş. Beşiktepe (2016c). A Review of Bosphorus Measurements during
2478 the TÜRBO Campaign (1999-2000), in Özsoy, E. et al. (editors), *The Sea of Marmara - Marine*
2479 *Biodiversity, Fisheries, Conservation and Governance*, Turkish Marine Research Foundation
2480 (TÜDAV) Publication #42, 79-95.
- 2481 Pektaş, H. (1953). Surface current in the Bosphorus and the Sea of Marmara. *Hydrobiology*, 1(4).
2482 Hydrobiology Research Institute, University of İstanbul Publications, 154–169 [in Turkish].
- 2483 Peliz, A., D. Boutov, R. M. Cardoso, J. Delgado, and P. M. M. Soares (2013), The Gulf of Cadiz–
2484 Alboran Sea sub-basin: Model setup, exchange and seasonal variability, *Ocean Modelling*,
2485 61(0), 49-67, doi:<http://dx.doi.org/10.1016/j.ocemod.2012.10.007>.
- 2486 Peneva, E., E. Stanev, V. Belokopytov, and P.-Y. Le Traon (2001). Water Transport in the
2487 Bosphorus Straits Estimated from Hydro-meteorological and Altimeter Data: Seasonal to
2488 Decadal Variability. *J. Mar. Sys.*, 31, 21-33.
- 2489 Pettenuzzo, D., W. G. Large, and N. Pinardi (2010), On the corrections of ERA-40 surface flux
2490 products consistent with the Mediterranean heat and water budgets and the connection
2491 between basin surface total heat flux and NAO, *J. Geophys. Res.*, 115, C06022,
2492 doi:10.1029/2009JC005631.
- 2493 Pfeifroth, U., R. Mueller, and B. Ahrens, 2013: Evaluation of satellite-based and reanalysis
2494 precipitation data in the tropical Pacific. *J. App. Met. and Clim.*, 52, 634-644,
2495 doi:10.1175/JAMC-D-12-049.1

- 2496 Poulain, P.-M., R. Barbanti, J. Font, A. Cruzado, C. Millot, I. Gertman, A. Griffa, A. Molcard, V.
 2497 Rupolo, S. Le Bras, and L. Petit de la Villeon (2007)
 2498 MedArgo: a drifting profiler program in the Mediterranean Sea. *Ocean Sci.*, 3, 379-395.
- 2499 Reid, J. L., On the contribution of the Mediterranean Sea outflow to the Norwegian-Greenland
 2500 Sea, *Deep Sea Res., Part A*, 26, 1199- 1223, 197
- 2501 Rixen M., et al. (2005), The Western Mediterranean Deep Water: A proxy for climate change,
 2502 *Geophys. Res. Lett.*, 32, L12608, doi:10.1029/2005GL022702.
- 2503 Rohling, E. J. and Bryden, H. L. (1992) Man-induced salinity and temperature increases in
 2504 western Mediterranean deep water. *Journal of Geophysical Research*, 97, 11191–11198.
- 2505 Romanou, A., G. Tselioudis, C.S. Zerefos, C.-A. Clayson, J.A. Curry, and A. Andersson, 2010:
 2506 Evaporation-precipitation variability over the Mediterranean and the Black Seas from
 2507 satellite and reanalysis estimates. *J. Climate*, 23, 5268-5287, doi:10.1175/2010JCLI3525.1.
- 2508 Ruti PM et al. (32 coauthors) (2015) MED-CORDEX initiative for the Mediterranean Climate
 2509 studies. *Bulletin of the American Meteorological Society*. doi: 10.1175/BAMS-D-14-00176.1
- 2510 Sammartino, S., J. García Lafuente, C. Naranjo, J.C. Sánchez Garrido, R. Sánchez Leal, and A.
 2511 Sánchez Román (2015). Ten years of marine current measurements in Espartel Sill, Strait of
 2512 Gibraltar, *submitted to Journal of Geophysical Research*
- 2513 Sammartino, S., J. García Lafuente, J. C. Sánchez Garrido, F. J. De los Santos, E. Álvarez Fanjul, C.
 2514 Naranjo, M. Bruno, and C. Calero (2014), A numerical model analysis of the tidal flows in
 2515 the Bay of Algeciras, Strait of Gibraltar, *Continental Shelf Research*, 72(0), 34-46,
 2516 doi:<http://dx.doi.org/10.1016/j.csr.2013.11.002>.
- 2517 Sánchez Garrido, J. C., G. Sannino, L. Liberti, J. García Lafuente, and L. Pratt (2011), Numerical
 2518 modeling of three-dimensional stratified tidal flow over Camarinal Sill, Strait of Gibraltar,
 2519 *Journal of Geophysical Research: Oceans*, 116(C12), C12026,
 2520 doi:<http://dx.doi.org/10.1029/2011JC007093>.
- 2521 Sánchez Garrido, J. C., J. García Lafuente, E. Álvarez Fanjul, M. G. Sotillo, and F. J. de los Santos
 2522 (2013), What does cause the collapse of the Western Alboran Gyre? Results of an
 2523 operational ocean model, *Progress in Oceanography*, 116(0), 142-153,
 2524 doi:<http://dx.doi.org/10.1016/j.pocean.2013.07.002>.
- 2525 Sánchez Román, A., G. Sannino, J. García Lafuente, A. Carillo, and F. Criado Aldeanueva (2009),
 2526 Transport estimates at the western section of the Strait of Gibraltar: A combined
 2527 experimental and numerical modeling study, *Journal of Geophysical Research: Oceans*,
 2528 114(C6), C06002, doi:<http://dx.doi.org/10.1029/2008JC005023>.
- 2529 Sánchez-Gómez, E., S. Somot, S.A. Josey, C. Dubois, N. Elguindi, and M. Déqué, (2011). Evaluation
 2530 of Mediterranean Sea water and heat budgets simulated by an ensemble of high resolution
 2531 regional climate models. *Climate Dynamics*, 37, 2067-2086. Doi: 10.1007/s00382-011-
 2532 1012-6.
- 2533 Sannino, G., A. Bargagli, and V. Artale (2004), Numerical modeling of the semidiurnal tidal
 2534 exchange through the Strait of Gibraltar, *Journal of Geophysical Research: Oceans*, 109(C5),
 2535 C05011, doi:<http://dx.doi.org/10.1029/2003JC002057>.

- 2536 Sannino, G., A. Carillo, and V. Artale (2007), Three-layer view of transports and hydraulics in the
 2537 Strait of Gibraltar: A three-dimensional model study, *Journal of Geophysical Research:*
 2538 *Oceans*, 112(C3), C03010, doi:<http://dx.doi.org/10.1029/2006JC003717>.
- 2539 Sannino, G., L. Pratt, and A. Carillo (2009), Hydraulic Criticality of the Exchange Flow through the
 2540 Strait of Gibraltar, *Journal of Physical Oceanography*, 39(11), 2779-2799,
 2541 doi:<http://dx.doi.org/10.1175/2009JPO4075.1>.
- 2542 Sannino, G., Garrido, J.C.S.,Liberti, L., Pratt, L. Exchange flow through the strait of gibraltar as
 2543 simulated by a s-coordinate hydrostatic model and a z-coordinate non hydrostatic model
 2544 (2014a). In book: The Mediterranean Sea: Temporal Variability and Spatial Patterns.
 2545 Editors: G. Borzelli, M. Gacic, P. Lionello, P. Malanotte-Rizzoli. American Geophysical Union.
 2546 pp. 25-50. ISBN: 978-1-118-84734-3.
- 2547 Sannino, G., Sözer, A. and E. Özsoy (2014b). MOTUS: A High-Resolution Modelling Study of the
 2548 Turkish Straits System Utilizing HPC, PRACE project report, 35p.
- 2549 Sannino, G., Carillo, A., Pisacane, G., Naranjo, C. On the relevance of tidal forcing in modelling
 2550 the Mediterranean thermohaline circulation (2015) *Progress in Oceanography*, 134, pp.
 2551 304-329. DOI: 10.1016/j.pocean.2015.03.002
- 2552 Sannino, G., Sözer, A. and E. Özsoy (2017). A High-Resolution Modelling Study of the Turkish
 2553 Straits System. *Ocean Dynamics* 67: 397. doi:10.1007/s10236-017-1039-2
- 2554 Schluessel, P., L. Schanz, and G. Englisch, 1995: Retrieval of latent heat flux and longwave
 2555 irradiance at the sea surface from SSM/I and AVHRR measurements. *Adv. Space Res.*, 16,
 2556 10,107- 10,116
- 2557 Schott, G. (1915), Die Gewasser des Mittelmeeres, *Annalen der Hydrographie und Maritimen*
 2558 *Meteorologie*, 43, 63-79.
- 2559 Schroeder K., S.A. Josey, M. Herrmann, L. Grignon, G.P. Gasparini, and H.L. Bryden (2010) Abrupt
 2560 warming and salting of the Western Mediterranean Deep Water after 2005: Atmospheric
 2561 forcings and lateral advection, *Journal of Geophysical Research*, 115, C08029,
 2562 doi:10.1029/2009JC005749, 2010.
- 2563 Schroeder, K., García-Lafuente, J., Josey, S. A., Artale, V., Nardelli, B. B., Carrillo, A., Gačić, M,
 2564 Gasparini, G. P., Herrmann, M., Lionello, P., Ludwig, W., Millot, C., Özsoy, E., Pisacane, G.,
 2565 Sánchez-Garrido, J. C., Sannino, G., Santoleri, R., Somot, S., Struglia, M., Stanev, E., Taupier-
 2566 Letage, I., Tsimplis, M. N., Vargas-Yáñez, M., Zervakis, V., G. Zodiatis (2012). Chapter 3:
 2567 *Circulation of the Mediterranean Sea and its Variability*, In: Lionello, P. (ed.), *The Climate of*
 2568 *the Mediterranean Region - From the past to the future*, Elsevier, 592 p.
- 2569 Schroeder, K., J. Garcia-Lafuente, S. A. Josey & 22 Co-authors 2012: ‘Circulation of the
 2570 Mediterranean Sea and its Variability’ in *The Climate of the Mediterranean: From the Past*
 2571 *to the Future*, 75 pp., P. Lionello (ed.), Elsevier.
- 2572 Schroeder K., Millot C., Bengara L., Ben Ismail S., Bensi M., Borghini M., Budillon G., Cardin V.,
 2573 Coppola L., Curtil C., Drago A., El Moumni B., Font J., Fuda J.L., García-Lafuente J., Gasparini
 2574 G.P., Kontoyiannis H., Lefevre D., Puig P., Raimbault P., Rougier G., Salat J., Sammari C.,
 2575 Sánchez Garrido J.C., Sanchez-Roman A., Sparnocchia S., Tamburini C., Taupier-Letage I.,
 2576 Theocharis A., Vargas-Yáñez M. and Vetrano A., 2013. Long-term monitoring programme of

- 2577 the hydrological variability in the Mediterranean Sea: a first overview of the
2578 HYDROCHANGES network. *Ocean Sci.*, 9: 301-324, doi:10.5194/os-9-301-2013.
- 2579 Schroeder, K., T. Tanhua, H.L. Bryden, M. Alvarez, J. Chiggiato, and S. Aracri. 2015.
2580 Mediterranean Sea Ship-based Hydrographic Investigations Program (Med-SHIP).
2581 *Oceanography* 28(3), <http://dx.doi.org/10.5670/oceanog.2015.71>.
- 2582 Schroeder, K., J. Chiggiato, H.L. Bryden, M. Borghini, S. Ben Ismail (2016) Abrupt climate shift in
2583 the Western Mediterranean Sea. *Sci. Rep.* 6, 23009. doi:10.1038/srep23009
- 2584 Schroeder, K., J. Chiggiato, S. A. Josey, M. Borghini, S. Aracri, S. Sparnocchia (2017) Rapid
2585 response to climate change in a marginal sea. *Sci. Rep.* 7, 4065. doi:10.1038/s41598-017-
2586 04455-5
- 2587 Serreze, M. C., A. Barrett, and F. Lo, 2005: Northern high latitude precipitation as depicted by
2588 atmospheric reanalyses and satellite retrievals, *Mon. Weather Rev.*, 133, 3407–3430.
- 2589 Simmons, H.L., and I.V. Polyakov, 2004: Restoring and flux adjustment in simulating variability
2590 of an idealised ocean. *Geophys. Res. Letters*, 31, L16301, doi:10.1029/2004GL020197.
- 2591 Smith, S. R., 2004: Focusing on improving automated meteorological observations from ships.
2592 *EOS, Trans Amer. Geophys. Union*, 85, 319.
- 2593 Smith, S.D., 1980: Wind stress and heat flux over the ocean in gale force winds. *J. Phys.*
2594 *Oceanogr.*, 10, 709-726.
- 2595 Somot S, Sevault F, Déqué M (2006) Transient climate change scenario simulation of the
2596 Mediterranean Sea for the twenty-first century using a high-resolution ocean circulation
2597 model. *Clim Dyn* 27(7–8):851–879
- 2598 Somot S, Sevault F, Déqué M, Crépon M (2008) 21st century climate change scenario for the
2599 Mediterranean using a coupled atmosphere-ocean regional climate model. *Global*
2600 *Planetary Change* 63(2–3):112–126. doi:10.1016/j.gloplacha.2007.10.003
- 2601 Soto-Navarro, J., F. Criado Aldeanueva, J. García Lafuente, and A. Sánchez Román (2010),
2602 Estimation of the Atlantic inflow through the Strait of Gibraltar from climatological and in
2603 situ data, *Journal of Geophysical Research: Oceans*, 115(C10), C10023,
2604 doi:<http://dx.doi.org/10.1029/2010JC006302>.
- 2605 Sözer, A. (2013). Numerical Modeling of the Bosphorus Exchange Flow Dynamics, Ph.D. thesis,
2606 Institute of Marine Sciences, Middle East Technical University, Erdemli, Mersin, Turkey.
- 2607 Sözer. A. and E. Özsoy (2017). Modeling of the Bosphorus Exchange Flow Dynamics, *Ocean*
2608 *Dynamics*, online, 67(3-4), 321-343. DOI 10.1007/s10236-016-1026-z
- 2609 Stanev, E. V., and E. L. Peneva (2002). Regional sea level response to global climatic change:
2610 Black Sea examples, *Global and Planetary Change*, 32, 33-47.
- 2611 Stuart-Menteth, A.C., I.S. Robinson, and P.G. Challenor, 2003: A global study of diurnal warming
2612 using satellite-derived sea surface temperature. *J. Geophys. Res.*, 108, 3155,
2613 doi:10.1029/2002JC001534.

- 2614 Sverdrup, H.U., M.W. Johnson and R.H. Fleming, 1942: The Oceans, Their Physics, Chemistry, and
2615 General Biology . Prentice Hall, New York, 1087 pp.
- 2616 Tanhua, T., D. Hainbucher, K. Schroeder, V. Cardin, M. Alvarez and G. Civitarese. 2013. The
2617 Mediterranean Sea system: A review and an introduction to the special issue. *Ocean*
2618 *Science* 9:789–803, <http://dx.doi.org/10.5194/os-9-789-2013>.
- 2619 Tsimplis, M. N., and H. L. Bryden (2000), Estimation of the transports through the Strait of
2620 Gibraltar, *Deep Sea Research Part I: Oceanographic Research Papers*, 47(12), 2219-2242,
2621 doi:[http://dx.doi.org/10.1016/S0967-0637\(00\)00024-8](http://dx.doi.org/10.1016/S0967-0637(00)00024-8).
- 2622 Tsimplis, M. N., F. M. Calafat, M. Marcos, G. Jordà , D. Gomis, L. Fenoglio-Marc, M. V. Struglia, S.
2623 A. Josey, and D. P. Chambers (2013), The effect of the NAO on sea level and on mass changes
2624 in the Mediterranean Sea, *J. Geophys. Res. Oceans*, 118, doi:10.1002/jgrc.20078.
- 2625 Tuğrul, S., Beşiktepe, Ş. B., Salihoğlu, İ. (2002) "Nutrient exchange fluxes between the Aegean
2626 and Black Seas through the Marmara Sea". *Medit. Marine Sciences*, 3, 33-42.
- 2627 Tutsak, E. (2013). Analyses of marine and Atmospheric Observations along the Turkish Coast,
2628 Institute of Marine Sciences, Middle East Technical University, Erdemli, Mersin, Turkey,
2629 Masters thesis, 125 pp.
- 2630 Tutsak, E., Gündüz, M. and E. Özsoy (2016). Sea level and fixed ADCP Measurements from
2631 Turkish Straits System During 2008-2011, in Özsoy E. et al. (editors), *The Sea of Marmara -*
2632 *Marine Biodiversity, Fisheries, Conservation and Governance*, Turkish Marine Research
2633 Foundation (TÜDAV) Publication #42, 62-78.
- 2634 Ünlüata, Ü., Oğuz, T., Latif, M. A., and E. Özsoy, (1990). On the Physical Oceanography of the
2635 Turkish Straits, in: *The Physical Oceanography of Sea Straits*, L. J. Pratt (editor), NATO/ASI
2636 Series, Kluwer, Dordrecht, 25-60.
- 2637 Vargas, J. M., J. García Lafuente, J. Candela, and A. J. Sánchez (2006), Fortnightly and monthly
2638 variability of the exchange through the Strait of Gibraltar, *Progress in Oceanography*, 70(2–
2639 4), 466-485, doi:[10.1016/j.pocean.2006.07.001](http://dx.doi.org/10.1016/j.pocean.2006.07.001)
- 2640 Vargas-Yáñez et al, 2009. Warming and salting in the Western Mediterranean during the second
2641 half of the 20th century: Inconsistencies, unknowns and the effect of data processing. *Sci.*
2642 *Mar.* 73(1).doi: 10.3989/scimar.2009.73n1007
- 2643 Vargas-Yáñez, M., P. Zunino, A. Benali, M. Delpy, F. Pastre, F. Moya, M. C. García-Martínez, and
2644 E. Tel (2010), How much is the western Mediterranean really warming and salting?, *J.*
2645 *Geophys. Res.*, 115, C04001, doi:10.1029/2009JC005816.
- 2646 Vargas-Yáñez et al, 2012. The effect of interpolation methods in temperature and salinity trends
2647 in the Western Mediterranean. *Medit. Mar. Sci.*, 13/1,118-125 doi: 10.12681/mms.28
- 2648 Vörösmarty, C.J., B. Fekete, and B.A. Tucker. 1998. River Discharge Database, Version 1.1 (RivDIS
2649 v1.0 supplement). Available through the Institute for the Study of Earth, Oceans, and Space
2650 / University of New Hampshire, Durham NH (USA). Wade, M., G. Caniaux, and Y. DuPenhoat,
2651 2011 : Variability of the mixed layer heat budget in the Eastern Equatorial Atlantic during
2652 2005-2007 as inferred using Argo floats. *J. Geophys. Res.*, 116, C08006,
2653 doi:10.1029/2010JC006683.

- 2654 Webster, P.J., and R. Lukas, 1992: TOGA COARE, the coupled ocean and atmosphere response
2655 experiment. *Bull. Amer. Meteorol. Soc.*, 73, 1377-1416.
- 2656 Weedon, G. P., and Coauthors, 2011: Creation of the WATCH Forcing Data and Its Use to Assess
2657 Global and Regional Reference Crop Evaporation over Land during the Twentieth Century.
2658 *J. Hydrometeorol.*, 12, 823–848, doi:10.1175/2011JHM1369.1.
- 2659 Weedon, G. P., G. Balsamo, N. Bellouin, S. Gomes, M. J. Best, and P. Viterbo. 2014. The WFDEI
2660 Meteorological Forcing Data Set: WATCH Forcing Data Methodology Applied to ERA-Interim
2661 Reanalysis Data. *Water Resources Research* 50, no. 9 (September 2014): 7505–14.
2662 doi:10.1002/2014WR015638.
- 2663 Weill, A., F. Baudin, H. Dupuis, L. Eymard, J.P. Frangi, E. Gérard, P. Durand, B. Bénech, J. Dessens,
2664 A. Druilhet, A. Réchou, P. Flamand, S. Elouragini, R. Valentin, G. Sèze, J. Pelon, C. Flamant,
2665 J.L. Brenguier, S. Planton, J. Rolland, A. Brisson, P. LeBorgne, A. Marsouin, T. Moreau, K.
2666 Katsaros, R. Monis, P. Queffeuilou, J. Tournadre, P.K. Taylor, E. Kent, R. Pascal, P. Schibler,
2667 F. Parol, J. Desclotres, J.Y. Ballois, M. André, and M. Charpentier, 1995: SOFIA 1992
2668 experiment during ASTEX. *The Global Atmos. and Ocean System*, 3, 355-395.
- 2669 Weill, A., L. Eymard, G. Caniaux, D. Hauser, S. Planton, H. Dupuis, A. Brut, C. Guérin, P. Nacass,
2670 A. Butet, S. Cloché, R. Pedreros, P. Durand, D. Bourras, H. Giordani, G. Lachaud, and G.
2671 Bouhours, 2003: Toward a better determination of turbulent air-sea fluxes from several
2672 experiments. *J. Clim.*, 16, 4, 600–618.
- 2673 Weissman, D.E., B.W. Stiles, S.M. Hristova-Veleva, D.G. Long, D.K. Smith, K.A. Hilburn, and W.L.
2674 Jones, 2012: Challenges to satellite sensors of ocean winds: addressing precipitation effects.
2675 *J. Atmos. Ocean. Tech.*, 29, 356-374.
- 2676 Weller R.A., S.P. Bigorre, J. Lord, J.D. Ware, and J.B. Edson, 2012: A surface mooring for air-sea
2677 interaction in the Gulf Stream. Part I: Mooring design and instrumentation. *J. Atmos. Ocean.*
2678 *Tech.*, 29, 1363-1376.
- 2679 Wöppelmann, M. Marcos, A. Coulomb, B. Martín Míguez, P. Bonnetain, C. Boucher, M. Gravelle,
2680 B. Simon, P. Tiphaneauet (2014), Rescue of the historical sea level record of Marseille
2681 (France) from 1885 to 1988 and its extension back to 1849–1851. *Journal of Geodesy*
2682 Volume 88, Issue 9, pp 869-885, doi: 10.1007/s00190-014-0728-6
- 2683 Xie, P., and P. A. Arkin, 1996: Global precipitation: a 17-year monthly analysis based on gauge
2684 observations, satellite estimates, and numerical model outputs. *Bull. Amer. Meteor. Soc.*,
2685 78, 2539-2558.
- 2686 Yelland, M.J., B.I. Moat, R.W. Pascal, and D.I. Berry, 2002: CFD model estimates of the airflow
2687 distortion over research ships and the impact on momentum flux measurements. *J. Atmos.*
2688 *Ocean. Tech.*, 19, 1477-1499, doi:10.1175/1520-0426.
- 2689 Yüce, H., (1993). Water level variations in the Sea of Marmara. *Oceanologica Acta*, 16, 4, 335-
2690 340.
- 2691

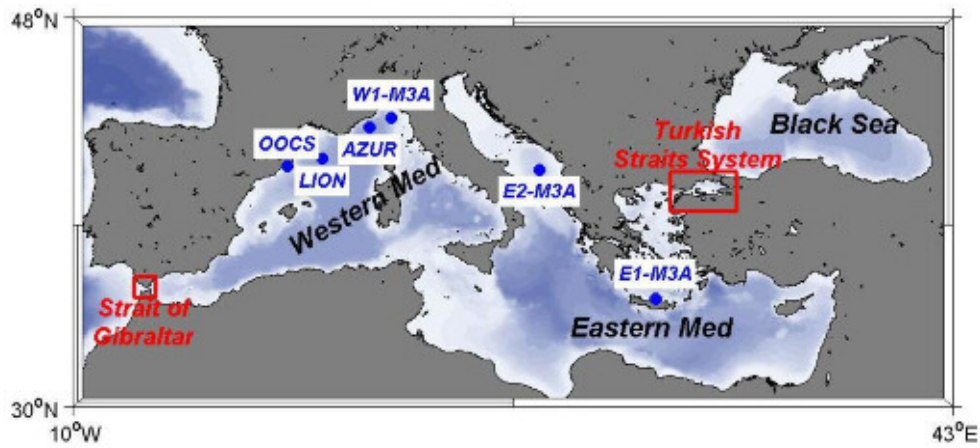


Figure 1: Mediterranean bathymetry with the location of the Strait of Gibraltar and the Turkish Straits System (for detail see Figures 4 and 9 respectively). The blue dots indicate the location of the open sea buoys described in section 2.

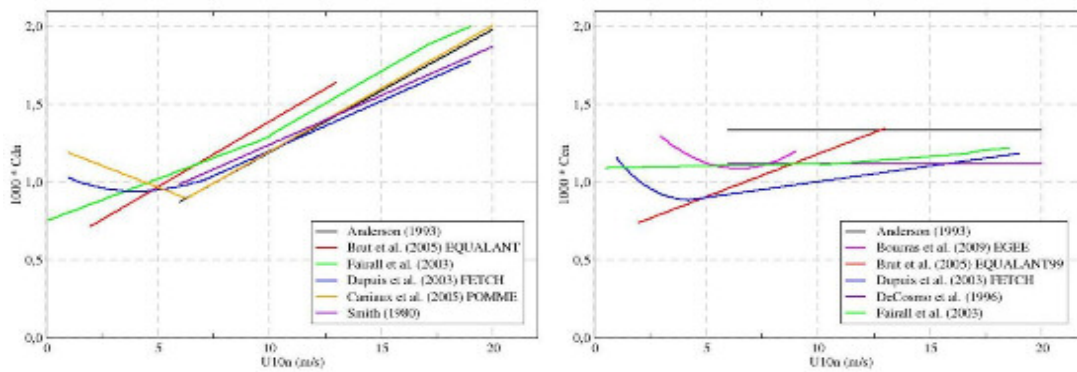


Figure 2: Exchange coefficient (multiplied by 1000) for the wind stress C_{dn} (left) and for the latent heat flux C_{en} (right) as a function of the wind velocity (at 10 m and in neutral stratification) for some recent parameterizations and in the range of sampled wind conditions.

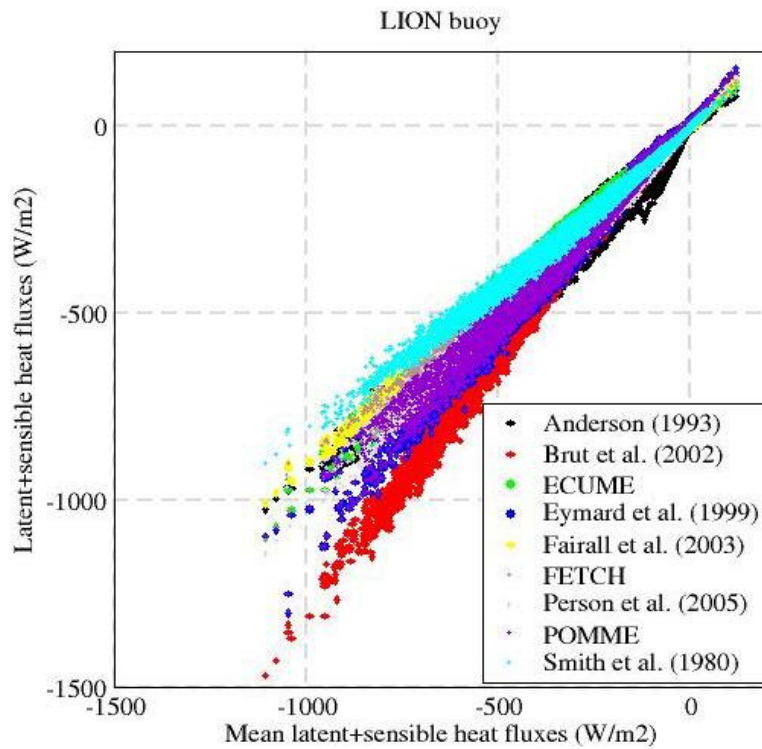


Figure 3: Spread of the sum of the latent and sensible heat fluxes calculated at the LION buoy in the north western Mediterranean Sea (period 2001-2013; N=68722) from nine flux bulk algorithms, as a function of the mean of the nine fluxes. Note that for a mean sensible plus latent heat flux of 1000 Wm^{-2} the spread is about 500 Wm^{-2}

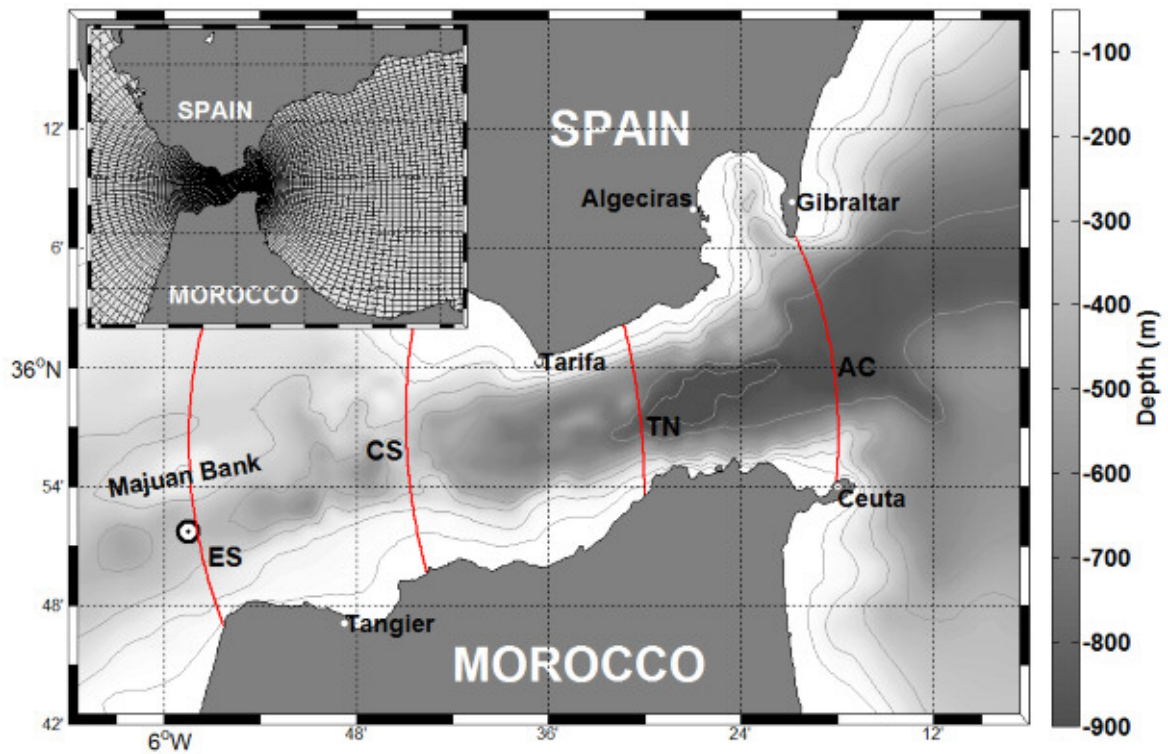


Figure 4. Map of the Strait of Gibraltar showing the bathymetry and the location of the relevant topographic features and sites cited in the text: ES, CS, TN, and AC indicate the position of Espartel sill, Camarinal sill, Tarifa Narrows and Gibraltar-Ceuta cross-strait sections, respectively. The monitoring site at Espartel sill is also indicated. The inset shows the numerical model domain used to accomplish the two hincasts discussed in the text.

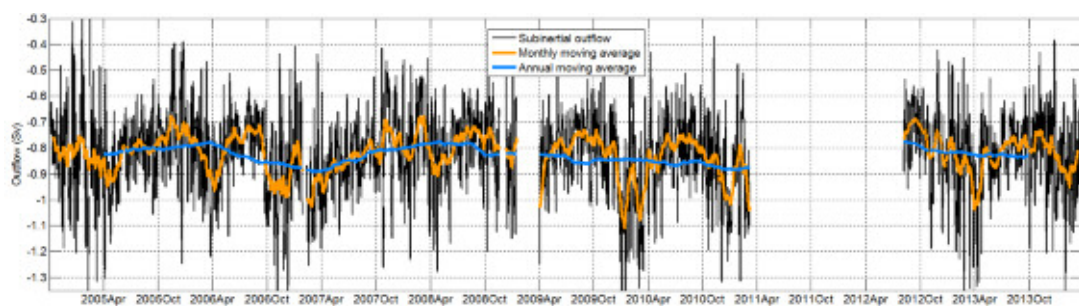


Figure 5.- Time series (black) of the outflow after removing tidal fluctuations by a low-pass 8-th order Butterworth filter, with pass and stop band frequencies of 38^{-1} and 28^{-1} h^{-1} , respectively. Two other versions with different degree of additional filtering are presented to illustrate the annual (orange) and interannual (blue) variability (adapted from Sammartino et al. (2015)).

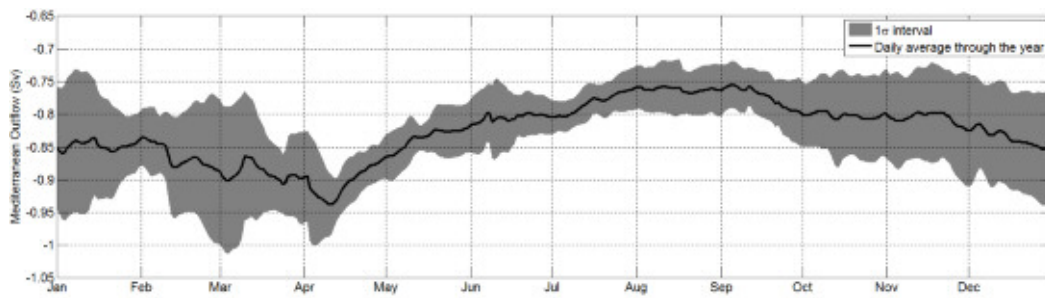


Figure 6.- Seasonal cycle of the outflow at Espartel. The black line is the mean value of the outflow in a given Julian day obtained by averaging the daily value of the outflow the same days of all the sampled years. Grey shade represents the standard deviation of the same statistics (adapted from Sammartino et al. (2015)).

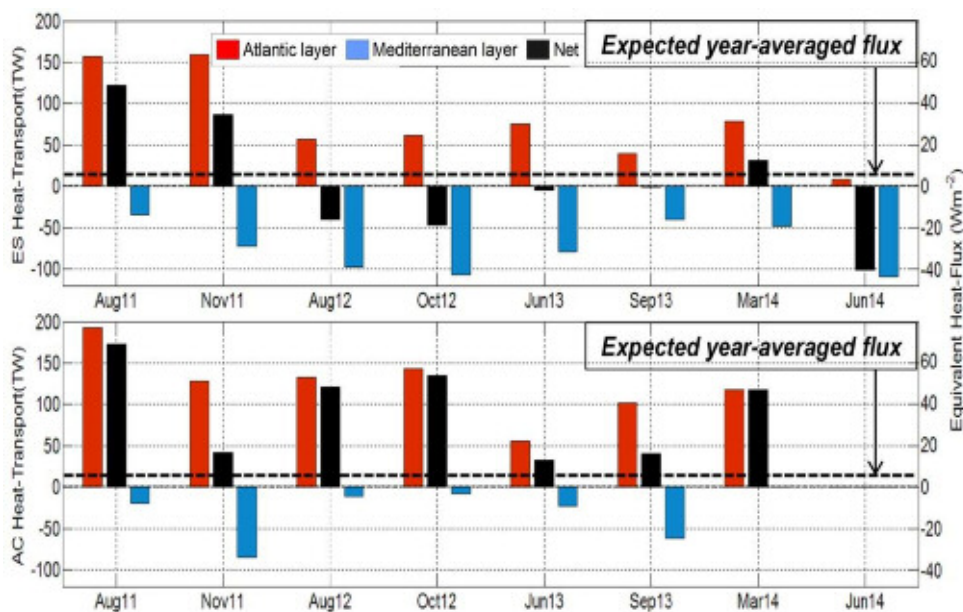


Figure 7. Heat transport computed from observations collected with a CTD probe that had a lowered ADCP incorporated, during different oceanographic cruises at the dates indicated in the x-axis. The top panel shows the transport across ES section and the bottom panel through the easternmost section of the SoG (AC, see Figure 1). The colored bars indicate the heat transport within each layer and their sum (net), being positive towards the Mediterranean Sea and negative towards the Atlantic Ocean. The dashed black line indicates the expected long-term mean according to values in the literature. The scale on the right shows the equivalent heat flux across the Mediterranean Sea surface to balance the heat transport through the SoG, which is computed by dividing the heat transport (left scale) by the area of the Mediterranean Sea.

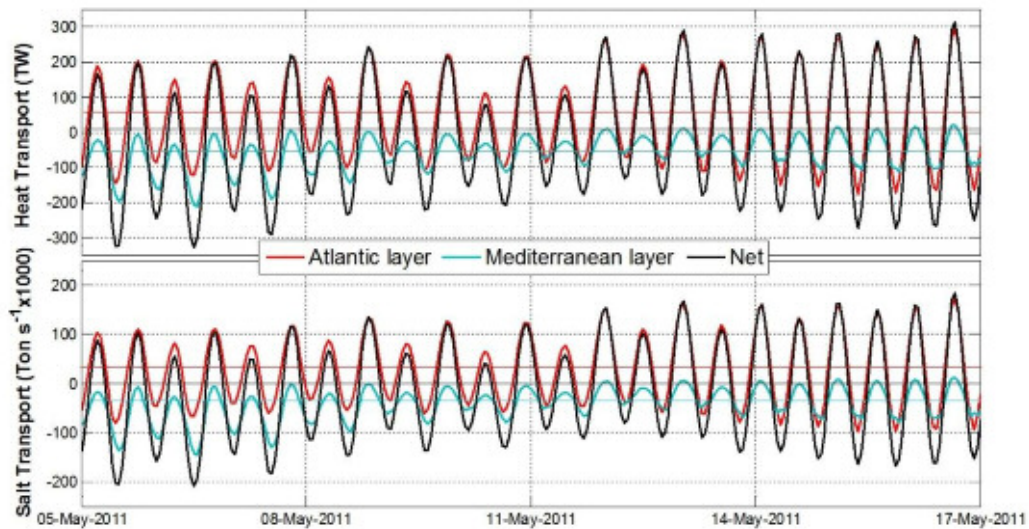


Figure 8.- Short fragment of the time series of heat (top) and salt (bottom) transports computed from the outputs of the numerical model at ES section. The time series include all ranges of variability, although the overwhelming prevalence of the semidiurnal tidal signal masks the variability at other frequencies (subinertial in this case). As in Figure 4, the color code indicate the heat and salt transport within each layer, which must not always be necessarily positive (towards the Mediterranean) in the Atlantic layer or negative (towards the Atlantic) in the Mediterranean layer. Horizontal lines indicate the time-average values of the transports with the same color code (see also Table 2).

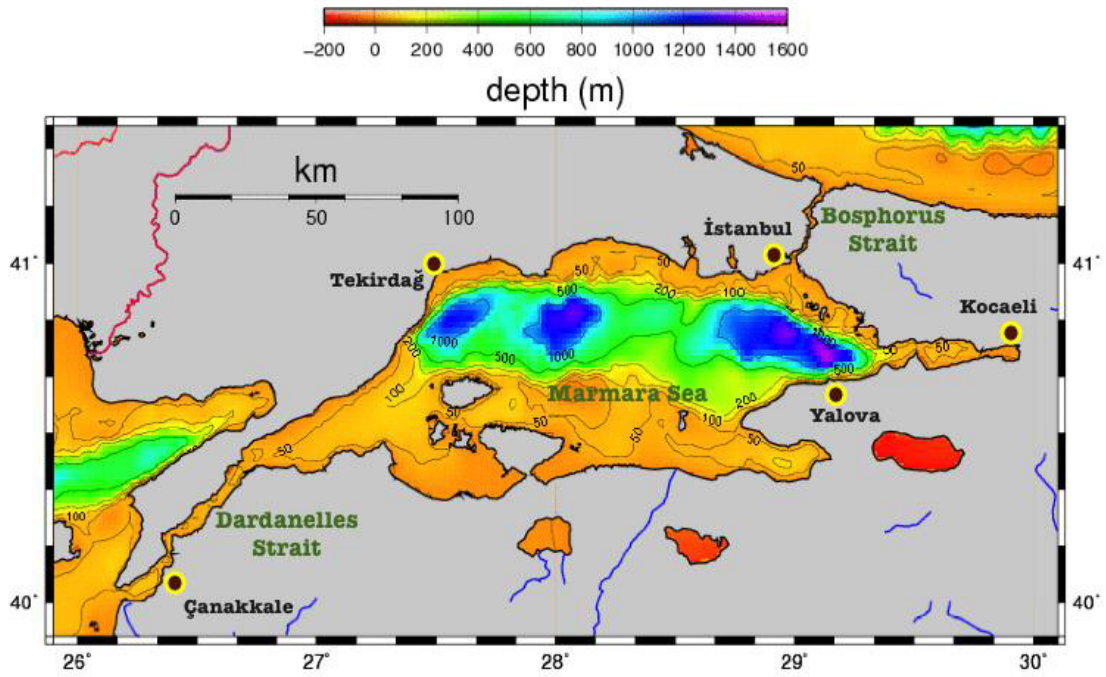


Figure 9. Location and bathymetry of the Turkish Straits System. Adapted from Schroeder et al., 2012.

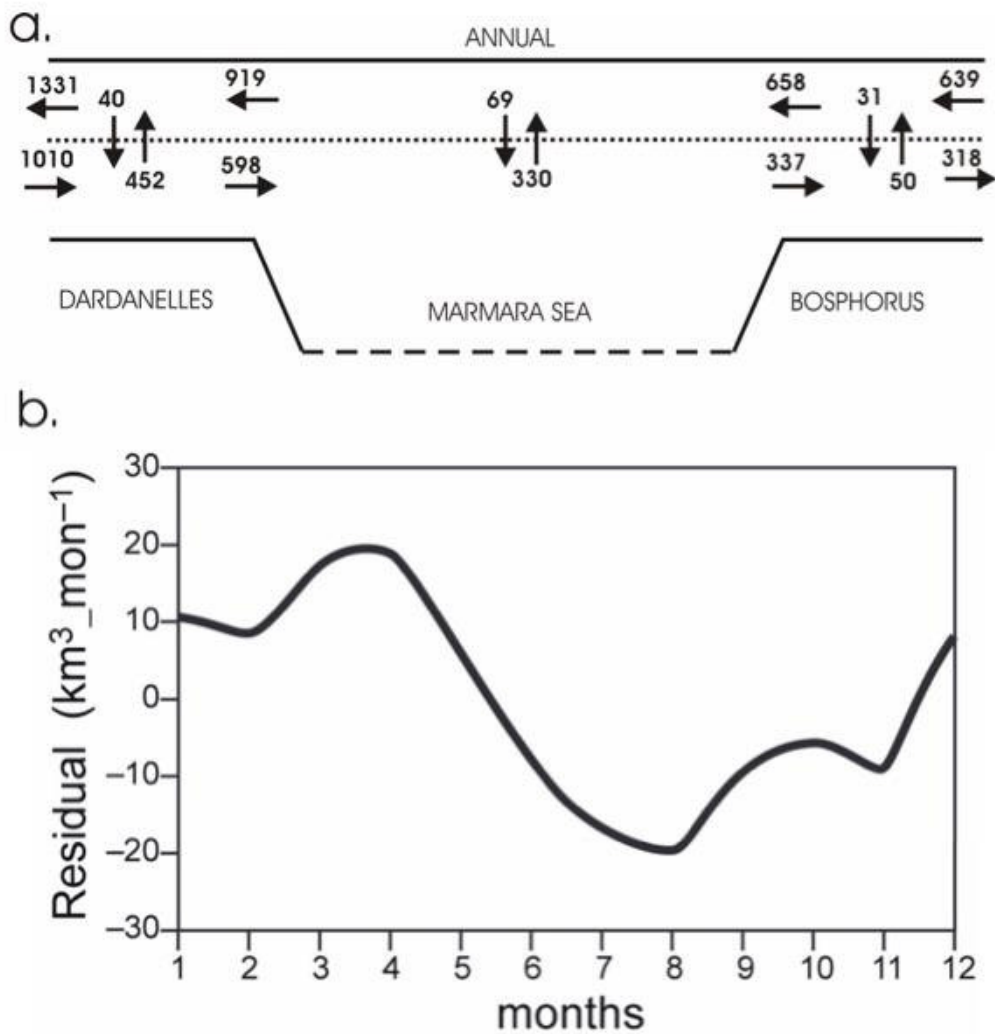


Figure 10: (a) Steady-state annual mean fluxes (km³/yr) through the TSS and between its individual compartments (after Beşiktepe, 2003); (b) seasonal anomalies of the net transport through the Bosphorus Strait based on data from 1923-1997 (Peneva et al., 2001). Reprinted from *The Climate of the Mediterranean Region - From the past to the future*, Elsevier, 592 p Lionello P. (ed). 2012

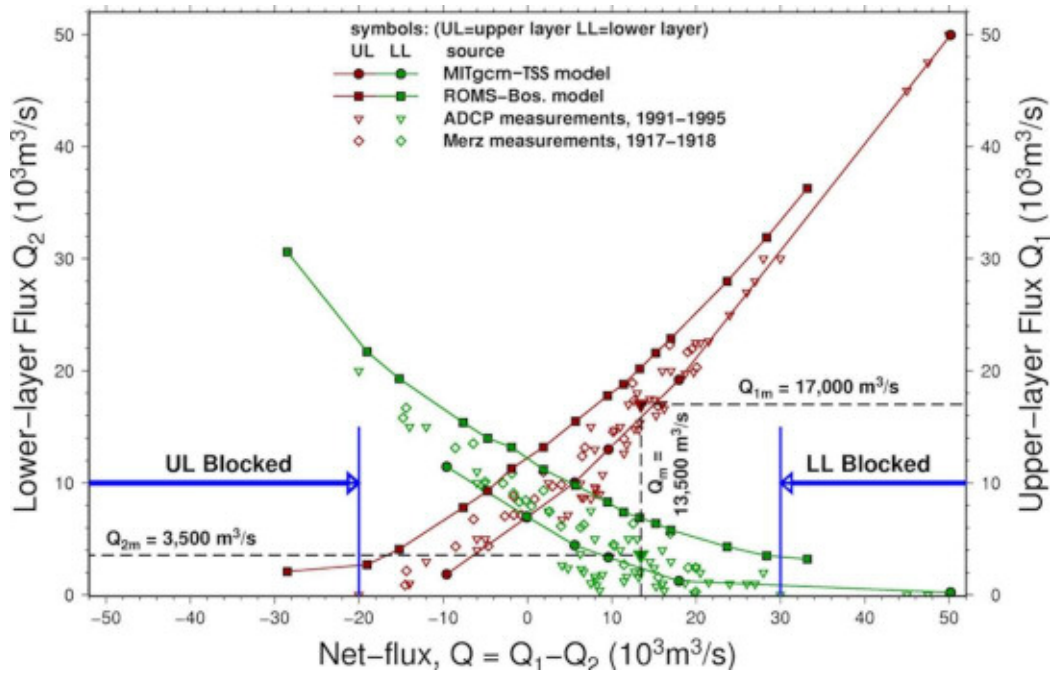


Figure 11. Upper-layer (Q_1) and lower-layer (Q_2) volume fluxes through the Bosphorus as a function of the net flux ($Q=Q_1-Q_2$), based on observational data and compared with the results from the Bosphorus model (ROMS) of Sözer (2013) and the TSS model (MITgcm) of Sannino et al. (2015). Data from ADCP measurements on board the R/V BİLİM (Özsoy et al., 1998) and the by Merz and Möller (Möller, 1928) are also shown. The average upper, lower layer and net flux average values obtained from the ADCP measurements are marked (large inverted triangles and dashed lines). The blue arrows show the ranges of net flux where either the upper layer (right) or the lower layer (left) are expected to be blocked.

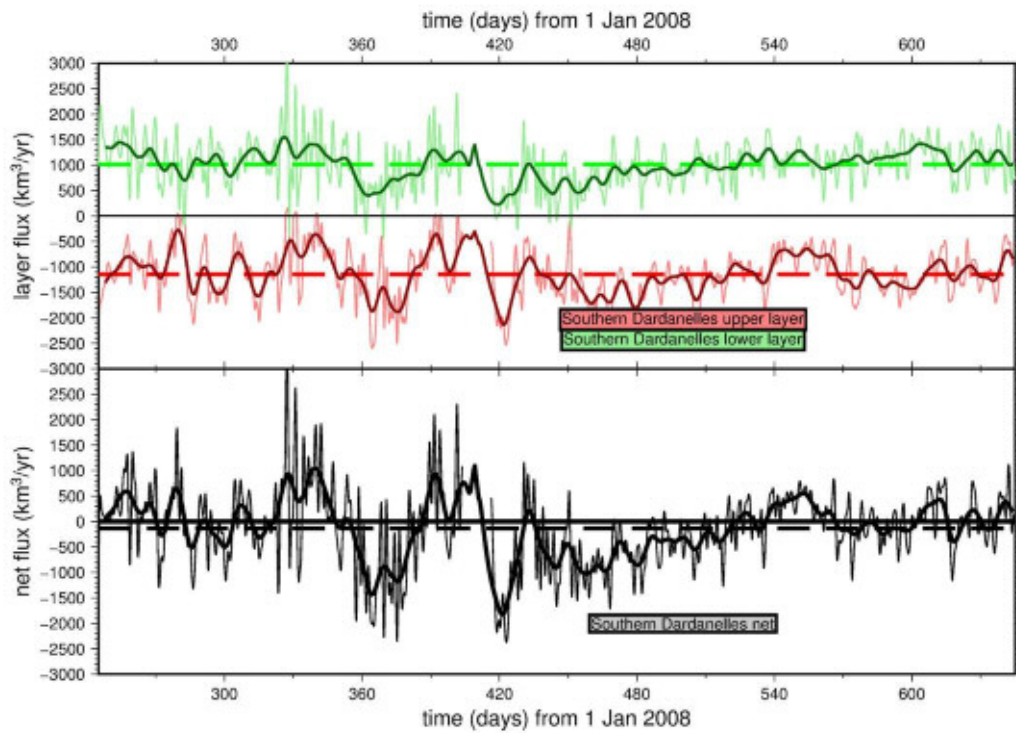


Figure 12. The upper, lower layer and net volume fluxes at the southern end of the Dardanelles Strait, computed from time series of current profiling measurements by Jarosz et al. (2013). The low pass filtered daily time series (black) with a cosine taper filter length of 11-points (~10d) and the mean values of each time series (dashed lines) are also shown.

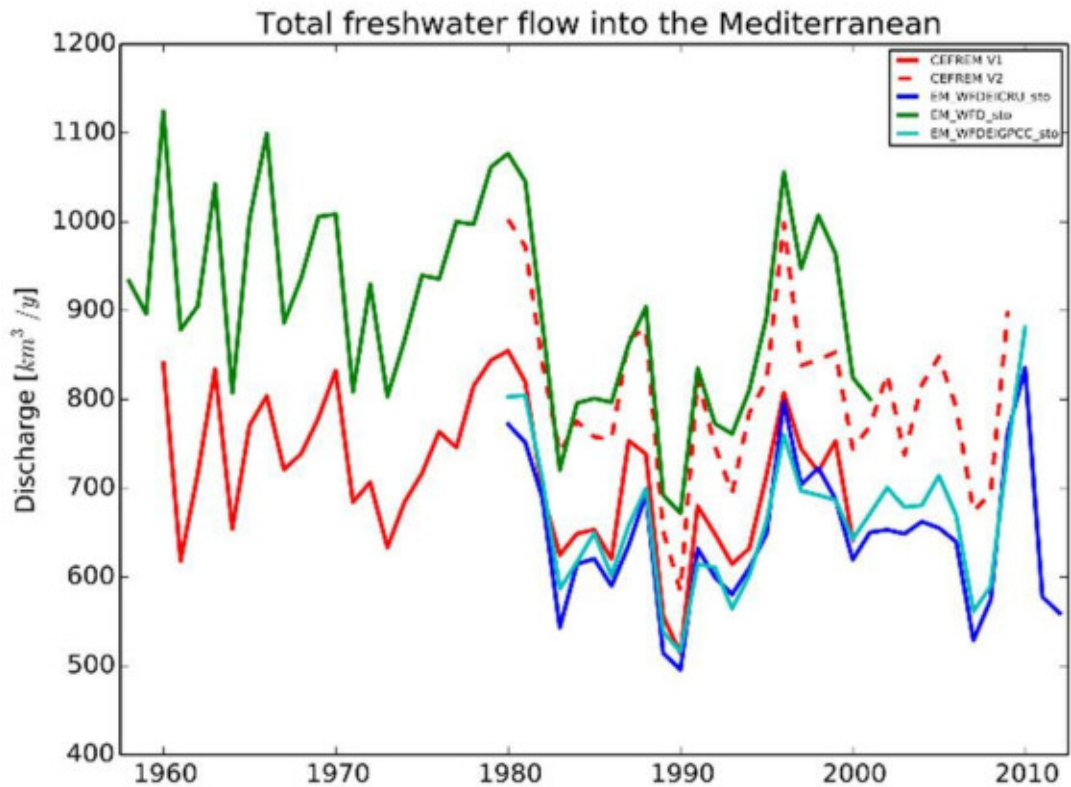


Figure 13 : The evolution of riverine input into the Mediterranean as as provided by CEFREM (Ludwig et al. 2009 for V1 and personal communication for V2) and simulated by the ORCHIDEE model forced with three different atmospheric conditions : 1) WFD (Weedon et al. 2011, labelled EM_WFD_sto), 2) WFDEI, precipitation corrected with CRU (Weedon et al. 2014, labelled EM_WFDEICRU_sto) and WFDEI corrected with GPCC (labelled EM_WFDEIGPCC_sto).

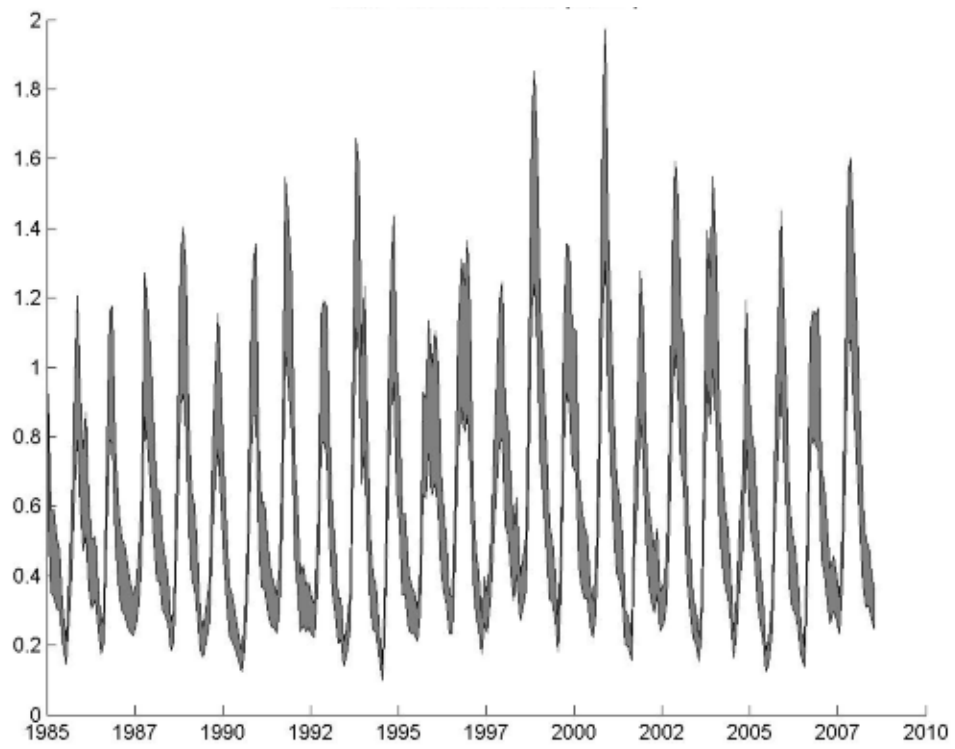


Figure 14. Temporal evolution of the heat flux (in W/m^2) associated to the river runoff. See section 5.5 for details.

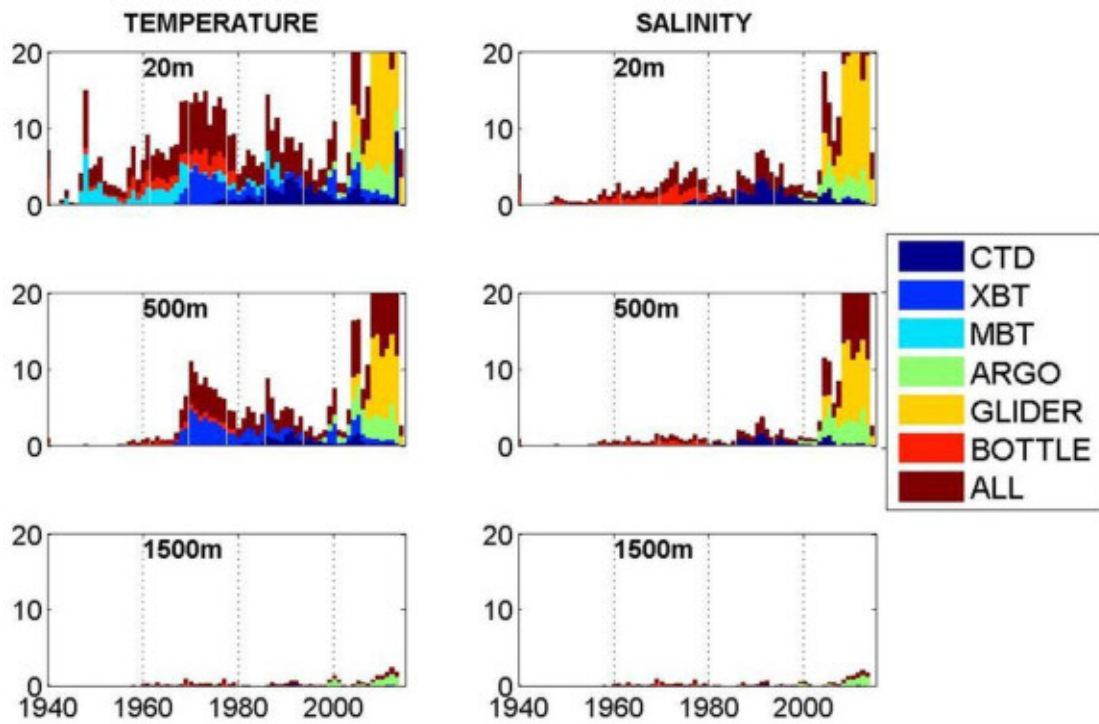


Figure 15. Temporal evolution of the amount of in-situ temperature (left) and salinity (right) data in the Mediterranean Sea from different platforms (vertical axis scaled by 10^3). The results are shown for 20 m (top), 500 m (middle) and 1500 m (bottom).

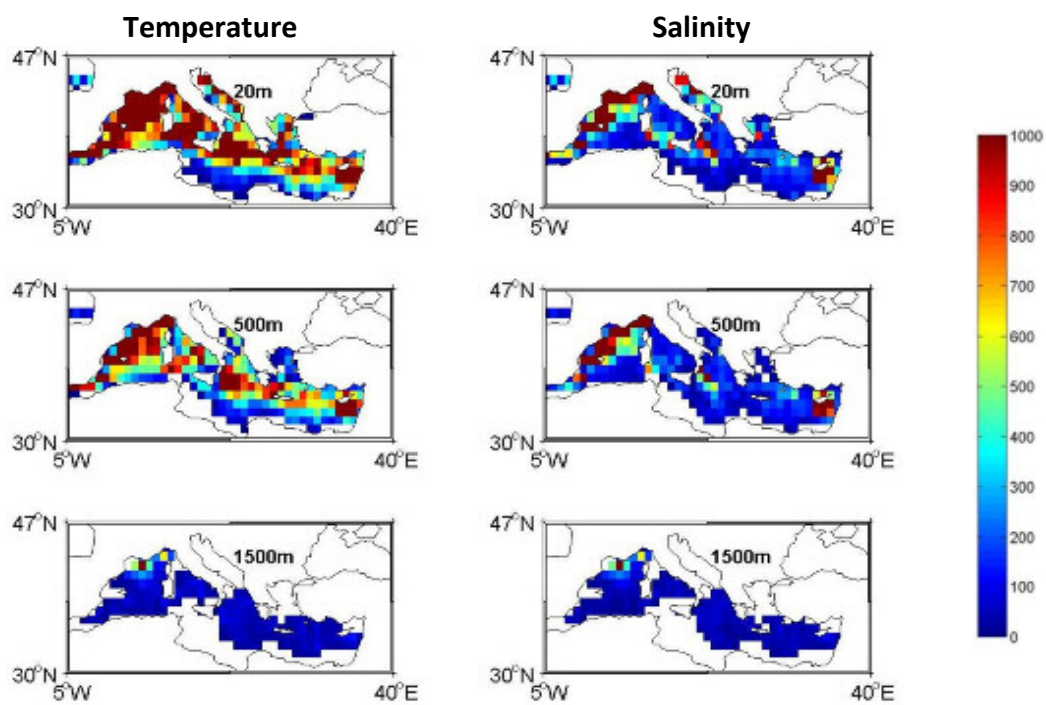


Figure 16. Number of observations of temperature (left column) and salinity (right column) gathered during the period 1940-2014 at different depths. The observations have been binned in $2^\circ \times 2^\circ$ boxes and all kind of observations have been included in the count.

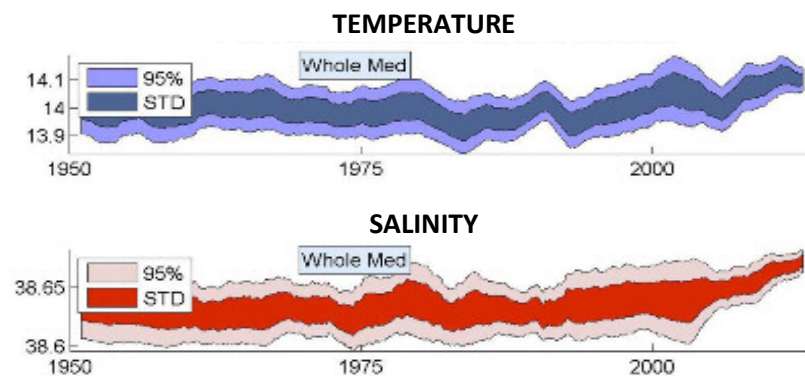


Figure 17. Time evolution of the 3D basin averaged temperature (top) and salinity (bottom) as obtained from Jordà et al. (2016). The dark patch indicates the normal error while the light patch indicates the 95% confidence interval.

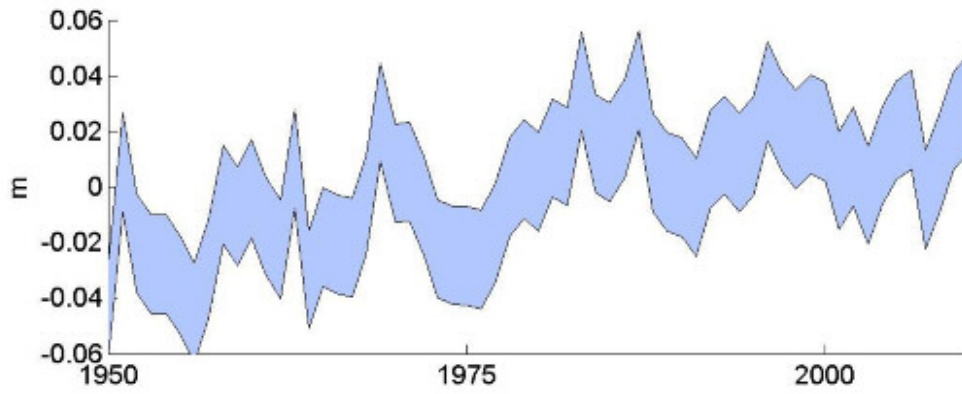


Figure 18. Mediterranean mass water content anomalies (in equivalent water thickness, in m) obtained from the combination of reconstructed basin mean sea level and water expansion from hydrographic datasets. The anomalies are computed with respect to the mean of the time series. The patch indicates the range of uncertainty as described in the text (adapted from Jordà and Gomis, 2013).

Table 1: Comparison of in-situ measurements of daily incoming long-wave and short-wave radiations with satellite estimates, in terms of bias and rms. Ship data collected during the SOFIA (NE Atlantic, Weill et al., 1995), SEMAPHORE (NE Atlantic; Eymard et al., 1996) and CATCH (NW Atlantic, Eymard et al., 1999) experiments; anchored buoy data for the POMME experiment (NE Atlantic; Mémery et al., 2005), while for 2006, several land or buoy pyranometers and pygeometers are operationally used for evaluation. Note the change of statistics between the SEMAPHORE and CATCH experiments in the incoming shortwave radiation due to an improved cloud classification for satellite retrievals. N is the number of days of the series.

Daily data (W/m ²)	Incoming longwave		Incoming shortwave		Reference
	Bias	RMS	Bias	RMS	
SOFIA (1992) <i>Ship data</i>	-2.1 (N=289)	11.3	23.6 (N=149)	75.5	<i>Eymard et al. (1999)</i>
SEMAPHORE (1993) <i>Ship data</i>	4.3 (N=640)	15.7	10.6 (N=197)	58.1	<i>Eymard et al. (1999)</i>
CATCH (1997) <i>Ship data</i>	0.3 (N=719)	17.0	-1.3 (N=232)	49.9	<i>Eymard et al. (1999)</i>
POMME (2001) <i>Buoy data</i>	-1.3 (N=246)	11.1	-1.5 (N=246)	10.6	<i>Caniaux et al. (2005)</i>
Year 2006	-1.2	15.6	-1.3	13.7	<i>LeBorgne et al. (2007)</i>

Table 2: Errors on the various components of the net heat flux computed with the COARE3.0 bulk algorithm (Fairall et al., 2003) at the LION buoy (period 2011-2013) in the North-western Mediterranean resulting from the observable errors. In parenthesis, the errors when adding the error due to the bulk algorithm. Note that this values have been obtained for a single measurement point and do not represent basin-wide averages.

	Mean values (2011-2013)	Error
Air temperature (°C)	16.3	0.2
SST (°C)	18.1	0.1
Relative humidity (%)	0.79	0.03
Wind (m.s⁻¹)	7.8	0.3
Latent heat flux (Wm⁻²)	-122	12.2 (19.1)
Sensible heat flux (Wm⁻²)	-14	0.0 (1.7)
Net shortwave radiation (Wm⁻²)	185	3.9
Net longwave radiation (Wm⁻²)	-48	6.9
Net heat flux (Wm⁻²)	+1	14.6 (20.8)
Wind stress (Nm⁻²)	0.15	0.018

Table 3 – Estimations of inflow (Q_A) and outflow (Q_M) and net flow (Q_{net}) through the Strait of Gibraltar published in literature. Gray-shaded rows indicate estimations based on salt ($Q_M S_M + Q_A S_A = 0$) and volume ($Q_A + Q_M = E$) conservation, and, eventually, on the hydraulically controlled flows theory, whereas the remaining values come from observations.

Reference	Q_A (Sv)	Q_M (Sv)	Q_{net} (Sv)
<i>Nielsen</i> [1912]	1.87	-1.78	0.09
<i>Schott</i> [1915]	1.74	-1.64	0.10
<i>Sverdrup et al.</i> [1942]	1.75	-1.68	0.07
<i>Carter</i> [1956]	0.95	-0.91	0.04
<i>Bethoux</i> [1979]	1.68	-1.60	0.08
<i>Lacombe and Richez</i> [1982]	1.21	-1.15	0.06
<i>Bryden and Stommel</i> [1984]	1.67	-1.59	0.08
<i>Bryden and Kinder</i> [1991]	0.92	-0.88	0.04
<i>Bryden et al.</i> [1994]	0.73	-0.68	0.05
<i>García Lafuente et al.</i> [2000]	0.92	-0.87	0.05
<i>Tsimplis and Bryden</i> [2000]	0.78	-0.67	0.11
<i>Baschek et al.</i> [2001]	0.81	-0.76	0.05
<i>Candela</i> [2001]	1.01	-0.97	0.04
<i>García Lafuente et al.</i> [2002]	0.96	-0.84	0.12
<i>Vargas et al.</i> [2006]	0.89	-0.82	0.07
<i>Sánchez Román et al.</i> [2009]	---	-0.78	---
<i>García Lafuente et al.</i> [2009]	---	-0.79	---
<i>Soto Navarro et al.</i> [2010]	0.81	-0.78	0.03
<i>Sammartino et al.</i> , [2015]	---	-0.85	---
Mean \pm std from observational estimates	0.86 \pm 0.10	-0.80 \pm 0.08	0.065 \pm 0.033

Table 4.- Time averaged exchange properties at the three notable sections of the SoG, estimated from different runs of the MIT-gcm numerical model applied to the domain showed in the inset of Figure 1 during the periods of hincast I (March 12 to June 24, 2011, upper box) and II (September 1 to November 27, 2011, lower box). The three rows correspond to Espartel Sill (ES), Camarinal Sill (CS) and Tarifa Narrows (TN) sections. Negative sign means transport towards the Atlantic Ocean. Numbers in italic within brackets indicate the associated uncertainty of the time-averaged value, which has been estimated as half the standard deviation of the subinertial series, according to the results by Sammartino *et al* (2015). Column $\Delta S_{effective} = S_M - S_A$ is the difference, expressed in units of the practical salinity scale, between the weighted Atlantic inflow and Mediterranean outflow salinity, which have been computed as $\bar{Q}_A \bar{S}_A$ and $\bar{Q}_M \bar{S}_M$, respectively, overbars representing time-averaged values. Last column is the Outflow Salinity Transport ($\bar{Q}_M \Delta S_{effective}$)

PERIOD	SECTION	Volume Transport, Q (Sv)			Salt Transport, QS (Ton $s^{-1} \times 1000$)			Heat Transport, QH (TW)			$\Delta S_{effective}$ ("PSU")	OST (Sv \times PSU)
		Q_A	Q_M	Q_{net}	QS_A	QS_M	QS_{net}	QH_A	QH_M	QT_{net}		
(I)	ES	0.959 (0.083)	-0.929 (0.102)	0.029 (0.173)	35.51 (3.09)	-36.34 (4.01)	-0.83 (6.61)	62.72 (5.43)	-51.06 (5.78)	11.66 (10.21)	1.953 (0.128)	-1.814 (0.080)
	CS	0.836 (0.098)	-0.817 (0.088)	0.019 (0.174)	31.04 (3.65)	-32.29 (3.48)	-1.26 (6.66)	55.21 (6.34)	-43.88 (4.77)	11.34 (10.23)	2.251 (0.109)	-1.839 (0.109)
	TN	0.845 (0.105)	-0.824 (0.089)	0.021 (0.174)	31.51 (3.92)	-32.61 (3.51)	-1.10 (6.64)	55.33 (6.72)	-44.04 (4.75)	11.29 (10.23)	2.154 (0.084)	-1.775 (0.123)
(II)	ES	0.918 (0.096)	-0.914 (0.094)	0.004 (0.167)	33.96 (3.56)	-35.73 (3.70)	-1.78 (6.37)	60.76 (6.78)	-49.97 (5.32)	10.78 (10.21)	1.992 (0.125)	-1.821 (0.080)
	CS	0.800 (0.106)	-0.805 (0.084)	-0.005 (0.169)	29.66 (3.93)	-31.84 (3.33)	-2.18 (6.42)	53.69 (7.24)	-43.31 (4.56)	10.38 (10.24)	2.292 (0.101)	-1.846 (0.112)
	TN	0.802 (0.112)	-0.807 (0.088)	-0.005 (0.169)	29.84 (4.15)	-31.94 (3.50)	-2.10 (6.42)	53.42 (7.54)	-43.23 (4.73)	10.18 (10.18)	2.205 (0.087)	-1.780 (0.124)

Table 5.- Contribution of the tidally-driven eddy fluxes to the time averaged exchange properties at the three notable sections of the SoG, estimated from hindcast II (September 1 to November 27, 2011) of the MIT-gcm numerical model applied to the domain showed in the inset of Figure 1. The rows correspond to Espartel Sill (ES), Camarinal Sill (CS) and Tarifa Narrows (TN) sections. Negative sign means transport towards the Atlantic Ocean. Percentage of the eddy fluxes contribution is in italic.

	SECTION	Volume Transport, $Q(\text{Sv})$			Salt Transport, $QS(\text{Ton s}^{-1}\times 1000)$			Heat Transport, $QH(\text{TW})$		
		Net	Eddy	(%)	Net	Eddy	(%)	Net	Eddy	(%)
INFLOW	ES	0.918	0.066	<i>7.2</i>	33.95	2.41	<i>7.1</i>	60.76	1.22	<i>2.0</i>
	CS	0.800	0.281	<i>35.1</i>	29.66	10.40	<i>35.1</i>	53.69	18.66	<i>34.8</i>
	TN	0.801	0.014	<i>1.7</i>	29.84	0.43	<i>1.4</i>	53.42	-0.60	<i>1.1</i>
OUTFLOW	ES	-0.914	-0.064	<i>7.0</i>	-35.73	-2.53	<i>7.1</i>	-49.97	-2.93	<i>5.9</i>
	CS	-0.805	-0.282	<i>35.0</i>	-31.84	-11.24	<i>35.3</i>	-43.31	-16.59	<i>38.3</i>
	TN	-0.807	-0.014	<i>1.8</i>	-31.94	-0.56	<i>1.8</i>	-43.24	-0.45	<i>1.1</i>

Table 6. Annual mean of water fluxes in the upper and lower layer at the southern limit of the Dardanelles Strait from different authors (adapted from Jarosz et al., 2013). Units are km³/year and in brackets the equivalence in Mediterranean sea level change (mm/yr). Negative values mean transports towards the Mediterranean.

<i>km³/year (mm/year)</i>	Upper layer	Lower layer	Net
Ünlüata et al. (1990)	-1258 (-503)	967 (387)	-291 (-116)
Beşiktepe et al. (1994)	-1218 (-487)	918 (367)	-300 (-120)
Özsoy and Ünlüata (1997)	-1181 (-472)	880 (352)	-300 (-120)
Tuğrul et al. (2002)	-1331 (-533)	1010 (404)	-321 (-128)
Kanarska and Maderich (2008)	-1225 (-490)	947 (379)	-278 (-111)
Jarosz et al. (2013)	-1158 (-463)	999 (400)	-158 (-63)
MEAN	-1228 (-491)	954 (382)	-275 (-110)
STD	61 (25)	49 (20)	59 (24)

Table 7 Projections of the change (in %) of basin average value at the end of the XXI century of different components of the Mediterranean water budget from different studies and scenarios.

<i>All values are expressed as %</i>	Precipitation	Evaporation	Prec. – Evap.	River Runoff	Dardanelles	Strait of Gibraltar	Sum of sources
<i>Mariotti et al. (2015)</i> Global CMIP5 ; RCP4.5 ; 2071-2098	-8.5	+7	-13.9	-14.8	N/D	N/D	N/D
<i>Adloff et al. (2015)</i> RCM ; A2 /A1B / B1 ; 2070-2099	[-2; -12]	[+8; +12.5]	[-16; -33]	[-4.5;-32]	[-25;-61]	[+31;+60]	[-31;-60]
<i>Sanchez-Gomez et al. (2009)</i> RCM ; A1B ; 2070-2099	[-4;-28]	[-6;+18]	[-15;-35]	[-5;-43]	[+25;-102]	N/D	[-20;-60]
<i>Mariotti et al. (2008)</i> CMIP3 ; A1B ;2070-2099	[+2;-23]	[+6;+9]	[-11;-25]	[-56;-87]	[-63;-85]	N/D	[-34;-42]

Table 8 Same that Table 7 for the heat fluxes through the sea surface and the Strait of Gibraltar.

<i>All values are expressed as %</i>	Surface heat flux	Gibraltar heat flux
<i>Adloff et al (2015)</i> RCM ; A2 /A1B / B1 ; 2070-2099	[+25;+75]	[0;+40]
<i>Dubois et al (2012) / Gualdi et al. (2013)</i> RCM ; A1B ; 2021-2050	[+60;+118]	[-11;+3]
<i>Somot et al. (2008)</i> RCM ; A2 ; 2070-2099	[+69]	N/D
<i>Somot et al. (2006)</i> RCM ; A2 ; 2070-2099	[+71]	N/D

Table 9 Projected changes of the basin average temperature, salinity and density at the end of the XXI century with respect to the values at the end of the XX century from different studies.

	T3D (°C)	S3D (psu)
<i>Adloff et al. (2015)</i> RCM ; A2 /A1B / B1 ; 2070-2099 vs. 1961-1990	[+0.93;+1.35]	[+0.28;+0.52]
<i>Macías et al. (2015)</i> RCM ; RCP4.5/RCP8.5 ; 2096-2099 vs. 2014-2017	[+1.30 ;+2.50]	[+0.6 ;+0.9]
<i>Carillo et al. (2012)</i> RCM ; A1B ; 2001-2050 vs. 1951-2000	[+0.38;+0.42]	[-0.08;+0.03]
<i>Somot et al. (2006)</i> RCM ; A2 ; 2099 vs CTRL	[+1.5]	[+0.23]

Table 10: Best estimates of the different components of the Mediterranean Sea heat budget (see eq. 1) with their associated uncertainties for the long term average and for the period 2005-2010. In brackets we include the indirect estimate in that case where it provides lower uncertainty than the direct estimate. The indirect estimate is obtained assuming that the budget is closed and using the information of the other components and its uncertainty has been obtained considering that the errors in the different components are uncorrelated. See the text for further details.

HEAT FLUX (W/m²)	1980-2010	2005-2010
<i>SURFACE FLUXES</i>	-3.0 ± 8.0 [-4.9 ± 4.3]	-3.0 ± 8.0 [-1.7 ± 5.1]
<i>GIBRALTAR</i>	4.5 ± 4.1	4.5 ± 4.1
<i>DARDANELLES</i>	0.1 ± 0.2	0.1 ± 0.2
<i>RIVERS</i>	0.6 ± 0.4	0.6 ± 0.4
<i>HEAT CONTENT CHANGE</i>	0.3 ± 0.3	3.5 ± 3.0

Table 11: As Table 10 but for the water mass budget.

WATER FLUX (m/yr)	1980-2010	2005-2010
SURFACE FLUXES	-0.8 ± 0.2	-0.9 ± 0.2
GIBRALTAR	0.8 ± 0.4 [0.5 ± 0.2]	0.85 ± 0.4 { 0.6 ± 0.2 }
DARDANELLES	0.1 ± 0.02	0.1 ± 0.02
RIVERS	0.2 ± 0.01	0.2 ± 0.01
WATER CONTENT CHANGE	$5 \cdot 10^{-4} \pm 10^{-3}$	$1 \cdot 10^{-3} \pm 3 \cdot 10^{-3}$

Table 12: As Table 10 but for the salt mass budget.

SALT FLUX (10^6 kg/s)	1980-2010	2005-2010
GIBRALTAR	-1.5 ± 6.5 [-0.1 ± 0.2]	-1.5 ± 6.5 [0.1 ± 0.3]
DARDANELLES	0.2 ± 0.2	0.2 ± 0.2
SALT CONTENT CHANGE	0.1 ± 0.1	0.3 ± 0.2